Interdisciplinary Development of Diagnostic Bioindicators for Healthy and Degraded Reefs and Adjacent Built Habitats

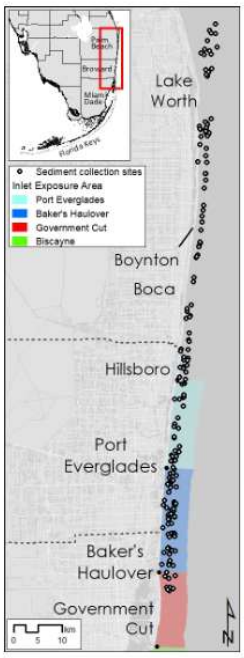

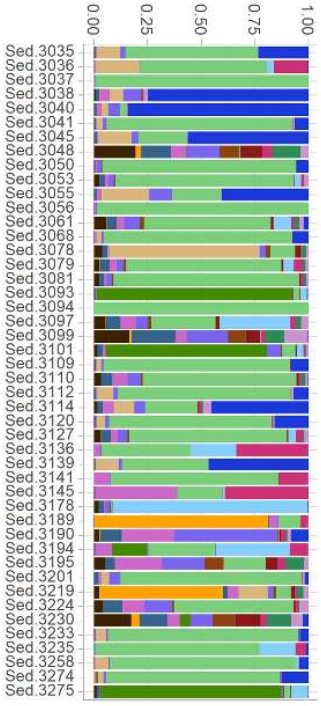

Interdisciplinary Development of Diagnostic Bioindicators for Healthy and Degraded Reefs and Adjacent Built Habitats

Final Report

Prepared By

Jose V. Lopez (NSU)

Brian Walker (NSU)

Nicholas Jones (NSU)

Paisley Samuel (NSU)

June 15, 2025

Completed in Fulfillment of DEP Agreement # C434B1 for

Florida Department of Environmental Protection

Coral Protection and Restoration Program

8000 N Ocean Dr.

Dania Beach, FL 33004

This report was funded through a contract agreement from the Florida Department of Environmental Protection's (DEP) Coral Protection and Restoration Program. The views, statements, findings, conclusions, and recommendations expressed herein are those of the author(s) and do not necessarily reflect the views of the State of Florida or any of its subagencies.

Acknowledgements

We are very thankful to Hunter Noren who coordinated sampling and the rest of the diving team who collected NCRMP samples in 2022 and 2024. We are also grateful to Dr. Lauren Krausfeldt for metagenomics analyses for qPCR conducted through her company, Microbial Matters Ltd. From the Molecular Microbiology and Genomics (MMG) Laboratory we thank volunteer Michelle Gorodosky and other graduate assistants such as Athena Capetanakis.

Management Summary (328 words)

We have applied multiple analyses to characterize sediments from the Kristin Jacobs Coral Aquatic Preserve (KJCAP) for new diagnostic markers in the context of *reef disturbance responses.* This project has now generated a wide array of interdisciplinary data: molecular microbiome and eukaryotic metabarcoding sequences, ambient environmental, nutrient and heavy metal (HM) measurements from sediments derived from approximately 253 KJCAP sites collected in the summer of 2022 and 2024. The samples were opportunistically collected as part of the National Coral Reef Monitoring Program (NCRMP). This resulted in one the most comprehensive and integrative surveys in recent times. One major goal established that *port-specific bacteria could be detected in reef sediments and decrease with increasing distances from ports, while also deeply characterizing sediment microbiomes and heavy metals.*
The total microbiome characterization encompassed 171 2022 and 82 2024 (n= 253) sediment samples but found few correlations with specific reef habitats. Indeed, many samples shared similar taxa, yet varying relative abundances of bacterial genera such as *Psychrobacter, Woeseia* and *Halomonas.* Reef sediments displayed an equally diverse eukaryotic meiofauna.

By comparing distributions of bacteria with previous Florida Keys data, several KJCAP sites appear qualitatively different from more pristine reefs. We have identified a few potential bioindicator bacteria such as *Woeseia* and Family Pirellulaceae, conspicuous by their absence or low abundance in KJCAP sites.

Variation in sediment microbiomes was most strongly influenced by the maximum temperature, total carbon, nickel, zinc and selenium concentrations and by latitude. Samples with higher total carbon had a higher Moraxellaceae abundance. Samples which had experienced higher maximum temperatures had higher Bacillaceae and Desulfocapsaeae, and samples with diverse microbiomes had lower total carbon, zinc and selenium concentrations, but higher nickel concentration.

Higher concentrations of some heavy metals (mercury, lead, zinc, barium etc) in sediments appeared nearer to ports and inlets than more remote reefs. Moreover, integrated statistical analyses and environmental modeling suggested a structuring of the KJCAP into “inlet exposure areas (IEAs), probably influenced by their closest southern ports/inlets.

Executive Summary

We have applied multiple analyses (microbiome, environmental) to characterize sediments from the Kristin Jacobs Coral Aquatic Preserve (KJCAP) and develop new diagnostic markers in the context of *reef disturbance responses.* The results follow previous FL DEP projects on Port Everglades Inlet (PEI) bacterial microbiome and heavy metals (HM) analyses. The KJCAP sediment sample collections spans over 160 Km and covers reef depths from 2 – 30 m. We also have generated a spatiotemporal map of sediment bacteria combined with contemporary environmental datasets ranging from Palm Beach to Miami-Dade county. Although not explicitly stated in this project, our data could be linked to concurrent studies of local water quality. The following hypotheses were posed for this project: a) PEI- specific bacteria can be detected in reef sediments associated with inlet exposure; b) PEI-specific microbe signatures will decrease in proportion to the distance from the port(s) and c) specific microbiome signatures will be found associated with specific parameters – e.g. less urbanized reef communities, or concentrations of specific heavy metals. We identify and quantify previously characterized PEI bacteria, we developed new quantitative PCR (qPCR) primers from archived PEI microbial sequences for higher sensitive detections. We amplified four bacterial genes - fucose, epimerase, hexulose and catalase, and then tested on various DNA derived of port or reef origins. PCR products were detectable in PEI control DNAs but not in adjacent reef sediments, indicating too much dilution of PEI bacteria on reef sediments.

Opportunistic sampling of a total of n=253 reef sediments collected as part of the 2022 and 2024 National Coral Reef Monitoring Program (NCRMP) seasons were characterized for their microbial community composition (e.g. “microbiomes”) via bacterial 16S rRNA amplicon sequence variant (ASV) analyses and eukaryotic meiofauna via metabarcoding methods. This is the first systematic survey of microbiomes at various depths (2 – 28 m) spanning from Palm Beach to Miami-Dade county. By comparing distributions of bacteria with earlier Florida Keys microbiome data, several KJCAP sites appear to lack specific, potential beneficial bioindicator rbacteria such as genus *Woeseia* and Family Pirellulaceae. Conversely have an increased relative abundance of fecal indicator bacteria (*E coli/Shigella*), *Psychrobacter*, and eukaryotic water molds at some KJCAP sites. Port-specific bacteria (e.g. Anaerolineaceae, Thiotrichaceae, Desulfobacteraceae) were also detected in the ASVs, but decreased with increasing distance from human-built structures.

Variation in sediment microbiomes was most strongly influenced by the maximum temperature in the month prior to sample collection, total carbon, nickel, zinc and Selenium concentrations and by latitude. Samples with higher total carbon, primarily southern sites in the Port Everglades and Haulover contributing areas, had a higher relative abundance of Moraxellaceae. Samples which had experienced higher maximum temperatures, particularly those near Boynton, had higher Bacillaceae and Desulfocapsaeae, and samples with diverse microbiomes had experienced moderate maximum temperatures, had lower total carbon, zinc and selenium concentrations, but higher nickel concentration. Higher concentrations of some trace metals (mercury, cadmium, barium etc) appeared nearer to ports and inlets than more remote reefs. Moreover, integrated statistical analyses and environmental modeling suggested a structuring of the KJCAP into “inlet exposure areas (IEAs), which in turn are influenced by their closest southern inlet.

TABLE OF CONTENTS

List of Figures

List of Tables

1. INTRODUCTION

3.2 Background

In general, molecular environmental DNA (eDNA) methods are applied across multiple habitats, such as coral reefs, to complement and enhance traditional survey techniques, increase detection and resolution of resident organisms (Alexander et al, 2020). Application of microbiome and eDNA methods has been conducted by the NSU Molecular Microbiology and Genomics (MMG) Laboratory for over a decade (Campbell et al 2015; O'Connell et al, 2018). Part of the impetus was determining possible sources of pathogens which could affect adjacent reefs (Studivan et al, 2022). In 2020 and 2021, the MMG laboratory was contracted by Florida Department of Environmental Protection (FL DEP) to characterize PEI and proximal Kristin Jacobs Coral Aquatic Preserve (KJCAP) surface sediments for the Coral Reef Conservation Program (CRCP). Sediment samples were collected from Port Everglades Inlet and surface sediments from the adjacent coral reef for two consecutive years 2020 -2021. CRCP 13 (B6F91C) results indicated that port (P) and adjacent reef ® sediments hold distinct bacterial communities. The results can also be accessed here – https://floridadep.gov/rcp/coral/documents/analysis-sediments-port-everglades-inlet-pei-microbiome-characterization-phase. Specific bacterial taxa showed statistically different abundances between the two habitats (Krausfeldt, Lopez et al, 2023). In a recent DEP project (#C0FEDD)", focus and measurements of heavy metals and metagenomics from eighteen deeper sediment cores (20 – 200 cm) were enhanced and showed high levels of some metals above continental crust values. This followed a preliminary analysis of heavy metals from core samples (Giarikos et al, 2023). However, the effects from contributing anthropogenic stressors in the PEI environment, and on its surrounding microbial communities, have not been fully interpreted. For example, lead (Pb) can incorporate into scleractinian coral skeletons, and possibly barium (Ba) as well which exhibit ionic radii (R Dodge, pers comm).

Since specific microbial communities are associated with port sediments, and inlet outflows probably affect water quality on the reefs, we proposed to examine the associations between microbial communities in reef sediments to the microbial communities in port sediments and how they are affected by exposure to port/inlet waters and other environmental conditions (Krausfeldt and Lopez et al 2023). The previous characterization of reef sediment microbiomes only included reef sites proximal (within 1 km) to PEI. We thus proposed to extend sampling and characterization for both PEI and reef-specific microbes through opportunistic sampling and archived National Coral Reef Monitoring Program (NCRMP) sediment samples.

We are aware of various quantitative reef models, estimates of flow rates and literature stating that effluent, sedimentation and fishing are major drivers that can predict or affect coral reef health and recovery (Jouffray et al, 2019). These can be applied to the KJCAP which has unique challenges due to its proximity to major south Florida urban centers. Although the KJCAP has been intensively studied for many years (Walker et al, 2012), stressors have only intensified on the reef via sedimentation, land-based sources of pollution, nitrification and disease outbreaks such as stony coral tissue loss disease (SCTLD). Early SCTLD appeared on *Dendrogyra cylindrus* not far from PEI (Jones et al. 2021), and port sediments can have adverse effects on corals (Serrano et al, 2023). Recently, a greater focus on land-based sources of pollutants and nutrients have gained the attention of focus groups and technical advisory committees. Nutrient inputs will affect microbial

communities, so our study will provide an extended baseline. This study is a component of an unofficial "phased" continuation of DEP projects in the MMG Lab. We also compared changes from two years of KJCAP community changes from NCRMP sampling (2022, 2024) to determine the profiles, and relative dynamics or stability of resident microbial communities. Concomitantly, for Goal 2 (Task 3), we also conduct eukaryotic metabarcoding and standard chemistry/nutrients methods on the NCRMP sediment samples to provide metadata on the existing reef meiofauna.

In this project, previously characterized microbiomes were used to meet DEP's goal of developing bioindicators for "diagnostic microbe(s) that could be indicative of disturbances or nutrient fluctuations in the coral reef environment" (Priorities I-IV). Our past FL DEP projects can assist in management decisions for monitoring. For example, the development of targeted and effective qPCR primers and probes for PEI bacteria presages remediation plans by the Army Corps of Engineers (Army Corp of Engineers 2022). The presence of such microbes could indicate further shifts of the environment to more eutrophic and compromised "regimes" (Jouffray et al 2019). Local managers have been struggling to connect biological and physical measurements as well as parameters in the context of reef health. Our molecular microbiome data generated through FL DEP projects (PO # B6F91C and # C0FEDD) can be linked to recent and ongoing measurements from PEI such as recent local NOAA work (https://repository.library.noaa.gov/view/noaa/32102), as well as collaborations with Giarikos and Hirons NSU laboratories (Giarikos et al, 2023). Comparisons with other reefs, microbial diversity and their management should also be instructive. Connecting FL DEP priorities with NCRMP actions provides a strong synergy and substantial cost savings for field work. The comparative efforts have now provided potentially new diagnostic tools and markers that can help define healthy vs degraded reef habitats.

1.2 Hypotheses and Goals

The following hypotheses were posed for this project

- PEI- specific bacteria can be detected in reef sediments associated with inlet exposure
- PEI-specific microbe signatures will decrease in proportion to the distance from the port(s)
- Specific microbiome signatures will be found associated with specific parameters – eg. Less urbanized reef communities, or concentrations of specific heavy metals.
- PEI sediments will support less meiofauna compared to reef sediments

To address the hypotheses, we have collaborated with Dr. Brian Walker's GIS and Spatial Ecology Laboratory and generated the following goals for this project:

- Goal 1 (Task 2) – Develop novel qPCR probes for PEI-sourced microbes to track their dispersal and extent of distribution;
- Goal 2 (Task 3) – Characterize archived 2022 and novel 2024 NCRMP reef sediment samples using 16S microbiome, chemical analyses, and eukaryotic "eDNA" metabarcoding methods;
- Goal 3 (Task 4) – Examine the relationship between reef sediment microbiomes and environmental conditions

This project addressed the following FL DEP FY 2024-2025 CPR Research Priorities (Ecosystem Restoration, Disturbance Response, Water Quality)

I. This project will address the potential role of "environmental co-factors (e.g. land-based run-off and pollution; eutrophication, sedimentation and turbidity) potentially causing or exacerbating coral disease etiologies and recovery."

II. This project will attempt to "identify traits indicative of resistant and/or resilient corals and understand what parameters (physical, chemical, and/or biological; individual and/or synergistic; organismal and/or environmental) drive these factors. "

III. This project can help "identify and/or develop methodologies for bio-indicators, (at the organismal and microscopic level), that can be used to understand the impact of WQ parameters on FCR. "

IV. This project will "advance diagnostics related to coral diseases that are causing significant mortality, relative to other coral diseases, on Florida's Coral Reef as part of Disturbance responses."

2. METHODS

2.1. Sediment collections

Sediment samples were collected in conjunction with NCRMP sampling. NOAA's Coral Reef Conservation Program (CRCP) established the NCRMP, which is "a strategic framework for conducting sustained observations of biological, climatic, and socioeconomic indicators in U.S. states and territories. NCRMP stems from the NOAA Coral Reef Conservation Program (CRCP) established as an integrated and focused monitoring effort for the US" (Lopez 2023). Co-PI Brian Walker's GIS Spatial Ecology laboratory coordinated and conducted NCRMP surveys in 2022 and 2024.

Since NCRMP sites were randomly distributed, the team used the opportunity to collect small amounts of surficial sediments at the data collection sites throughout Miami-Dade, Broward, and West Palm Beach counties. Samples were collected by using a 15 ml Falcon tube to scoop from the top 5 cm of sediment. Once 10-12 ml of sediment was obtained, the tubes were placed in a mesh bag until the divers ascended at the conclusion of the dive. Samples were immediately transferred to a cooler with wet ice. At the conclusion of the day, all sediment tubes were transferred to a 4° C fridge in the Lopez MMG lab for processing.

Sediment sample collections occurred opportunistically from June 2022 through October 2022 (Figure 1) and from June 2024 through November 2024. As a result, the NSU MMG laboratory archived a total of 253 random sediment samples across the KJCAP: 171 samples in 2022 and 82 samples in 2024. The 171 samples for microbiome study represents 52% of a total of 325 sites sampled in 2022. These sites span around 160 km, ranging from sites near Jupiter Inlet in Palm Beach County to past Government cut in Miami-Dade County, and covers reef depths from 2 – 30 m. The full list of 2022 and 2024 NCRMP sites are shown in the Appendix.

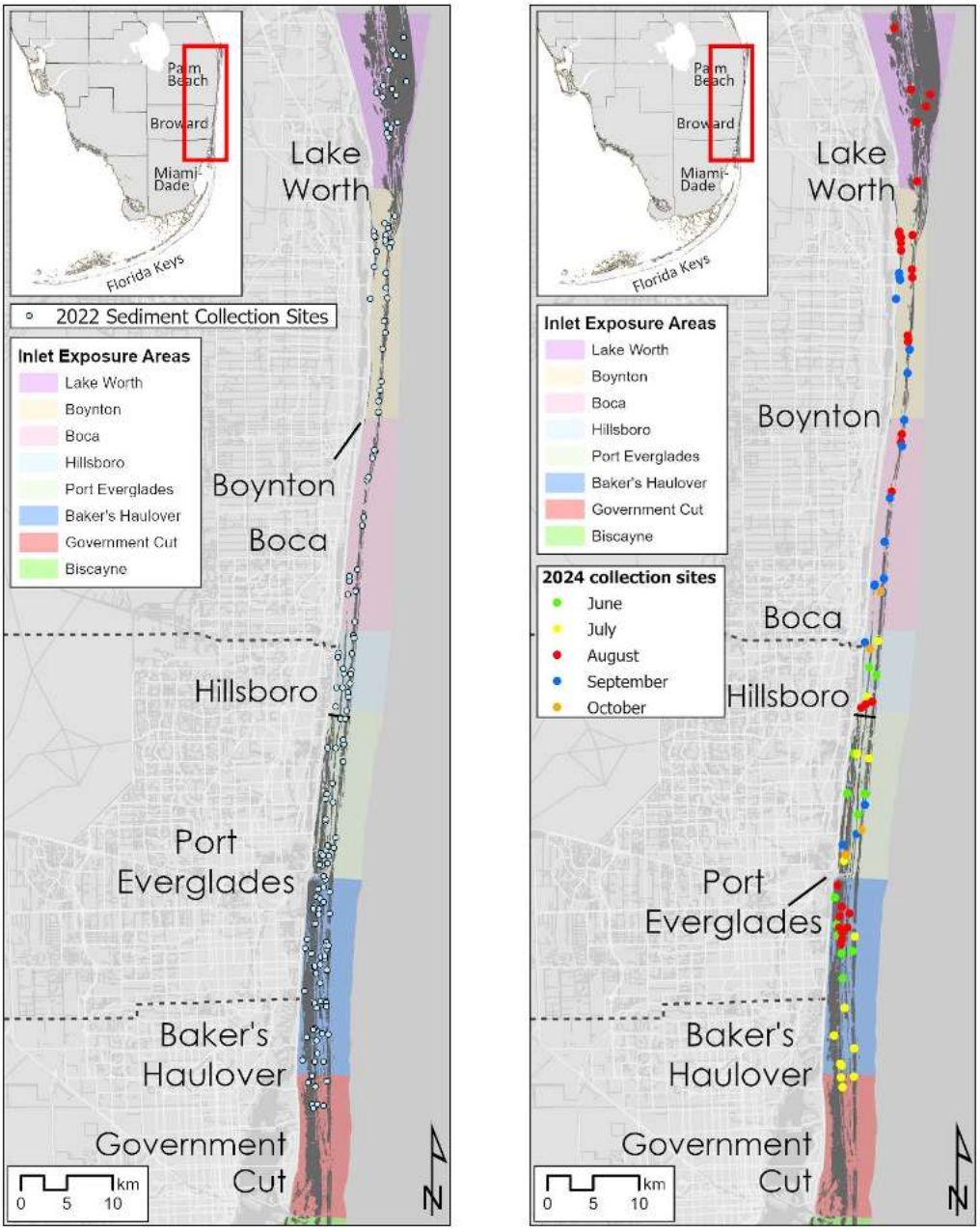

Figure 1- Map of the 2022 (left) and 2024 (right) sediment collection sites along the KJCAP. These sites are colorized by the month of collection highlighting that time of collection often corresponded to distinct sampling locations. Sites were also categorized by their spatially associated inlet exposure area where the coastline north of each inlet to the next inlet was considered to have the most exposure to the southern inlet's outflow based on hydrographic modeling (Walker et al. 2024). For example, all sites in the blue area between Baker's Haulover and Port Everglades were categorized as Haulover exposure.

Table 1 Reef habitat class abbreviations in the KJCAP based on Kilfoyle et al 2018

Map Habitat Class	Habitat Strata
Deep Ridge Complex	DPRC
Linear Reef-Inner	INNR
Linear Reef-Middle	MIDR
Linear Reef-Outer	OFFR
Ridge-Deep	OFFR (RGDP in Martin County only) *
Ridge-Shallow	NEAR
Other Delineations (Artificial, dredged inlets, sand borrow areas)	OTHR
Aggregated Patch Reef-Deep	PTDP
Aggregated Patch Reef-Shallow	PTSH
Patch Reef	PTSH <20m; PTDP >20m
Colonized Pavement-Deep	OFFR
Colonized Pavement-Shallow	NEAR
Unconsolidated Sediment	SAND
Scattered Coral/Rock in Sand	PTSH <20m; PTDP >20m
Seagrass	SGRS
Spur and Groove	OFFR
No Map Data	UNKW

*The Ridge-Deep was included in the OFFR strata for the southern portion of the reef tract. However, in Martin County, it was recognized as distinctly different and thus kept as a separate stratum.

Habitat class abbreviations are based on Kilfoyle et al 2018 shown in Table 1

2.2. Tracking PEI sourced microbes

2.2.1 Quantitative PCR (qPCR)

Specific PEI-only bacterial sequences have been used for qPCR primer design (Krausfeldt, Lopez et al, 2013). For example, we found higher abundances of Anaerolineaceae, Thiotrichaceae, Desulfobacteraceae, and Desulfobulbaceae bacteria in the PEI compared to reef sites. Novel qPCR primers of PEI-specific bacteria will be designed and then tested experimentally, starting with controls spiked into mixed genomic DNA cocktails to determine the lower limits of qPCR detection. Methods will follow standard protocols (Mougin et al 2020).

Briefly, previous DNA metagenomics reads were functionally classified using Enzyme Commission (EC) annotations. To identify genes that were enriched in top sediments of the port (sites DCC, PEC, PHQ) and not in the coral sediments (grabs and traps), Maaslin2 was implemented with linear model using abundances of genes (CPM). Genes that were identified to be missing from coral samples and only present in the port sites. Raw reads from the top sediments of the port were imported into Kbase for adapter removal using Trimmomatic v0.36, and then assembled with metaSPAdes v3.15.3. Assemblies were annotated with DRAM v0.1.2 to link genes unique to the port to the correct EC number and all genes representing that EC number were extracted. This generated a list of candidate genes for potential qPCR primers shown in Table 2 . These are genes with more details are available in this file "genes_and_sequences_unique_to_port.xlsx" in our shared project folders.

Table 2. List of candidate genes for potential qPCR primers. for potential qPCR primers

EC number	EC description	Associated KOID	KO description
2.4.2.48	.tRNA.guanine.15..transglycosylase	K18779	7-cyano-7-deazaguanine tRNA-ribosyltransferase
4.1.2.43	-hexulose-6-phosphate synthase	K08093	-hexulose-6-phosphate synthase
1.11.1.6	catalase	K03781	catalase: katE, CAT, catB, srpA
4.2.1.147	5,6,7,8-tetrahydromethanopterin hydro-lyase	K10713	5,6,7,8-tetrahydromethanopterin hydro-lyase
1.5.98.2	5,10-methylenetetrahydromethanopterin reductase	K00320	5,10-methylenetetrahydromethanopterin reductase
3.5.4.43	atzB; hydroxydechloroatrazine ethylaminohydrolase	K03382	atzB; hydroxydechloroatrazine ethylaminohydrolase
1.1.1.27	GDP-L-fucose synthase	K02377	GDP-L-fucose synthase
2.1.1.245	co-methyltransferase	K00194	acetyl-CoA decarbonylase/synthase, CODH/ACS complex subunit delta and gamma
2.1.1.245	co-methyltransferase	K00197	5-methyltetrahydrosarcinapterin---corrinoid/iron-sulfur protein Co-methyltransferase;

2.3. **Task 3: Microbiome analyses and metabarcoding**

2.3.1.1. Microbiome characterization by 16S rRNA sequencing

Because coral reefs are touted as one of the most biodiverse ecosystems on the planet, it behooves researchers to profile species composition and richness. Sequencing of bacterial communities ("microbiomes"), environmental DNA (eDNA) and infaunal metabarcoding can partly accomplish this, and over the past few years has become a powerful tool for monitoring reef ecosystem diversity (Shinzato et al, 2021; Lopez 2024).

Bacterial 16S rRNA gene amplicons were sequenced using standard Earth Microbiome Project protocols for the Illumina MiSeq platform routinely used in the MMG Laboratory (Thompson et al., 2017; Easson and Lopez 2019). The 515F and 806R primers amplified the ~300bp sequence of the V3 and V4 region of the 16S gene (Caporaso et al., 2011). Modified 16S primers were also applied (Apprill et al, 2015) . The PCR products were then cleaned using AMPure XP beads to purify the 16S V3 and V4 amplicon away from free primers and primer dimer species. The final DNA (and RNA) concentrations were checked to high precision using a Qubit® 4.0 Fluorometer and diluted to a normalization of 4 pM. All the samples were library pooled and then quality checked using an Agilent 4150TS Tapestation Bioanalyzer. The pooled DNA product were loaded into the Illumina MiSeq DNA sequencer in the MMG Laboratory for 16S rRNA sequencing using the *MiSeq* Reagent Kit *v3 at 6*00 cycles following a modified Illumina workflow protocol.

After bacterial 16S rRNA gene amplicon sequencing, the Quantitative Insights into Microbial Ecology v.2 (QIIME2) pipeline was applied to the raw sequences to demultiplex, quality filter, assign taxonomy, and reconstruct phylogeny. The QIIME2-generated sequences will be assigned taxonomy through a learned SILVA classifier (silva-132-99- 515-806-nb-classifier.qza). Moreover, alpha and beta diversity of bacterial microbiomes was assessed using the statistical software QIIME2 and R Studio following routine methods performed in the MMG laboratory of Halmos College of Arts and Sciences (HCAS) to produce diversity analysis and visualizations from the FASTQ DNA sequence files (Caporaso et al., 2010). Quality filtering and data trimming was conducted in DADA2 using the "dada2 denoise" command, which will then be used to create a feature-table.

The R Studio statistical software packages "vegan" and "phyloseq" 14aveolaed to assess diversity between samples (McMurdie & Holmes, 2012; Oksanen et al., 2013). Alpha

diversity, which describes the species richness and evenness within a sampling location, will be looked at for each sample. These were determined using multiple measures such as Observed and Chao1 for species richness estimators, Pielou's evenness index, and Shannon and Inverse Simpson indices for relative abundance diversity (Kim et al., 2017; Lande, 1996). Statistical differences between samples were calculated after normality determination using Shapiro-Wilks normality test, statistical differences between samples were calculated using Analysis of Variance (ANOVA) or Kruskal-Wallis one-way analysis of variance test (Krausfeldt and Lopez et al 2023).

The 16S rRNA ASV taxonomic data were used to compile basic statistics of the most abundant bacterial taxa across reef sites. In effort to find correlations to the 2022 bacterial communities at each site, the following environmental metadata were included in analyses and groupings –

- Temperature
- Habitat type
- Depth
- Geographic location (inner, middle or outer reef)
- Geographic location (county, inlet exposure area or IEAs – see discussion below)
- Hydrographic measurements
- Nutrients
- Trace metal concentrations

None of the above metadata were available for the 2024 NCRMP samples for this project and thus integrated analyses with 2024 NCRMP microbiome samples was not possible (and requires a post hoc Phase II). The samples were being collected during 2024 with no definite schedule for sampling completions, and so metadata integration with analyses of 2024 samples could not be included in the current results.

All 16S rRNA sequence data has been uploaded to local repositories at NSU, and also to the National Center for Biotechnology Information (NCBI) Short Read Archive (SRA) under NCBI BioProject number PRJNA1276599.

2.3.2. Eukaryotic metabarcoding

2.3.2.1.1.1. 18S rRNA sequencing

Eukaryotic metabarcoding has been established for marine habitats, but still remains a non-trivial task to set up (Leray et al, 2013; Pawlowski et al 2022). We applied an 18S rRNA sequencing approach previously described in survey of eukaryotic nekton in the Gulf of Mexico (Easson et al, 2020). The same genomic DNAs prepared for 16S rRNA microbiome analyses were used for 18S rRNA sequencing and eukaryotic metabarcoding.

2.3.2.1.1.2. Eukaryotic Metabarcoding with Cytochrome Oxidase I

Metabarcoding was performed by Jonah Ventures Inc., with their protocol partially shown here – https://jonahventures.com/faq/
Final indexed amplicons from each sample were cleaned and normalized using mag-bind normalization. A 15µl aliquot of PCR amplicon was purified and normalized using Cytiva SpeedBead magnetic carboxylate modified particles (#45152105050250). Samples were then pooled together by adding 5µl of each normalized sample to the pool.

Sequencing – Sample library pools were prepped for sequencing on an Oxford Nanopore Technologies MinION (Oxford, England) using the Ligation Sequencing Kit V14 (cat# SQK-LSK114). Final basecalling was completed using AWS Batch and EC2 g5.xlarge instances running ONT's dorado software (v0.7.1) in super high accuracy mode using the dna_r10.4.1_e8.2_400bps_sup@v5.0.0 basecalling model.

Bioinformatics – Raw Nanopore sequencing output was converted from pod5 to fastq format using dorado v0.7.1 [1] and the super-high accuracy basecalling model. Cutadapt v3.4 [2] was then used to trim outer adapters and reorient reads in a consistent 5' to 3' direction. The resulting reads were sorted into individual samples by demultiplexing with pheniqs v2.1.0 [3], allowing no more that one mismatch in each of the paired 10 bp molecular indices. Cutadapt was then used again to extract the target amplicon by removing the gene primers, discarding any reads where one or both primers were not found or where the resulting amplicon sequences were < 298 bp or > 328 bp. Exact sequence variants (ESVs) were then identified for each sample using the unoise3 denoising algorithm [4] as implemented in vsearch [5]. Only reads that were observed 4 or more times and with a maximum expected error rate [6] > 1 bp were considered as candidate ESVs and putative chimeras were filtered using the uchime3 algorithm [7]. Final read counts were determined for each sample by mapping unfiltered raw reads to the identified ESVs using the vsearch function usearch_global with an minimum identity of 95%. For each final ESV, a consensus taxonomy was assigned using a custom best-hits algorithm and a reference database consisting of publicly available sequences on NCBI GenBank [8], as well as Jonah Ventures voucher sequences records. Reference database searching used vsearch to conduct exhaustive semi-global pairwise alignments, and final match quality was quantified using a custom, query-centric approach, where the % match ignores terminal gaps in the target sequence, but not the query sequence. A consensus taxonomic assignment was then generated using either all 100% matching reference sequences or all reference sequences within 1% of the top match, accepting the reference taxonomy for any taxonomic level with > 90% agreement across the top hits.

2.4. **Nutrient and Trace Metal Analyses**

As part of Task 3 and in order to generate additional metadata, frozen NCRMP sediment samples were preserved at -20^{o}C and sent to Florida International University's CAChE Nutrient Analysis Laboratory for analyses of 16 trace metals and primary nutrients (Total Carbon -TC, Total Nitrogen-TN and Total Phosphorus-TP). The survey included the

following sixteen trace metals: Ag, As, Ba, Cd, Co, Cr, Cu, Pb, Hg, Mn, Mo, Ni, Se, Sn, V, and Zn.

This core facility is considered a NELAC-accredited nutrient analysis laboratory and will perform trace metal and dissolved carbon analyses of ECA reef sediments. All analyses will be performed according to the standard operating procedures used by the facility (https://environment.fiu.edu/facilities-research-groups/cache-nutrient-analysis-core/). For example, all samples for nutrient analyses will be prepared according to standard protocols written in Methods for Chemical Analysis of Water and Wastes (EPA-600/4-79-02, US EPA). The FIU CAChE Nutrient Analysis Core Facility's personnel, procedures, equipment, facilities, and quality system are in compliance with the requirements of FAC Rule 64E-1 and the 2016 NELAP Standards. The FIU CAChE Nutrient Analysis Core Facility was last accredited by the State of Florida Dept of Health, Bureau of Public Laboratories under Certificate #: E76930-34. TP values are given in ug/g (PPM). Percentages of N and C can be easily converted to ppm by multiplying the values by 10000 (1%=10000ppm).

2.5. **Task 4-Examining the relationship between reef sediment microbiomes and environmental conditions**

Multivariate analysis was conducted in Primer 7 (Clarke and Gorley, 2006). Spatiotemporal variation in the microbiome was statistically analyzed using Permutation Analysis of Variance (PERMANOVA; Anderson, 2001; McArdle and Anderson, 2001) and PERMDISP. Prior to the generation of Bray–Curtis similarity coefficients, data were square root transformed to reduce the influence of dominant bacterial families. Then a type 3 Permanova was performed with 9999 permutations of residuals under a reduced model to assess differences in centroid position. Variation in the microbiome was assessed in two models: spatial (Inlet contributing area and Strata) and spatiotemporal (Inlet contributing area and Month), as the 3-way model with all factors was too complex. Multivariate results were considered significant at $p < 0.05$. Permdisp was used to assess variation in dispersion from centroids in each factor and was performed with 9999 permutations. Any samples that were obvious outliers in the data were removed prior to analysis, leaving 157 microbiome samples.

Four types of environmental data (spatial, temperature, nutrients and heavy metals) were quantified at each NCRMP site to capture the environmental regime at the time of sample collection. The spatial factors latitude, longitude, depth, distance from the shoreline and distance from the nearest inlet were measured. The temperature regime at each NCRMP site was calculated from daily measured in situ data in a two-step process. First, the daily temperature over the previous year was estimated at each NCRMP site using a spatial join with nearby SECREMP (Southeast Florida Coral Reef Evaluation and Monitoring Project) sites where temperature data is recorded using Hobo v2 temp loggers. The type of spatial join between NCRMP sites and temperature data from SECREMP sites was determined by the distance between sites. If an NCRMP site was within 2 km of a SECREMP site, the temperature data at the SECREMP site was used, if the NCRMP site was 2 to 10 km then the mean of the closest two SECREMP sites was used, if the NCRMP site was greater than 10 km from a SECREMP

site then the mean of the nearest three SECREMP sites was used. Second, after estimating the daily temperature at each NCRMP site, multiple variables were calculated which were predicted to influence the microbiome at the time of sampling. These temperature variables included the maximum, mean and standard deviation of daily water temperatures prior to sample collection calculated at various temporal durations (the previous day, over the previous week and over the previous month). Further, the thermal extreme history at the site was quantified as both the heat stress duration over the prior year (number of days in situ water temperature was 1 °C above the maximum of the mean summertime (July-September) SST (see Jones et al. 2020)) and the Degree heating weeks (DHW) at the time of sampling, which were obtained from NOAA's Coral Reef Watch (NOAA CRW 2018). The heat stress threshold was calculated as 30.79 °C. Nutrient and heavy metal concentrations were measured in the sediment samples used to identify the microbiome by the Florida International University CAChE Nutrient Analysis Core Facility. The FIU CAChE NELAC laboratory applied Method Detection Limits (MDL) and Practical Quantitation Limits (PQL) approved and effective as of 08/01/2022 for water quality constituents.

Once the environmental regime was calculated for each sample and prior to data analysis, the predictors were tested for collinearity by calculating the Spearman's rank correlation coefficient, which is well suited to assess non-linear relationships and data which are non-normal. Correlations were considered significant at a threshold of 0.7 and one of the collinear predictors removed prior to statistical analysis. Longitude was correlated with depth and latitude and removed. The site temperature the day before sample collection was correlated with the maximum temperature 1 week prior, the mean temperature 1 week prior and the mean temperature 1 month prior, and with each other, and only site temperature retained. Heat stress duration was correlated with DHW and DHW removed as it is primarily a coral metric. The heavy metals/elements Arsenic, Beryllium, Copper, Chromium, Mercury, Molybdenum, Silver and Vanadium were removed either due to high correlation with other predictors (e.g., Arsenic, Chromium) and/or a high number of missing samples (e.g., Beryllium, Copper, Molybdenum, Silver, Vanadium). This left 19 environmental predictors: latitude, depth, distance from the closest inlet, distance from shore, Site temperature the previous day, max temperature the previous month, temperature SD the previous week, temperature SD the previous month, heating stress duration, Total Nitrogen, Total Phosphorus, Total Carbon, Cadmium, Cobalt, Lead, Nickel, Selenium and Zinc.

To assess the influence of these environment predictors on the microbiome a distance-based linear model (DISTLM) was conducted. Prior to analysis, all environmental predictors were visually assessed for normality to conform with assumptions. All environmental predictors except Barium, Lead and Selenium concentration were square root transformed. All environmental predictors were then normalized (each sample subtracted from the mean and divided by the standard deviation for the variable) for comparability of scale. The DISTLM analysis was performed under the BEST selection procedure with 9999 permutations and the best model determined using the corrected Akaike Information Criterion (AICc) from all possible combinations of environmental predictors. In the event that multiple models had equivalent AICc's (i.e., < 2 difference between models; Burnham and Anderson, 2004), the simplest model

with the fewest predictor variables was selected as the model which explained the most variation in the microbiome. Environmental predictors identified as particularly important in marginal tests (i.e., $p \leq 0.01$) were included in the final model if AICc scores were equivalent. The most parsimonious model was ordinated using distance-based redundancy analysis (dbRDA; Legendre and Anderson, 1999), where each point represented the microbiome in each sample and vectors represent either the origin of differences in the microbiome or the environmental predictors which explain the variation.

3. RESULTS/DISCUSSION

3.1 *Quantitative PCR of selected NCRMP samples.*

3.1.1. Task 2 – Testing of novel qPCR primers for PEI-sourced microbes

Before testing the designed PEI-primers using qPCR methods, end-point PCR was conducted to verify that the primers will amplify PEI DNA, which were used to create the primers. These are shown in Appendix 6.3 NCRMP samples were also run to test the hypotheses that port bacteria could be detectable on reefs. After running a 1% agarose gel electrophoresis to view the PCR products of the primers, the PEI samples (Port PHQ and Port PEC) successfully amplified with the primers while the NCRMP samples (NCRMP 3112, NCRMP 3190, NCRMP 3045 – see Appendix 6.1) did not amplify (Figure 2).

Although the primers were unsuccessful in amplifying using endpoint PCR, we applied them in qPCR trials to determine whether the extra sensitivity of the latter would enable detection. Figures 2- 3 show the standard curves for the two sets of qPCR primer amplifying the genes for catalase and hexulose, respectively. Within both curves, the efficiency (E%) is considerably above 110%, indicating that there was a presence of inhibitory factors which could include multiple factors such as poor DNA quality, excessive DNA concentration, or the accumulation of PCR reaction inhibitors. In qPCR, the combination of a standard curve and a melt curve is used to effectively assess the performance of a set of qPCR primers. Unfortunately, we were only able to generate the melt curve for the hexulose primer set (Figure 3). The melt curve depicts two general peak ranges, 70-75°C and 80-90°C, when only one peak is expected. Those peak ranges suggest the formation of primer-dimers during the PCR process**.**

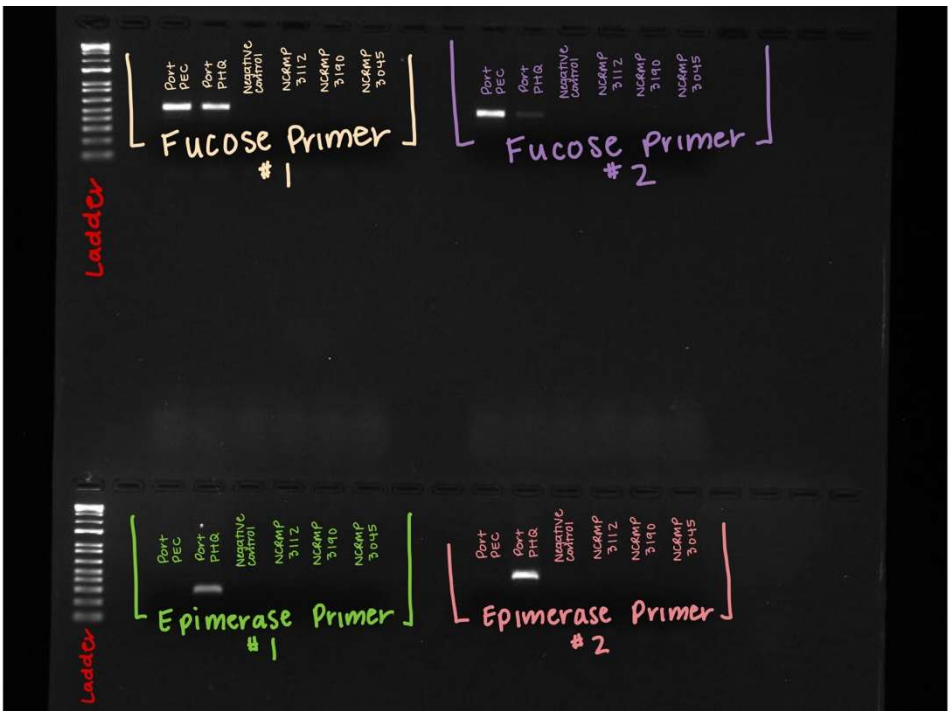

Figure 2 PCR results for two different genes with four sets of qPCR primers.Above each band resolved by agarose gel electrophoresis is the source DNAs based on previous core sampling: Port Everglades Inlet (PEI), Park Education Center (PEC), Park Headquarters (PHQ), or South Turning Basin (STB). Gene sequences were derived from PEI-specific DNA sequences. Other numbered lanes designate reef samples from the NCRMP sample sites described in Appendix 6.1.

Figure 3. PCR results for two different genes, catalase and hexulose. Sample designations are similar to those in Figure 2.

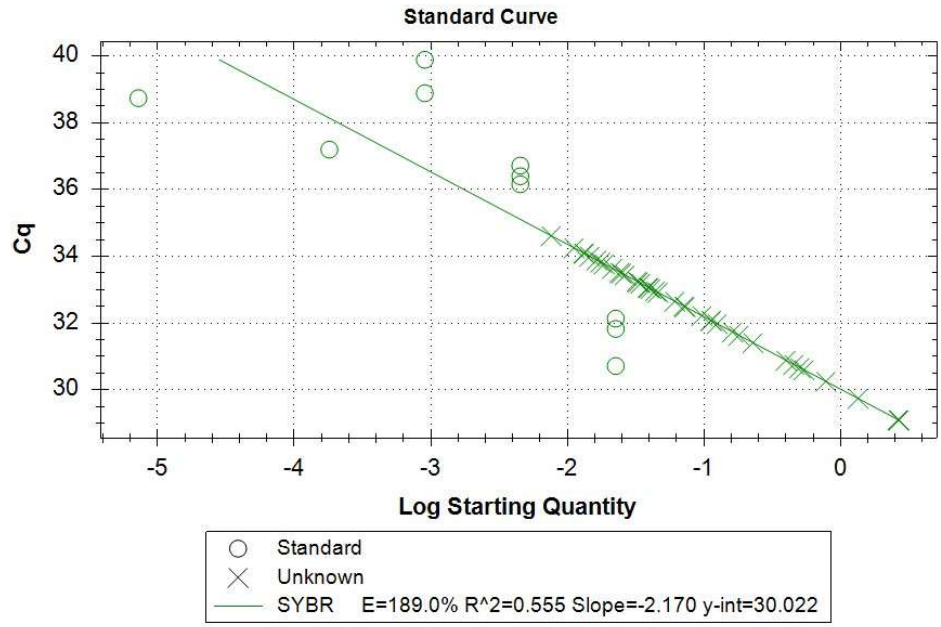

Figure 4. Example of qPCR standard curve with catalase gene data. Points depicted using an "X" signify the triplicate replicates of 12 samples used for testing the primer. Point depicted using an "O" signify the triplicate replicates of 6 serial dilution standards to create the curve.

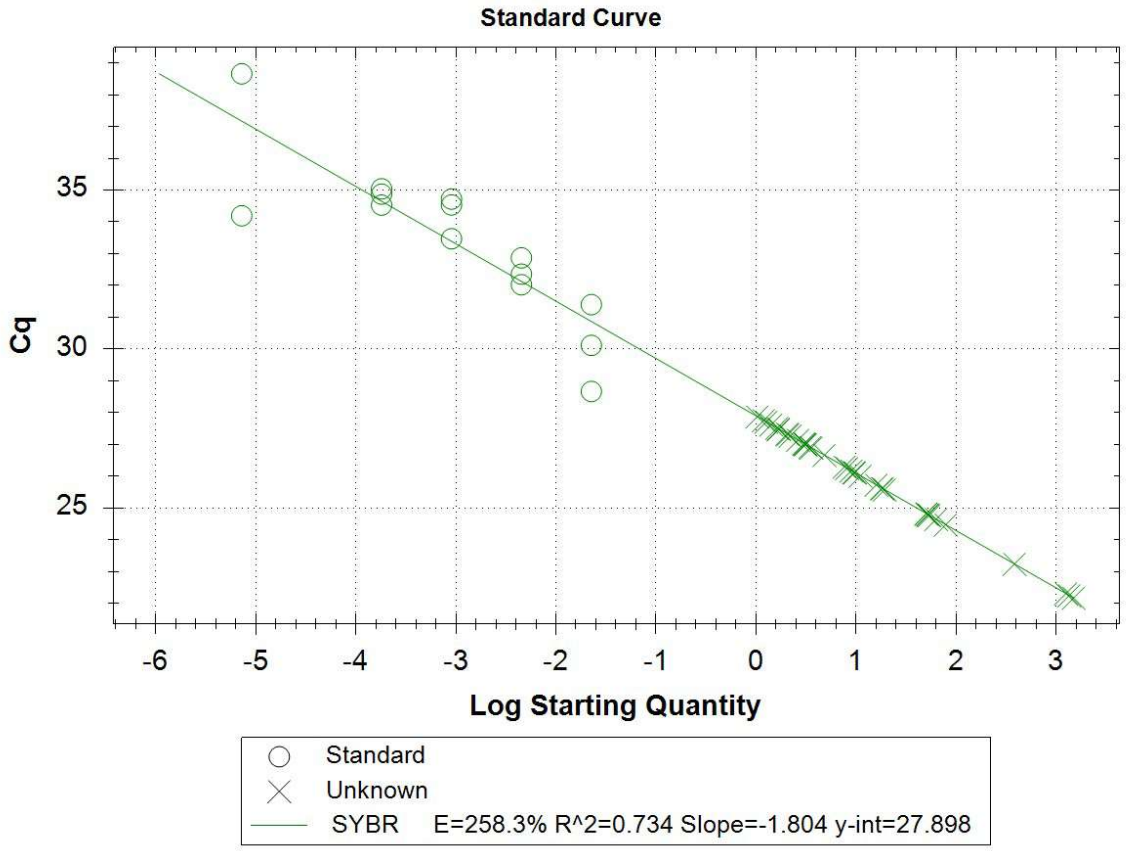

Figure 5.qPCR standard curve for hexulose. Points depicted using an "X" signify the triplicate replicates of 12 samples used for testing the primer. Point depicted using an "O" signify the triplicate replicates of 6 serial dilution standards to create the curve.

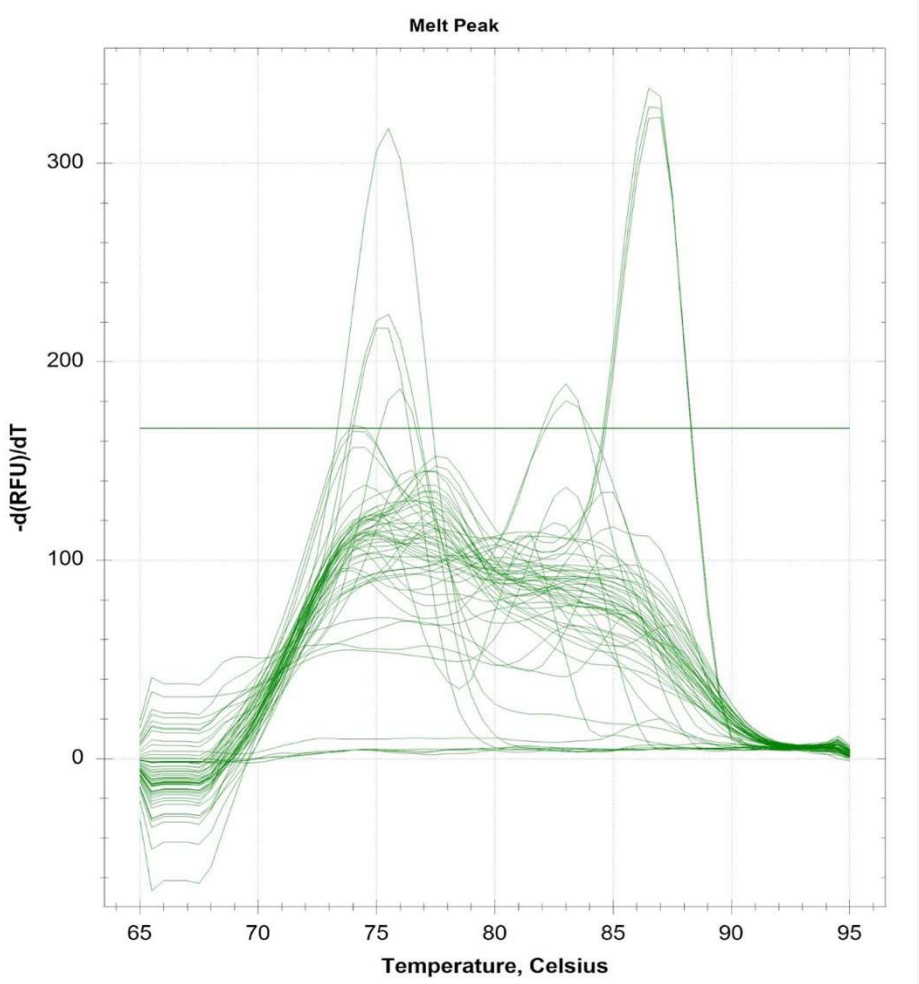

Figure 6. Hexulose gene qPCR melt curve.All curved lines depicted here represent both standards and samples run during qPCR.

3.2 Bacterial microbiome sequencing and analyses of 2022 and 2024 NCRMP samples

3.2.1 16S rRNA sequences and analyses

This activity encompassed Task 3, which characterized archived 2022 and novel 2024 NCRMP reef sediment samples using 16S microbiome, chemical analyses, and eukaryotic "eDNA" metabarcoding methods. The microbiomes of 2022 and 2024 KJCAP sediment samples were sequenced and characterized for 283 samples according to standard protocols and required three different Illumina MiSeq DNA sequencing runs. Sequencing read statistics of 2022 NCRMP sediment samples were as follows: 13,499,364 total reads generated, average of 82,313 reads per sample, and 12,596 ASVs identified. Sequencing reads statistics of 2024 NCRMP sediment samples were as follows: 12,326,000 total reads generated, average of 171,194 reads per sample, and 45,893 ASVs identified.

Full taxonomic profiles of the 2022 16S rRNA data are in these tables of shared drives and called

"taxonomy_168_NOEUKS.csv", and "NCRMP2022_Top20Families_PerSample B".

It is not possible to visualize all microbial taxa in the 2022 dataset (e.g. 12,596 ASVs), and moreover, most bacterial genera and species are in very low proportions (< 0.1%). Thus, to provide quantitative views of KJCAP microbial diversity, relative abundances of the most the most common (top 15 – 20) bacterial taxa across the KJCAP are shown in the following relative abundance stacked bar charts (Figures 7 – 15). These graphs are presented in the context of taxonomic ranking (phylum, family and genera), though 16S rRNA sequences generally do not resolve to the bacterial species level. Also, the top abundances are shown with respect to various environmental metadata groupings (such as habitat type, strata, or the closest inlet).

Alpha diversity measurements were performed, but no significant differences were found between any major groupings above, including county or depth. Moreover, no obvious major microbial patterns were observed, though we were surprised to see several sites with a dominance of genus *Bacillus* (Figure 9), which is not a typical marine bacterial taxon. This same prevalence was not observed in the 2024 microbial dataset, and so we suspect that some of the *Bacillus* identifications are due to more contamination in 2022 (Figure 13).

Canonical Correspondence Analysis (CCA) analyses of the ASV data (Figures 16 – 19) integrates metadata with each microbiome sample and the results supported the general lack of significant correlation for many environmental variables. A secondary analyses followed up in section 3.3.2 and found some significance with respect to temperatures, as well as zinc and arsenic. This will be discussed in greater length in the Conclusion in section 4.

Among rarer taxa, we also identified *Porticoccus* ASVs known to be associated with white plague II disease consortia in *Orbicella aveolate* (Sunagawa et al, 2009). It was interesting to see the appearance of Filomicrobia and related Hyphomicrobia genera, as these are known as facultative methylotrophs capable of growth on reduced C_1 compounds such as methanol, methylated amines or formate (Rainey et al, 1998).

The finding of multiple incidences of *Ruegeria* (Family *Rhodobacteraceae*) in the KJCAP datasets was promising (Figure 13), since this genus has been indicated as a beneficial coral symbiont and potential probiotic (Kitamura et al, 2021; Peixoto et al, 2021).

The presence of PEI-dominant bacteria was detected in 16S rRNA data and taxonomic signatures of reef sediment samples. Dominant bacterial taxa first identified at PEI such as Anaerolineaceae, Thiotrichaceae, Desulfobacteraceae, and Desulfobulbaceae, appeared at fairly high relative abundances at most of inlets except northern most Jupiter inlet (Figures 20-21). This suggests common microbial activities at distinct inlets and ports. Of course, many of these functions remain to be described for their potential impacts on reefs.

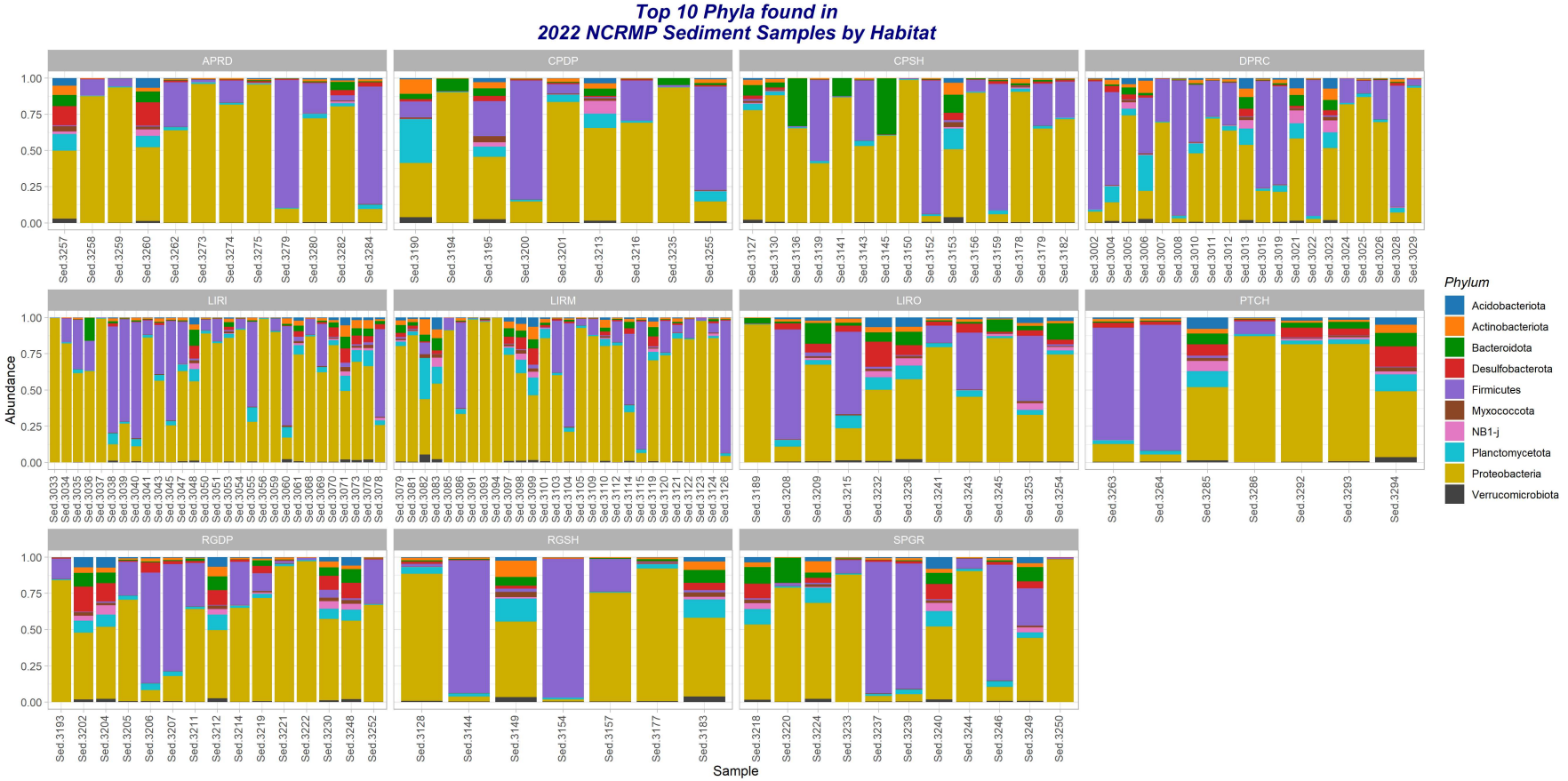

Figure 7. Relative abundances of Top 10 bacterial phyla from NCRMP 2022 samples found at various KJCAP reef habitats. Relative abundances of Top 10 bacterial phyla from NCRMP 2022 samples found at various KJCAP reef habitats. Habitat codes are shown in Table but also repeated here DPRC – Deep Ridge Complex; INNR - Linear reef Inner; MIDR - Linear reef Middle; OFFR - Linear reef Outer; PTCH – Patch Reef; APRD – Aggregated patch reef Deep; CPSH Colonized Pavement – Shallow ; CPSD Colonized Pavement – Deep; PTCH – Spur and Groove; RGDP – Ridge Deep; RGSH – Ridge Shallow

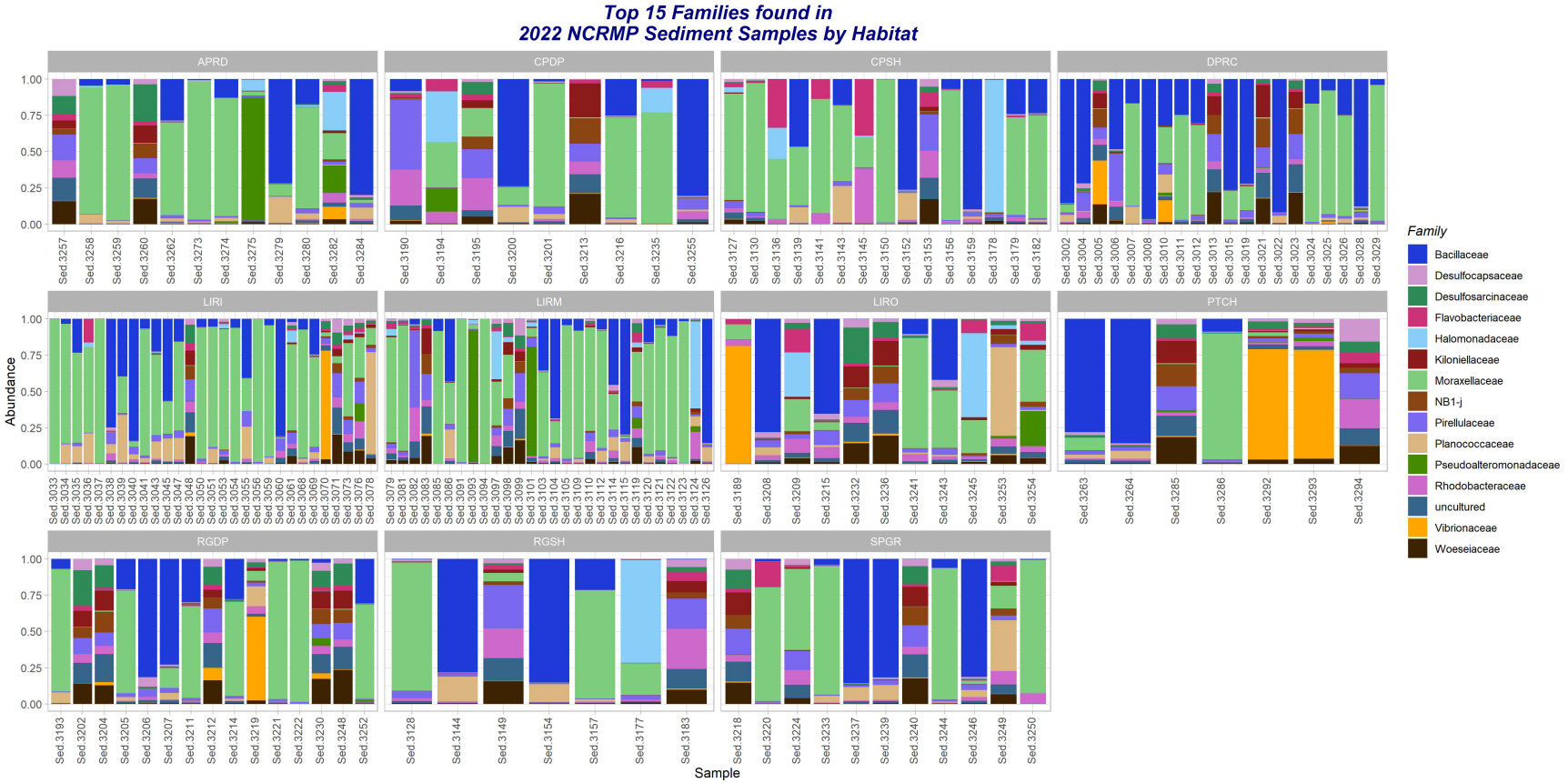

Figure 8.Relative abundances of Top 15 bacterial families from NCRMP 2022 found at various KJCAP reef habitats. Habitat codes are shown in Table but also repeated here DPRC – Deep Ridge Complex; INNR - Linear reef Inner; MIDR - Linear reef Middle; OFFR - Linear reef Outer; PTCH – Patch Reef; APRD – Aggregated patch reef Deep; CPSH Colonized Pavement – Shallow ; CPSD Colonized Pavement – Deep; PTCH – Spur and Groove; RGDP – Ridge Deep; RGSH – Ridge Shallow

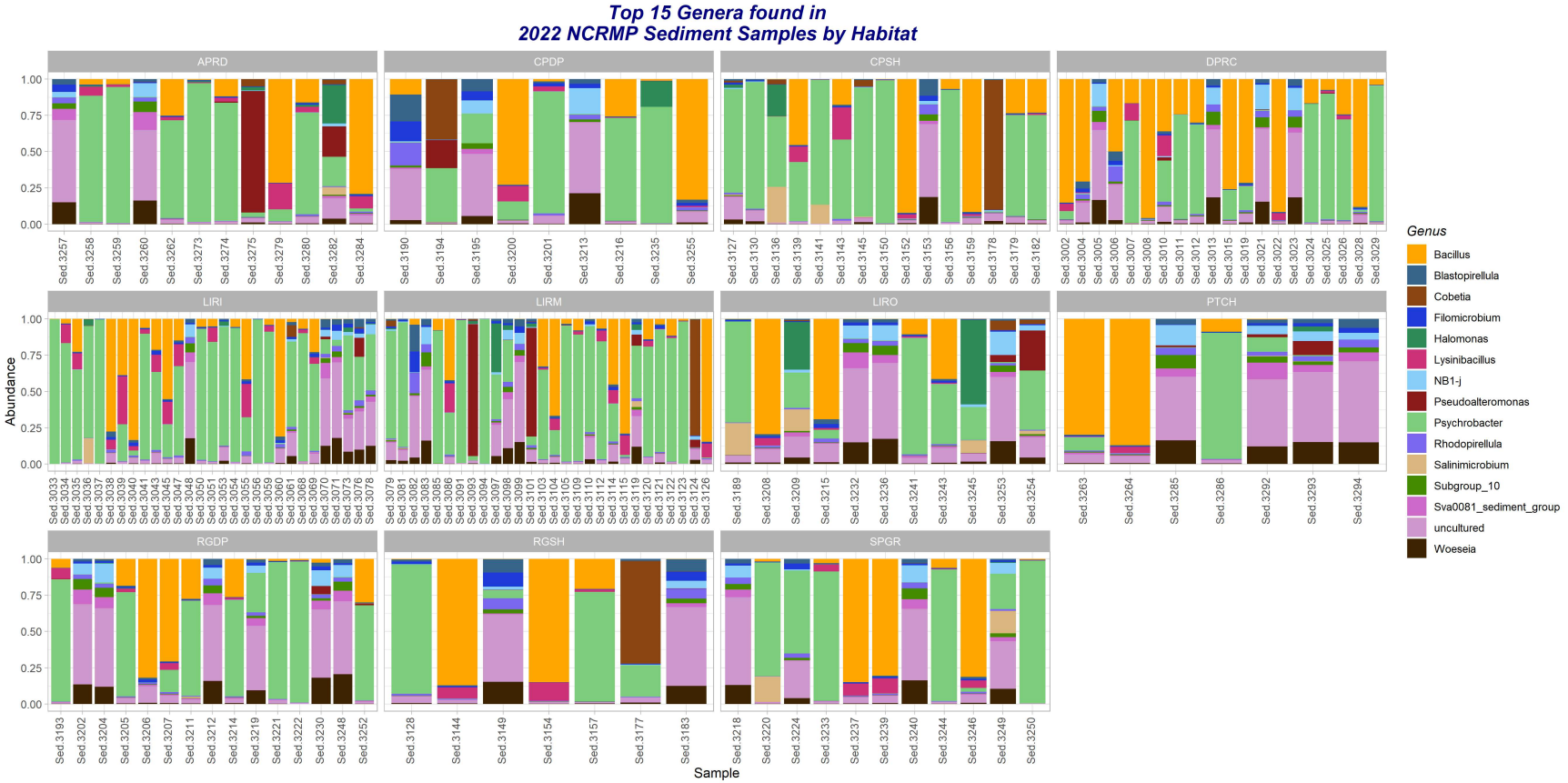

Figure 9.Relative abundances of Top 15 bacterial genera from NCRMP 2022 found at various KJCAP reef habitats. Habitat codes are shown in Table but also repeated here DPRC – Deep Ridge Complex; INNR - Linear reef Inner; MIDR - Linear reef Middle; OFFR - Linear reef Outer; PTCH – Patch Reef; APRD – Aggregated patch reef Deep; CPSH Colonized Pavement – Shallow ; CPSD Colonized Pavement – Deep; PTCH – Spur and Groove; RGDP – Ridge Deep; RGSH – Ridge Shallow.

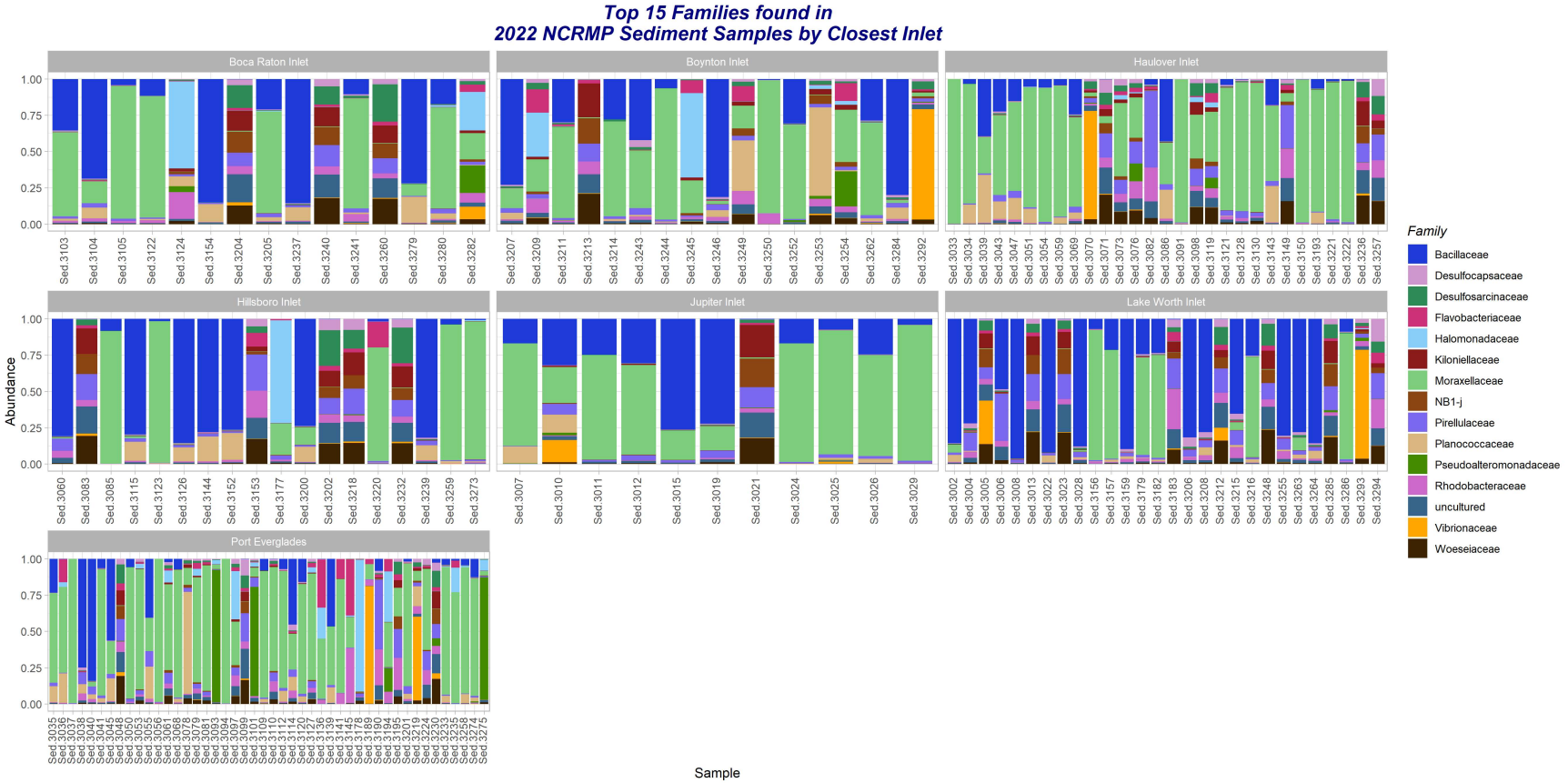

Figure 10.Relative abundances of Top 15 bacterial families from NCRMP 2022 found at sites closest to inlets. This includes Jupiter, Lake Worth, Boca Raton, Boynton, Haulover, Hillsboro, and Port Everglades.

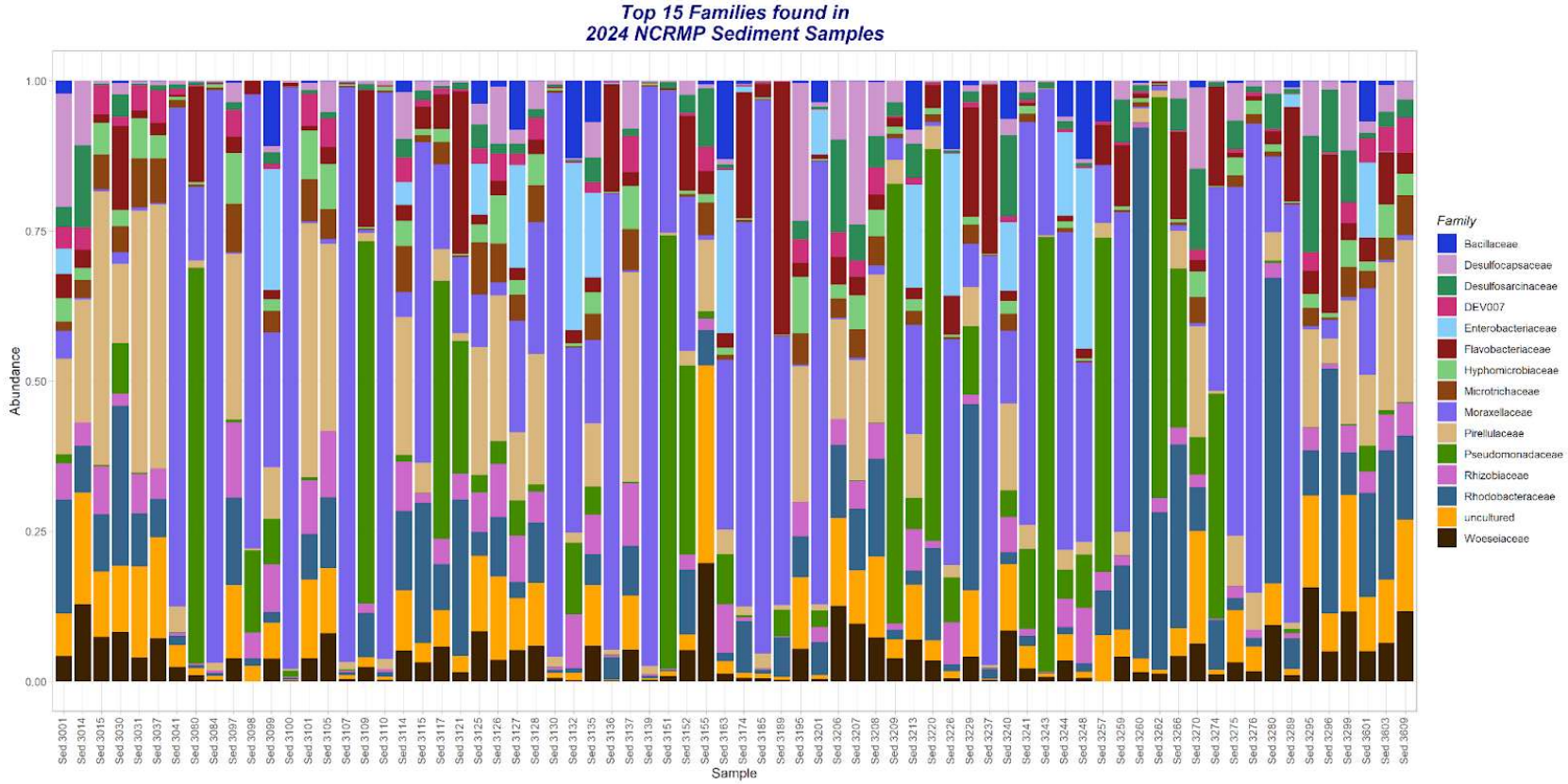

Figure 11.Top 15 families found in 2024 NCRMP sediments

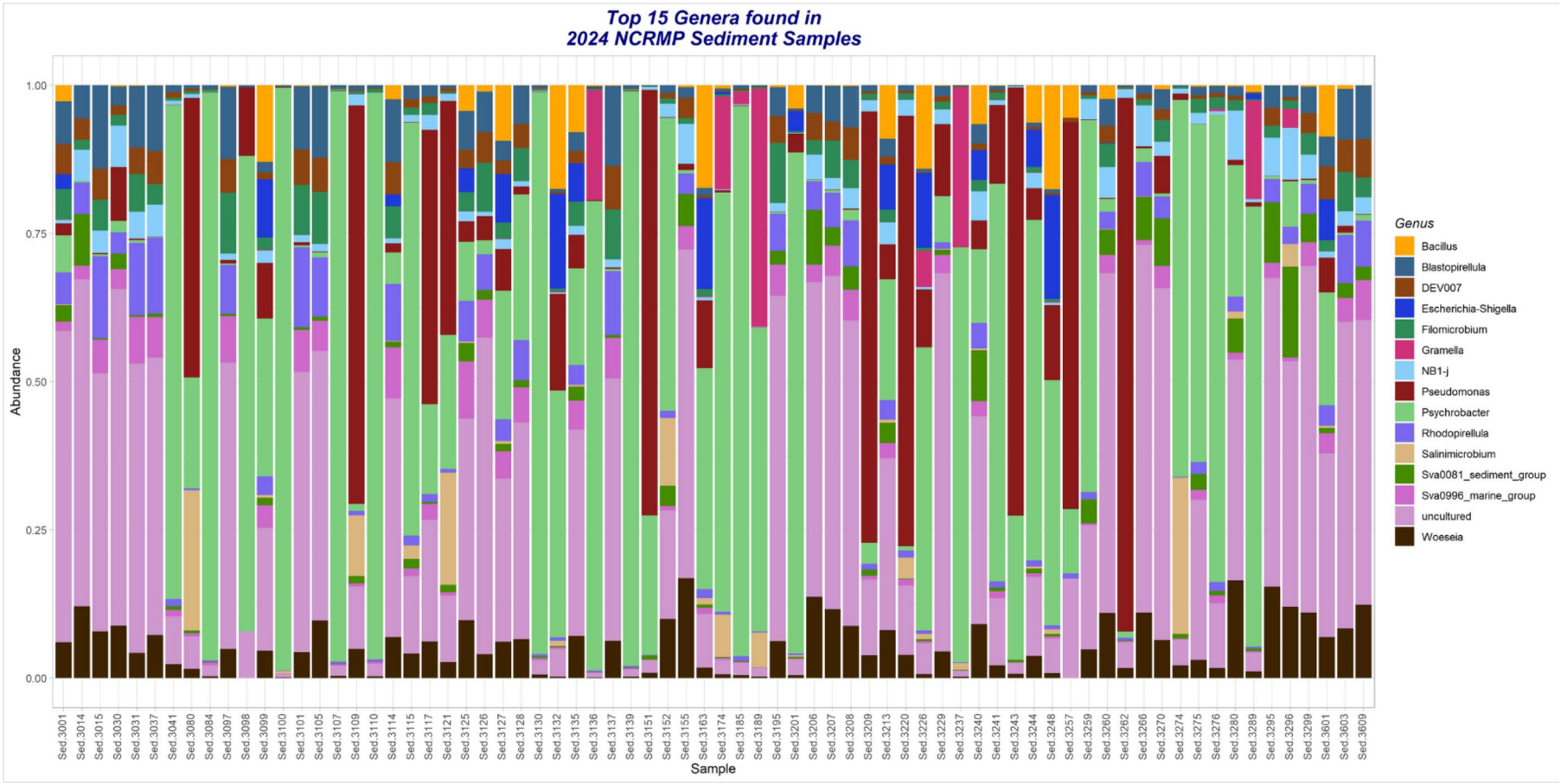

Figure 12. Top 15 genera found in 2024 NCRMP sediments

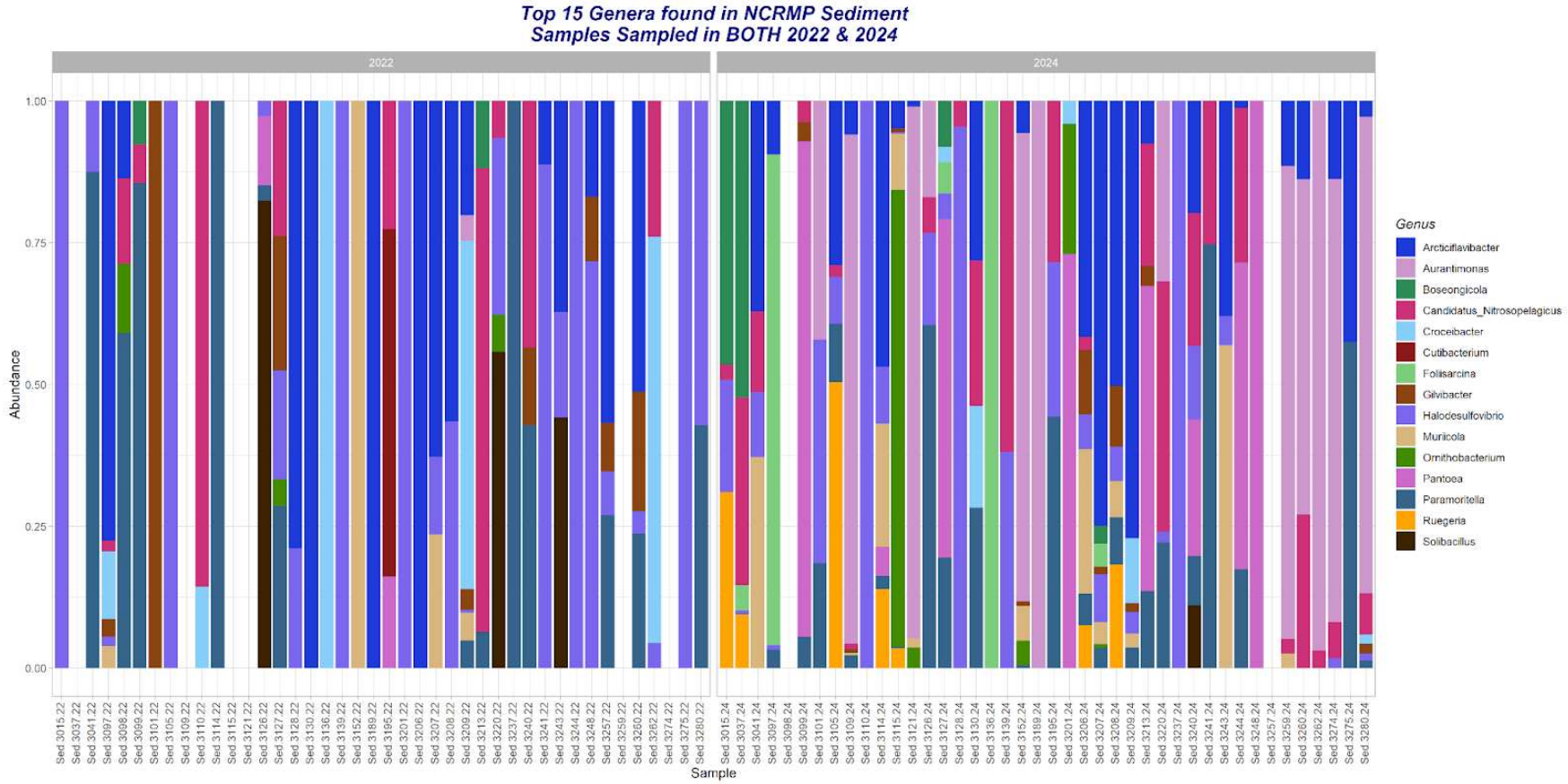

Figure 13. Top 15 genera found in both 2022 and 2024 NCRMP sediments

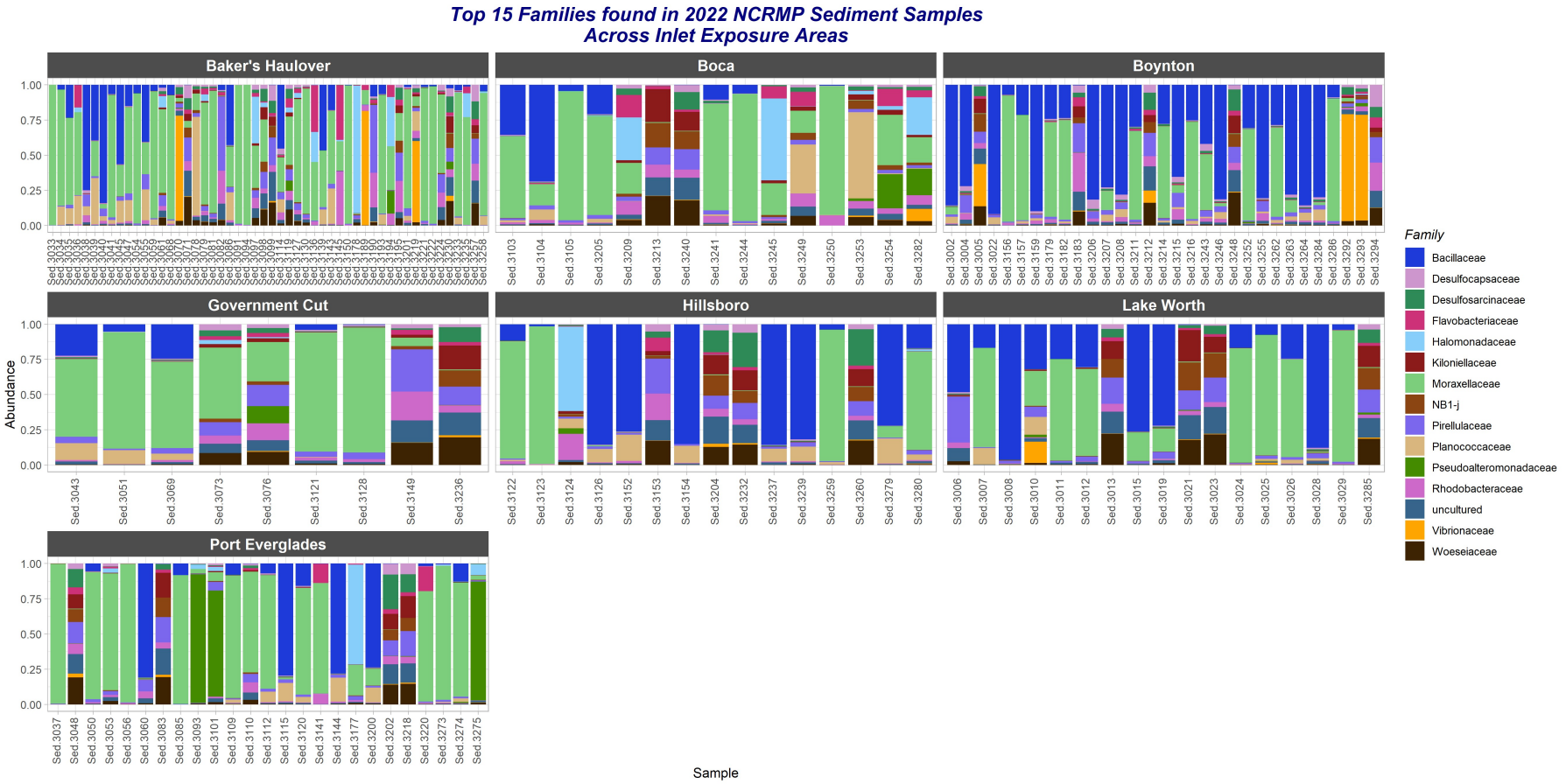

Figure 14. Top 15 families associated with specific Inlet Exposure Areas (IEAs) from NCRMP 2022

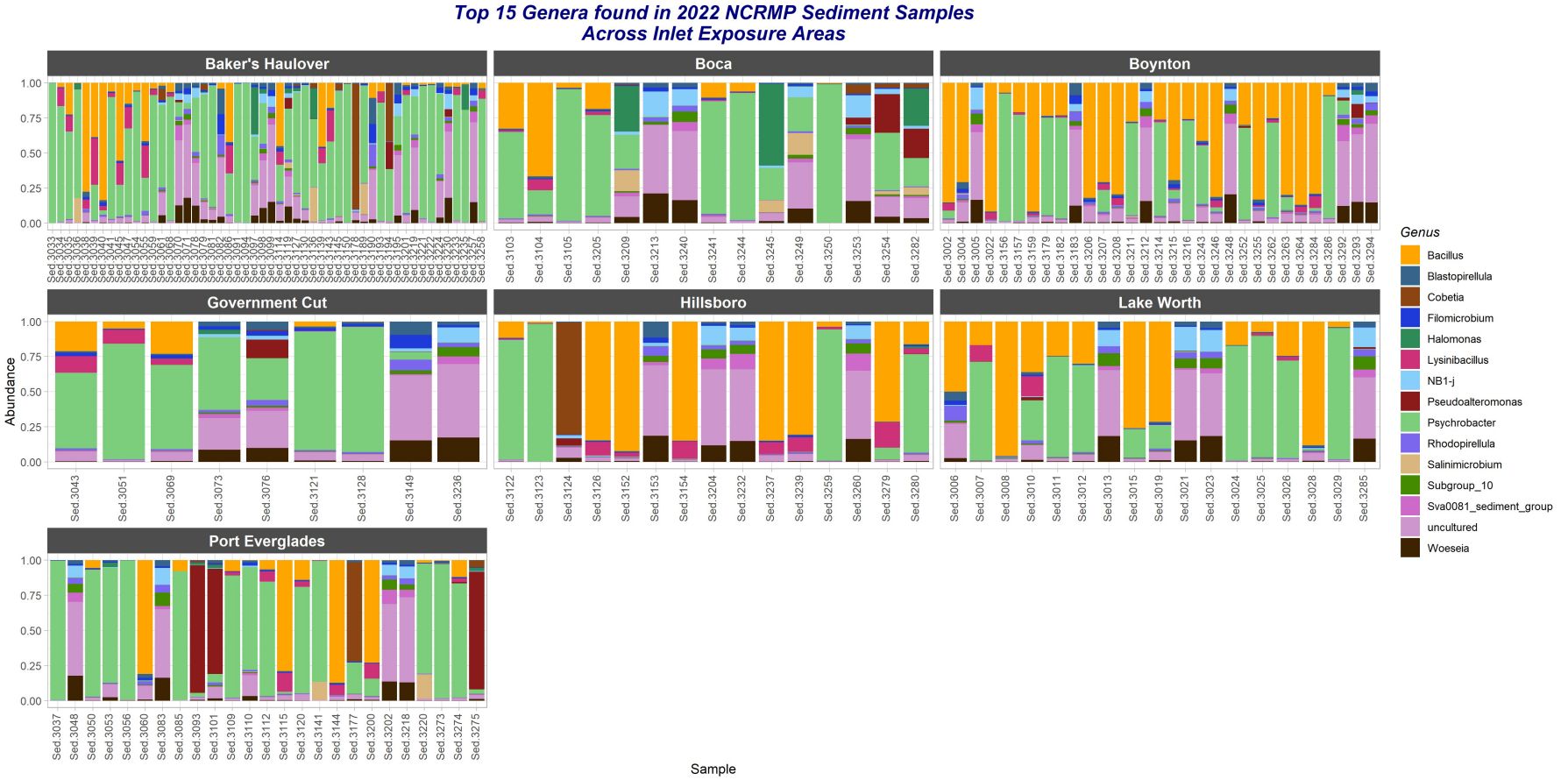

Figure 15. Top 15 genera associated with specific Inlet Exposure Areas (IEAs) from NCRMP 2022.

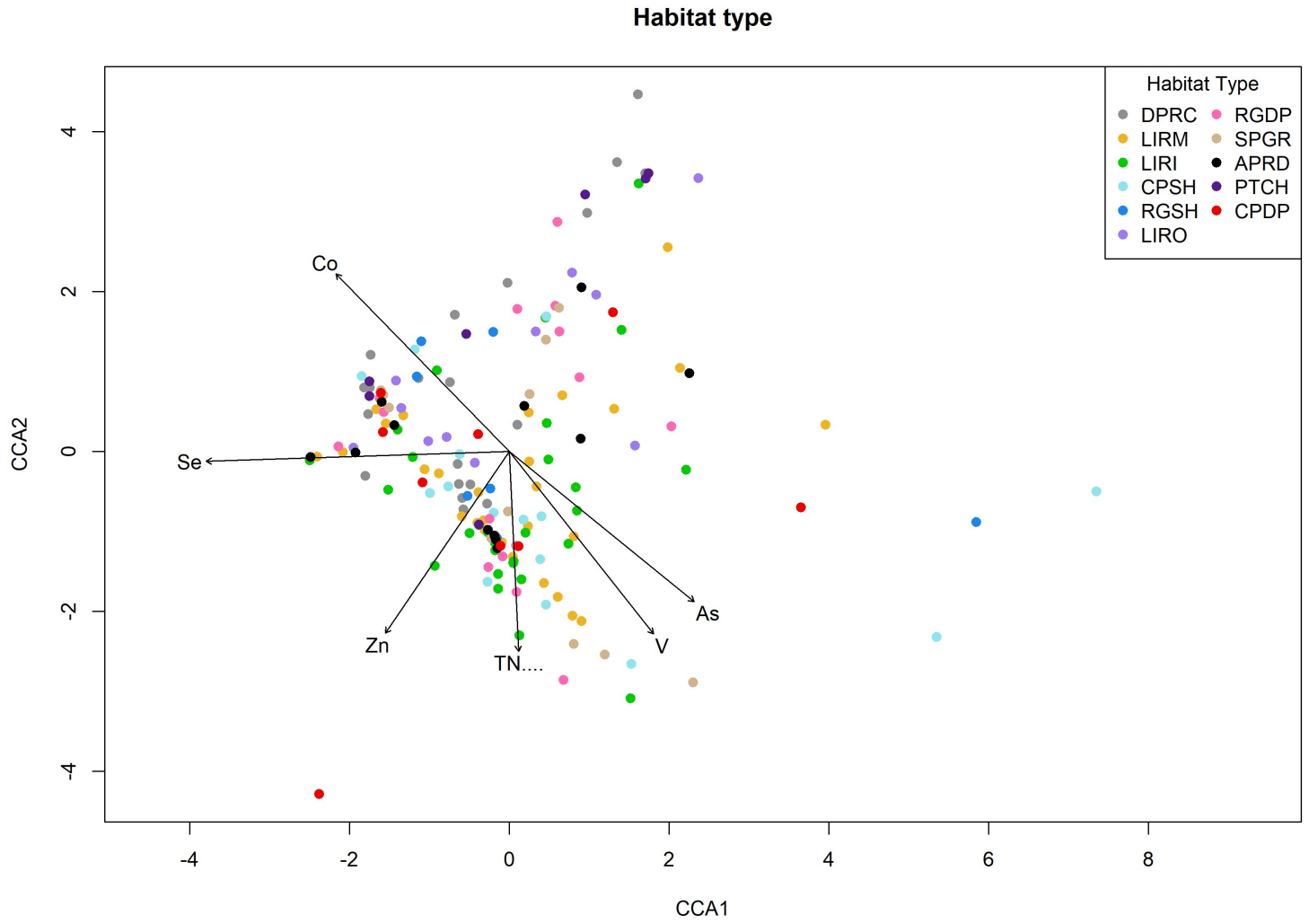

Figure 16. A Canonical Correspondence Analysis (CCA) plot of 16S rRNA data from NCRMP 2022 and most significant environmental metadata in the context of habitat types. (Oksanen et al., 2020). Colors represent the origins of the different sampling types shown in Table 1.

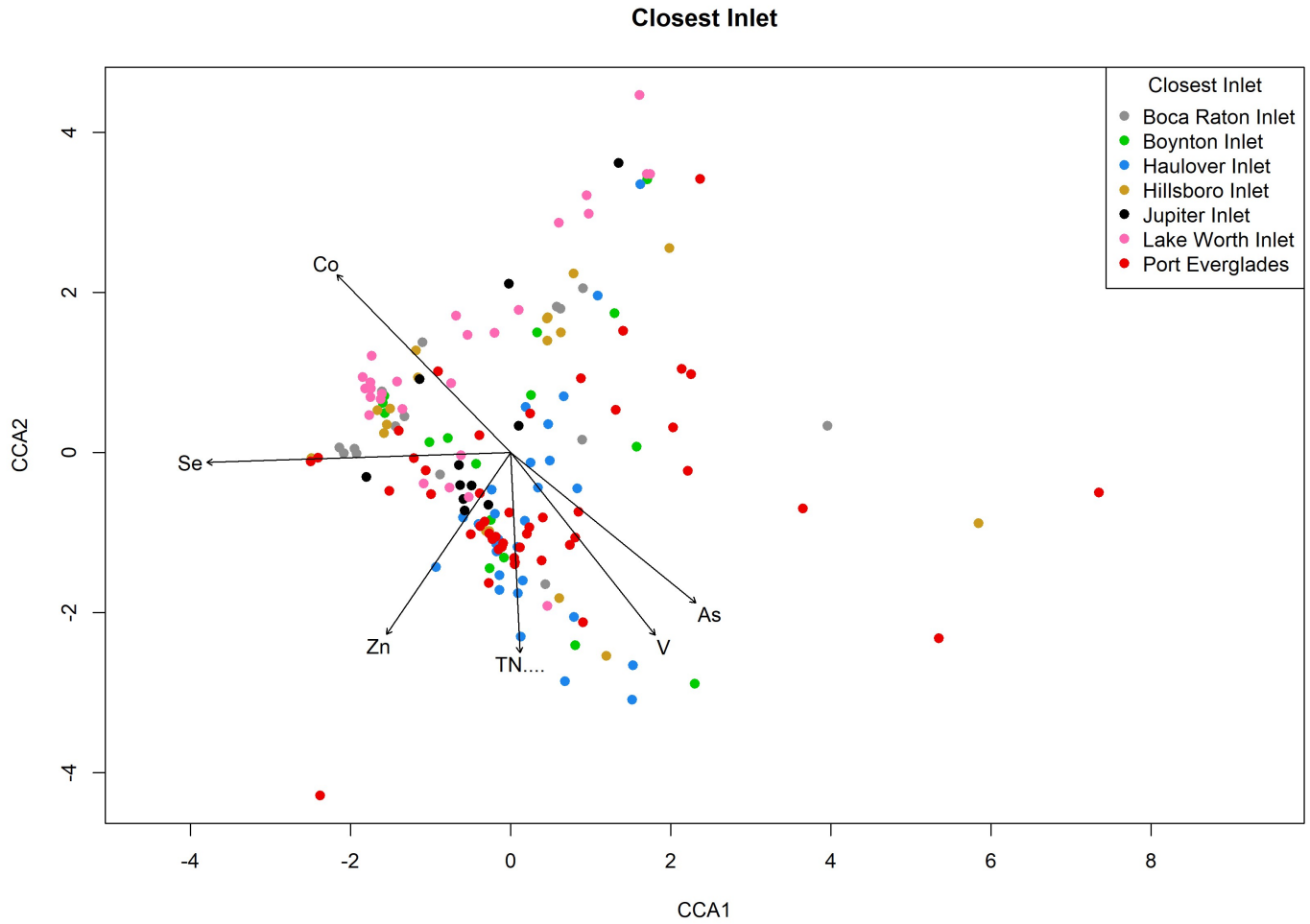

Figure 17. A Canonical Correspondence Analysis (CCA) plot of 16S rRNA data and most significant environmental metadata in the context of distance from closest inlet. (see Table 1 for key to abbreviations and Appendix 1 for sample IDs).

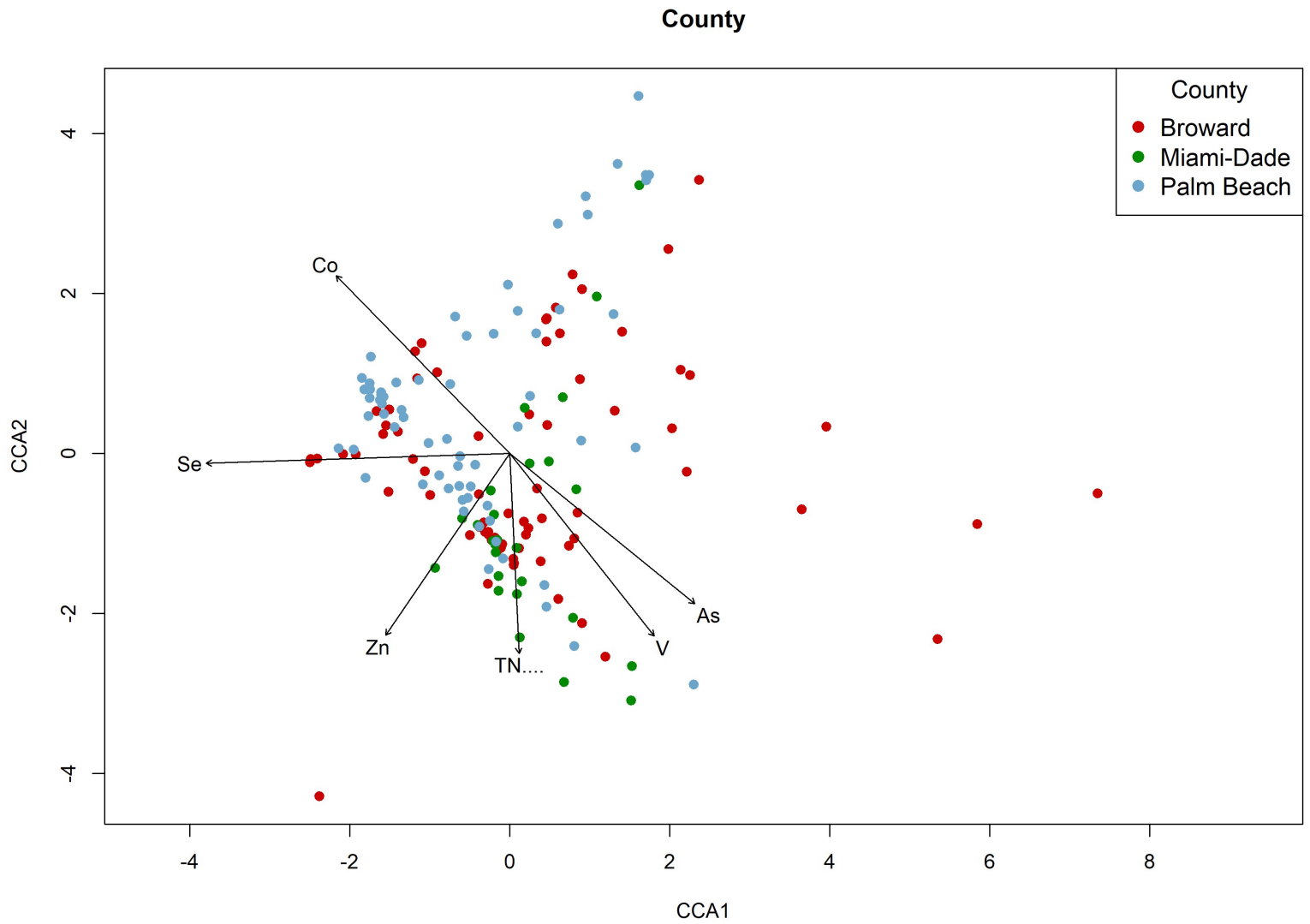

Figure 18. A Canonical Correspondence Analysis (CCA) plot of 16S rRNA data and most significant environmental metadata based on county of origin.

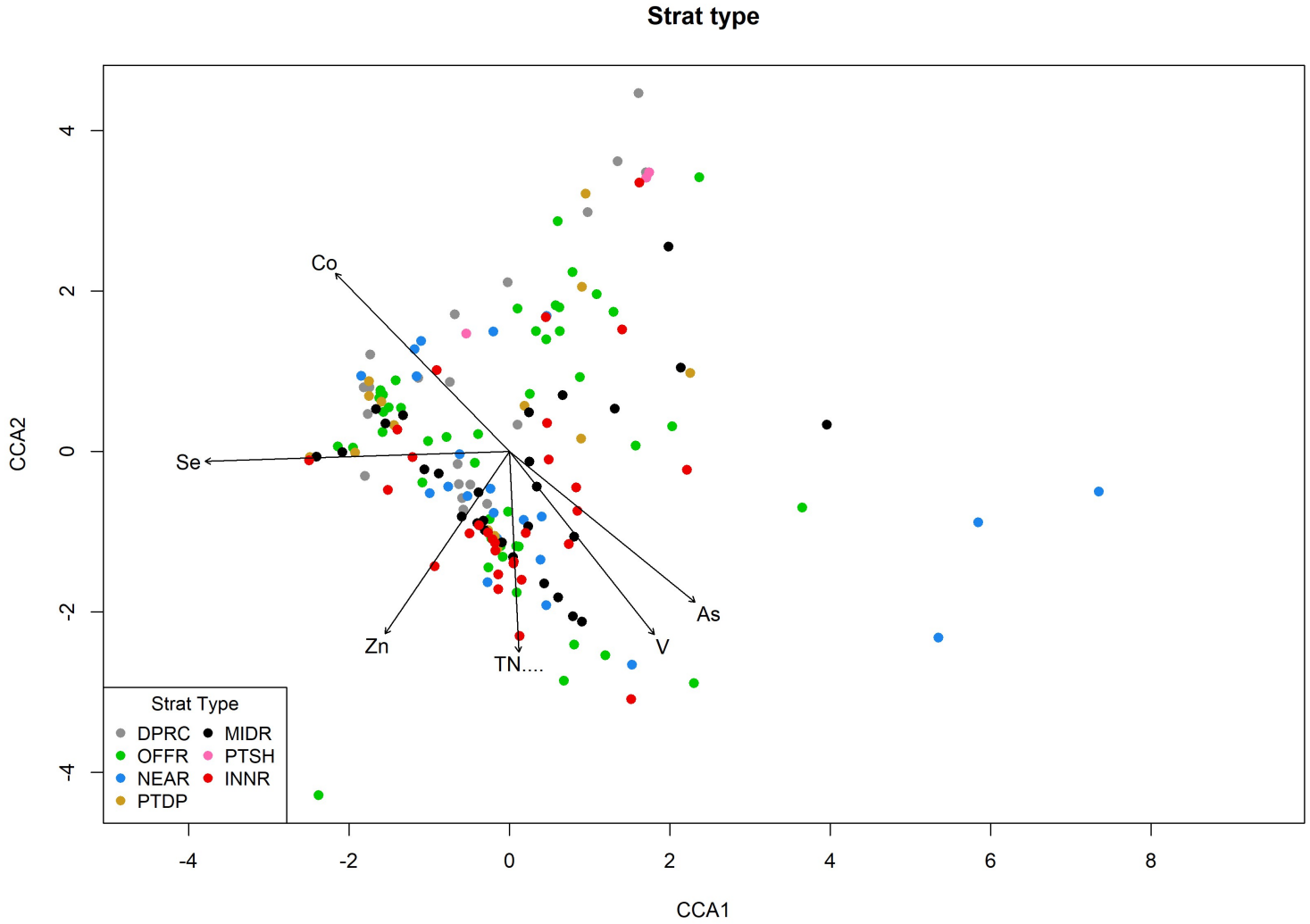

Figure 19. A Canonical Correspondence Analysis (CCA) plot of 16S rRNA data from NCRMP 2022 and most significant environmental metadata based on strata type.

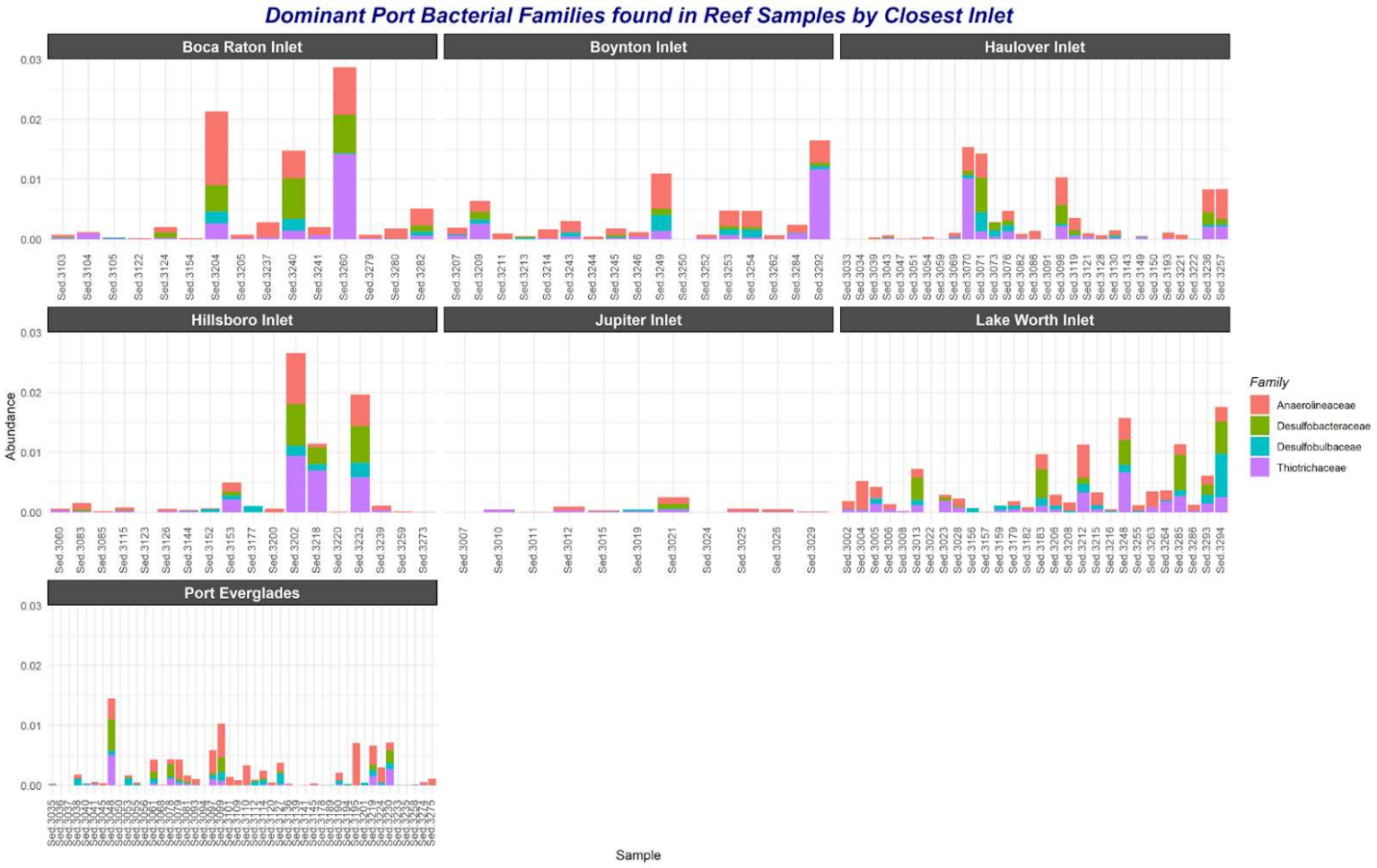

Figure 20. Dominant port bacterial families found in 2022 sediment samples by nearest inlet..

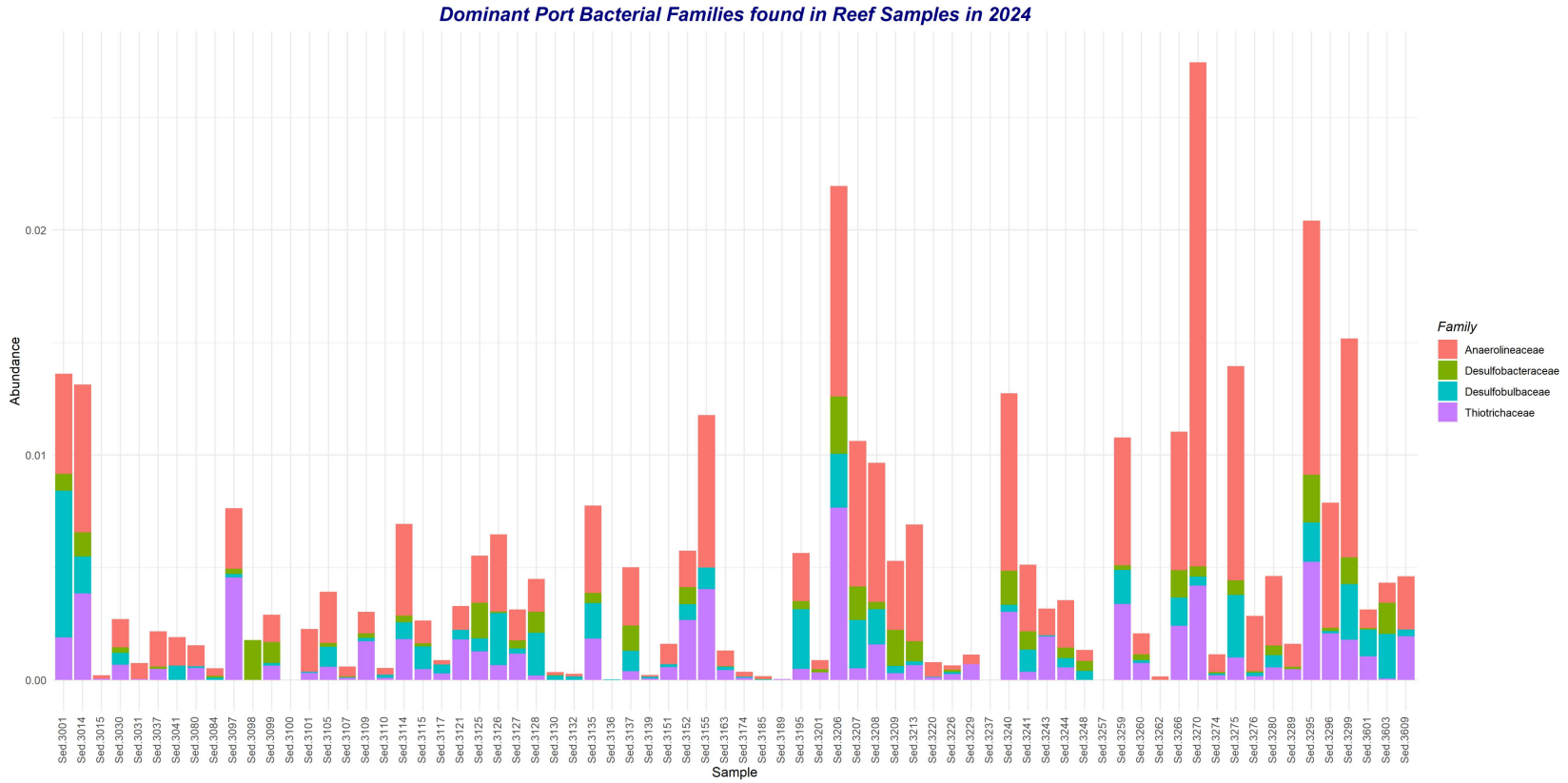

Figure 21. Dominant port bacterial families found in 2024 sediment samples by nearest inlet.

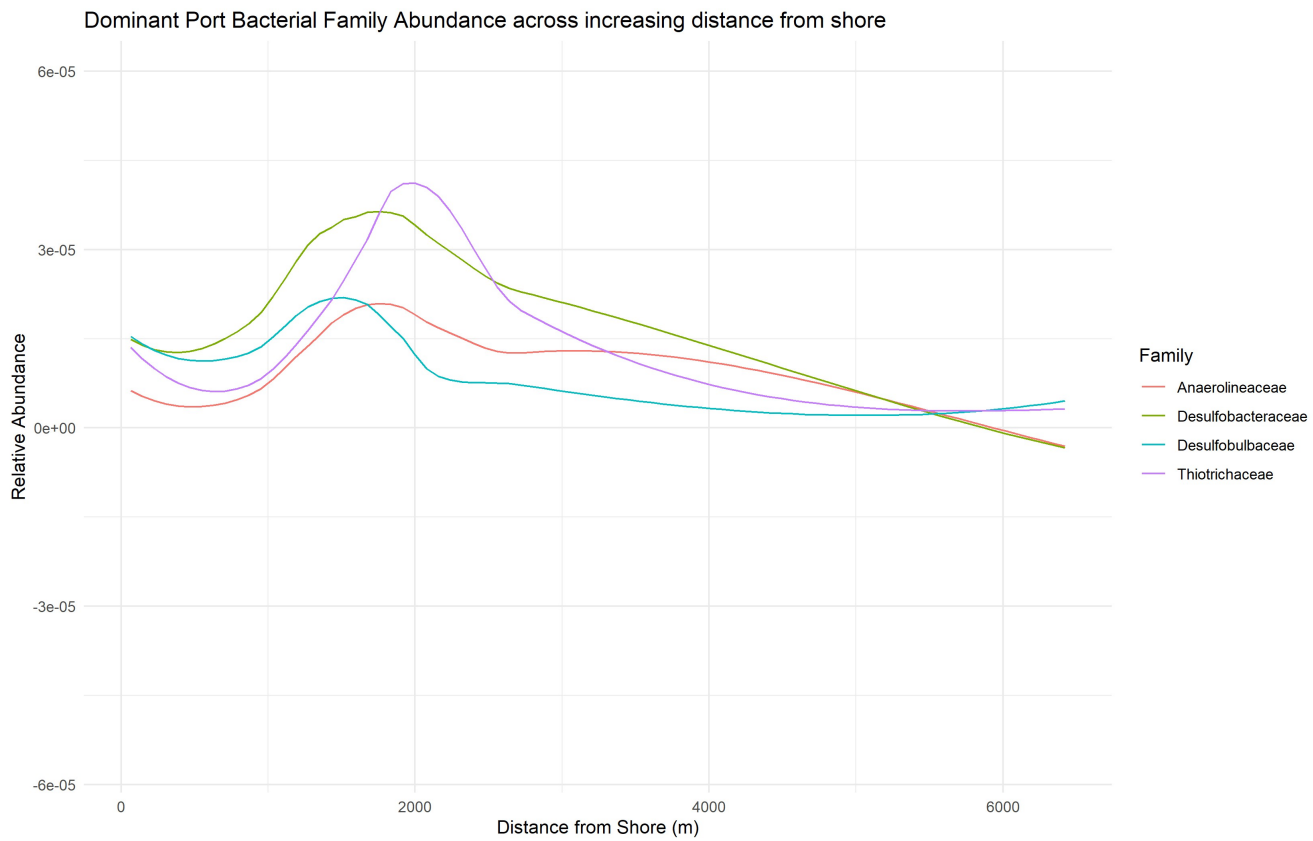

Figure 22. Relative abundances of four dominant port bacterial families based on distance from shore based on 16S rRNA data. Microbial families stem from a previous Port Everglades Inlet study (Krausfeldt et al., 2023)

3.2.2 Eukaryotic metabarcoding of selected samples.

The orders, Peronosporales (1,617 entries) and Pythiales (1,026 entries) are water molds and interestingly occurred within the top 5 eukaryotic entries in the total COI dataset. These organisms mainly constitute saprophytic detritovores. At the phylum level, water molds appeared 3x more likely than Cnidaria. Metabarcoding results identified 39 unique phyla, 352 unique orders and 1,254 unique eukaryotic families (Figure 23). The finding of matches to Lepidoptera in a marine habitat is curious, but could indicate that no suitable matches for an arthropod exist for the particular query sequences. Peronosporaceae and Pythiaceae are typically pathogenic water molds.

Phyla:

- Arthropoda — 8,734 entries
- Oomycota — 3,099 entries
- Bacillariophyta — 2,654 entries
- unk_phylum — 1,526 entries
- Cnidaria — 1,042 entries

Orders:

- Diptera — 2,321 entries
- Naviculales — 1,871 entries
- Lepidoptera — 1,730 entries
- Peronosporales — 1,617 entries
- Pythiales — 1,026 entries

Families:

- Peronosporaceae — 1,615 entries
- Pythiaceae — 1,021 entries
- Sellaphoraceae — 821 entries
- Pinnulariaceae — 683 entries
- Desmodoridae — 571 entries

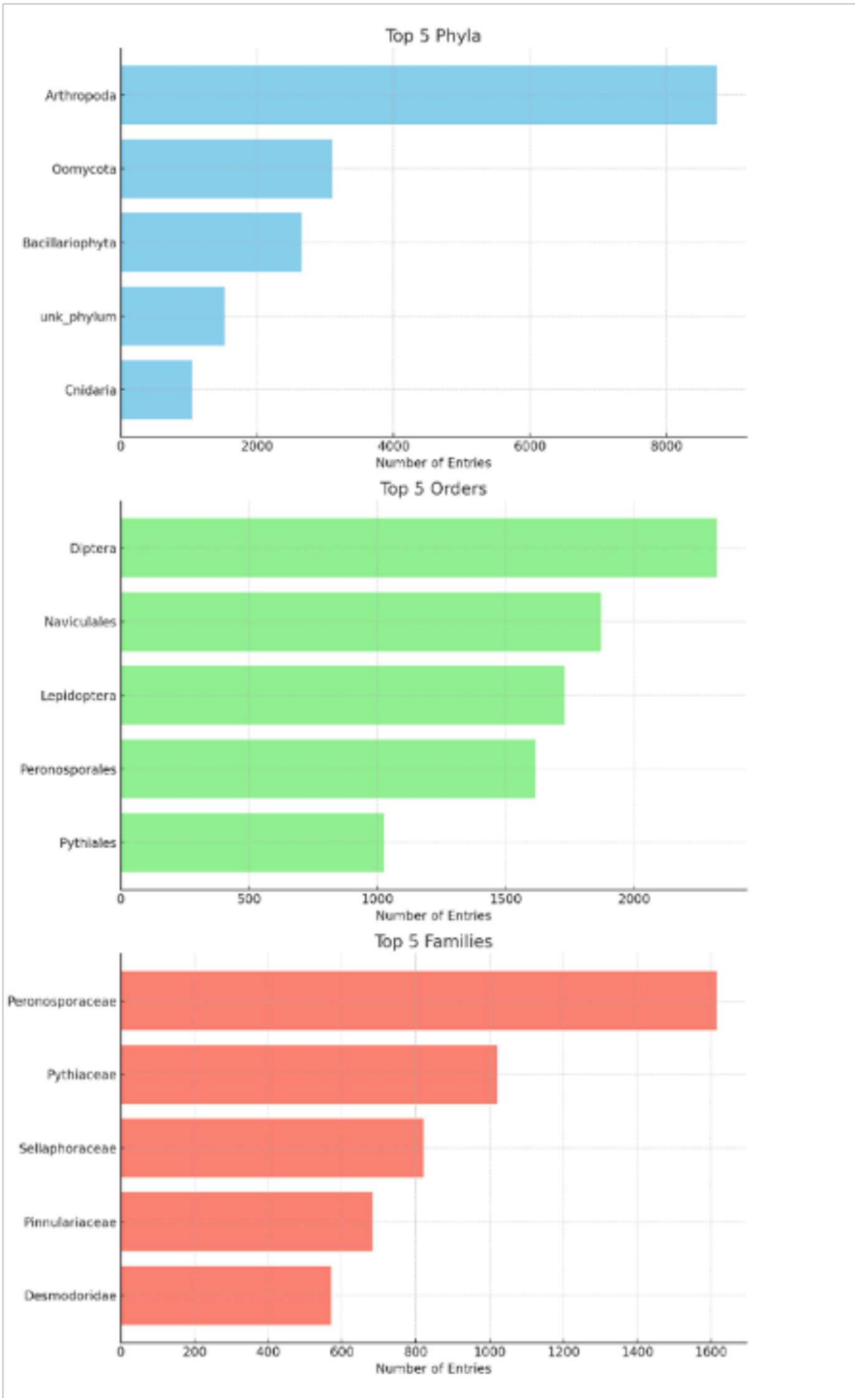

Figure 23. Count of top 5 eukaryotic a) phyla, b) orders and c) families based on COI metabarcoding from 50 2022 sediment samples.

Multiple studies have used molecular metabarcoding to characterize eukaryotic biodiversity in complex communities over the last decade (Taberlet et al, 2018).

Although several ubiquitous genes are available across eukaryotic genomes (rRNA, rubisco), the mitochondrial cytochrome oxidase subunit I (COI) has risen to one of the most robust and common markers used in metabarcoding, due to a) a large database and universal primers available for comparison, b) its inherent variation c) lack of variable introns and ability to denoise protein coding genes and d) the multiplicities of mitchochondria (Andujar et al 2018; Shinzato et al, 2021). Molecular biodiversity surveys have extended to reef structures and sediments (IP et al 2023).

3.2.3 Nutrient and Trace Metal analyses

Fortunately, trace or heavy metal (HM) analyses were conducted, since some of the sediment samples were below the recommended minimal volumes of 20 grams per sample. This capacity was important because obtaining as much environmental data as possible often provides a better context to better interpret the microbial data in the previous section (Knight et al, 2012)

All analyses were performed according to the standard operating procedures used by the facility (https://environment.fiu.edu/facilities-research-groups/cache-nutrient-analysis-core/). For example, all samples for nutrient analyses will be prepared according to standard protocols written in Methods for Chemical Analysis of Water and Wastes (EPA-600/4-79-02, US EPA). The FIU CAChE Nutrient Analysis Core Facility's personnel, procedures, equipment, facilities, and quality system are in compliance with the requirements of FAC Rule 64E-1 and the 2016 NELAP Standards. The FIU CAChE Nutrient Analysis Core Facility was last accredited by the State of Florida Dept of Health, Bureau of Public Laboratories under Certificate #: E76930-34.

Heavy metals from the collected sediments were analyzed at 159 sites and showed high spatiotemporal variation. Manganese (Mn) (15.1 ± 4.1 SD mg/kg), Barium (Ba) (6.8 ± 1.7 SD mg/kg), and Chromium (Cr) (3.1 ± 1.0 SD mg/kg) had the highest mean concentrations across all sites followed by Vanadium (Va) (2.1 ± 1.3 SD mg/kg), Zinc (Zn) (1.3 ± 0.8 SD mg/kg), Lead (Pb) (1.1 ± 0.4 SD mg/kg), and Arsenic (As) (0.99 ± 0.7 SD mg/kg) (Table 3). Most metals were detected in most samples except for Silver (Ag) which was only found in 30/159 samples (18.9%) and was therefore not used in any analyses.

Heavy metal concentrations not only varied significantly from each other in many cases but also varied greatly in space as evidenced by mapping their concentrations per site. Figures 24 and 25 illustrate the heavy metal concentrations by analyte by site where the highest values (darkest points) and lowest values (lightest points) are often found clustered in certain areas of the maps. The spatial patterns of heavy metal concentrations varied significantly depending on the analyte (Figure 26). Comparisons of mean concentrations across all sites in each Inlet Exposure Area (IEA) showed that Zinc (1.96 ± 0.3), Lead (1.4 ± 0.2), Arsenic (1.3 ± 0.2), Copper (0.3 ± 0.1), Molybdenum (0.08 ± 0.02), and Mercury (0.02 ± 0.003) were significantly highest in the southern

IEAs and much lower in the north (Zn = 1.2 ± 0.3; Pb = 1.2 ± 0.07; As = 0.8 ± 0.05; Cu = 0.16 ± 0.02; Mo = 0.02 ± 0.01; Hg = 0.007 ± 0.001). Conversely, Cobalt (0.07 ± 0.004), Nickel (0.7 ± 0.04), and Cadmium (0.04 ± 0.003) were significantly higher in the northern IEAs compared to the south (Co = 0.03 ± 0.004; Ni = 0.5 ± 0.07; Cd = 0.03 ± 0.003). Manganese, Barium, Chromium, and Selenium were relatively consistent throughout.

Heavy Metals also varied by site depth,, but varied differently depending on the analyte (Table 4). Scatterplots of the various heavy metal concentrations by depth revealed that Arsenic, Vanadium, Chromium, Manganese, and Beryllium concentrations significantly decreased with increasing depth in the southern inlet exposure regions. Conversely, Nickel, Cadmium, Cobalt and Selenium had significant positive relationships with increasing depth off Boynton and/or Lake Worth. However, the relationship of heavy metal concentration and depth in the north remains unclear because there were not enough shallow sample sites in the northern IEAs (Figure 27).

Table 3. Descriptive statistics of heavy metals at all sites in 2022 sorted from highest concentration (mg/kg) (left) to lowest (right).

	Mn	**Ba**	**Cr**	**Va**	**Zn**	**Pb**	**As**	**Ni**
Mean	15.136	6.754	3.112	2.084	1.334	1.034	0.985	0.476
Std Dev	4.120	1.677	1.029	1.294	0.796	0.390	0.708	0.156
Std Err Mean	0.330	0.133	0.082	0.104	0.063	0.031	0.056	0.012
Upper 95% Mean	15.788	7.016	3.273	2.289	1.459	1.095	1.096	0.501
Lower 95% Mean	14.485	6.491	2.951	1.880	1.208	0.973	0.874	0.452
N	156	159	159	156	158	159	159	159
	Cu	**Se**	**Mo**	**Co**	**Cd**	**Be**	**Hg**	**Ag**
Mean	0.286	0.182	0.048	0.045	0.029	0.023	0.015	0.014
Std Dev	0.216	0.069	0.081	0.017	0.012	0.012	0.011	0.021
Std Err Mean	0.018	0.005	0.007	0.001	0.001	0.001	0.001	0.004
Upper 95% Mean	0.321	0.192	0.062	0.048	0.031	0.025	0.017	0.022
Lower 95% Mean	0.252	0.171	0.035	0.042	0.027	0.021	0.013	0.006
N	151	159	144	159	159	157	152	30

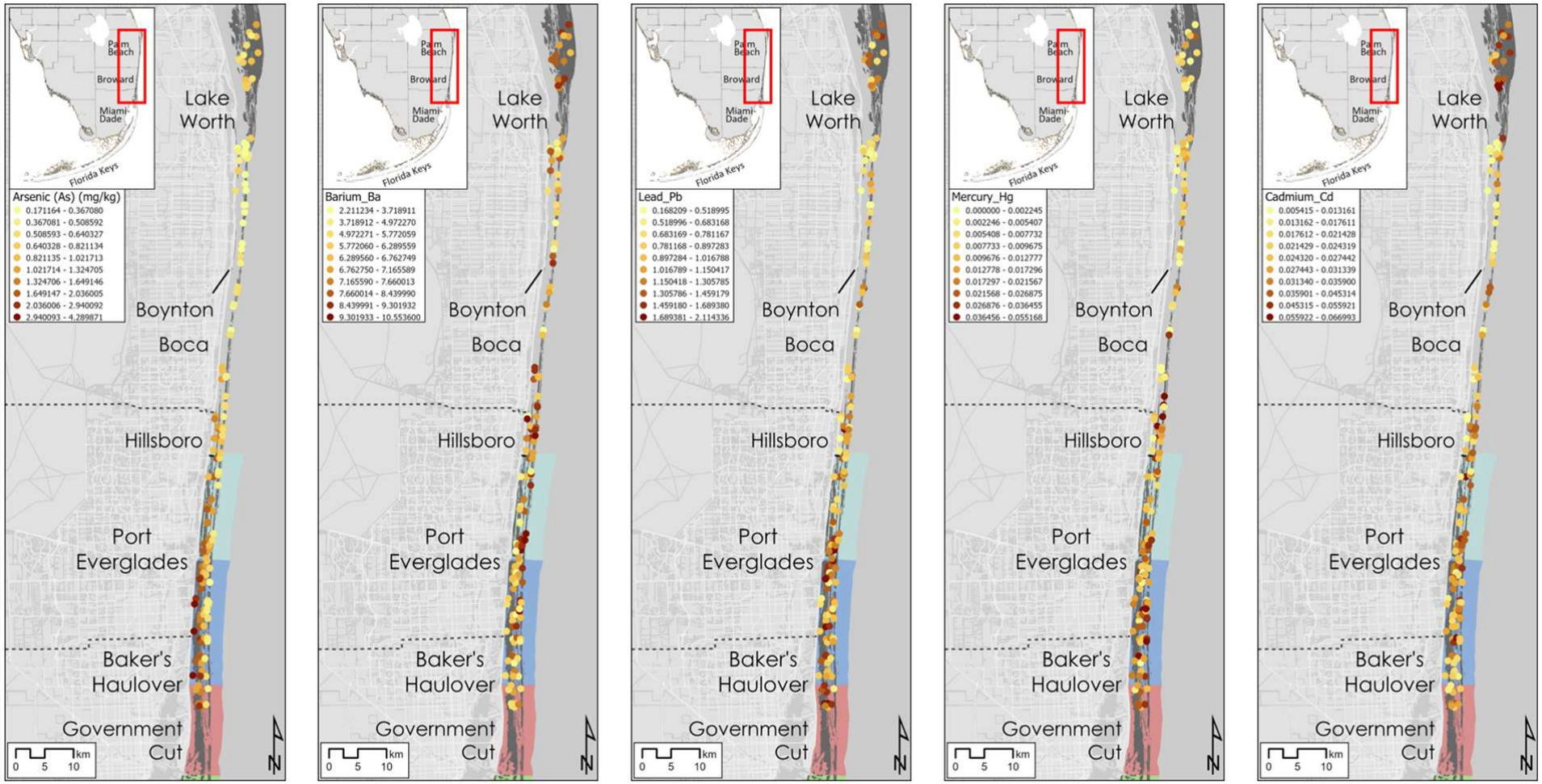

Figure 24. Maps of Arsenic, Barium, Lead, Mercury, and Cadmium heavy metal concentrations by site. .Colors represent 10 natural breaks in the data for each analyte. Yellow indicates low values and brown indicates high. Units are mg/kg.

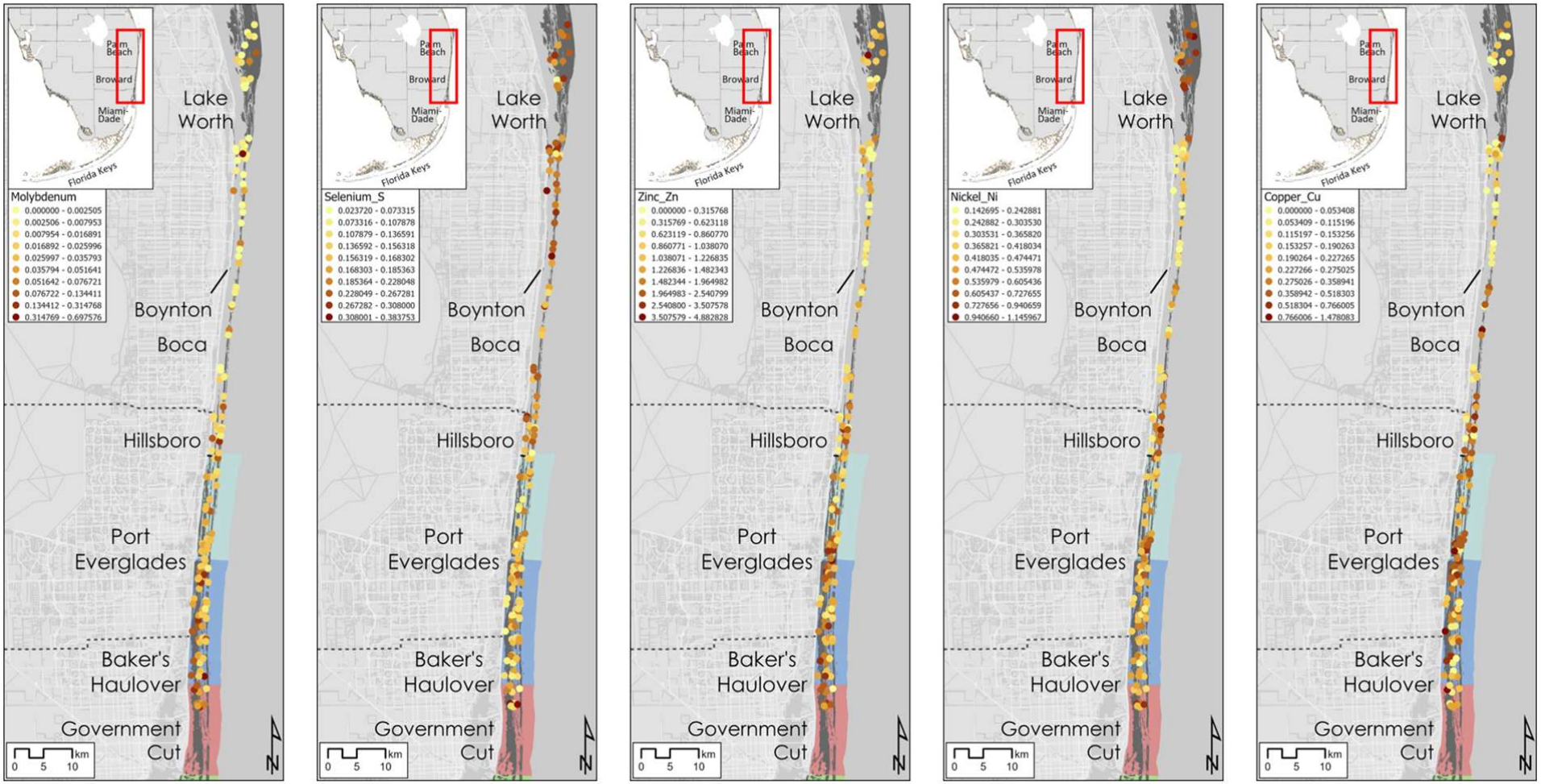

Figure 25. Maps of Molybdenum, Selenium, Zinc, Nickel, and Copper heavy metal concentrations by site. Colors represent 10 natural breaks in the data for each analyte. Yellow indicates low values and brown indicates high. Units are mg/kg.

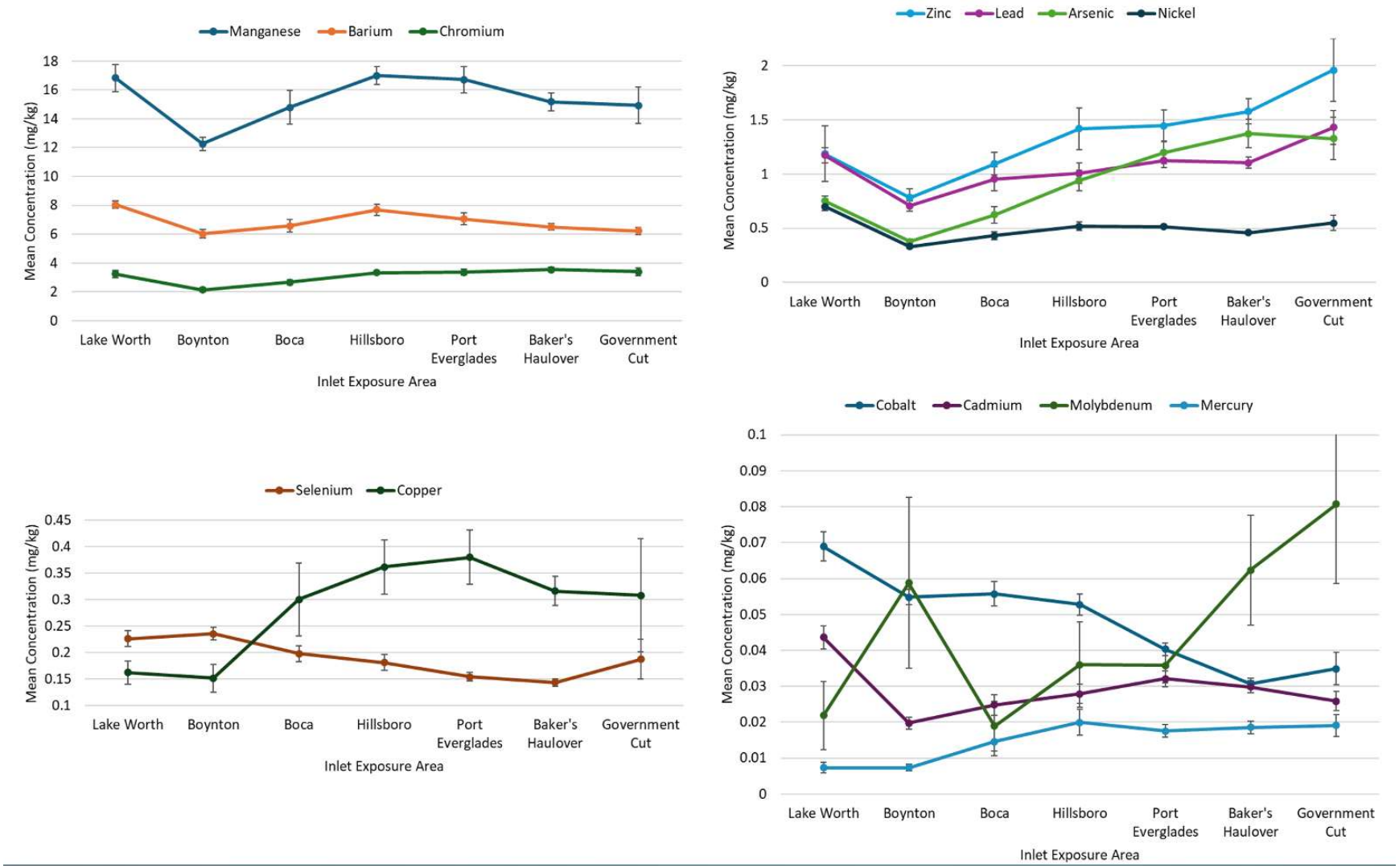

Figure 26. Mean heavy metal concentrations across all 2022 sites by Inlet Exposure Area. Analytes were plotted in groups by their scale from top left to bottom right. Plots are organized from north to south from the left. Error bars indicate one standard error of the mean.

Table 4. R^2 values of linear fit of heavy metals. Red indicates a decrease with depth and green indicates an increase with depth. Bold indicates significance (p<0/05).

	Inlet Exposure						
Heavy Metals	**Gov Cut**	**Haulover**	**PortEv**	**Hillsboro**	**Boca**	**Boynton**	**Lake Worth**
Arsenic (As)	**0.47**	**0.53**	**0.64**	**0.45**	**0.41**	0.10	0.16
Vanadium (V)	**0.59**	**0.48**	**0.57**	0.09	0.00	0.00	0.22
Chromium (Cr)	0.22	**0.22**	**0.39**	0.07	0.15	0.09	0.09
Manganese (Mn)	0.40	**0.28**	**0.39**	0.05	0.03	0.04	0.00
Beryllium (Be)	0.23	0.02	**0.46**	**0.39**	0.05	0.07	0.00
Zinc (Zn)	0.02	**0.08**	0.08	0.09	**0.37**	0.03	0.00
Barium (Ba)	0.28	0.06	**0.35**	0.18	**0.38**	0.00	0.01
Nickel (Ni)	0.07	0.00	0.01	**0.50**	0.23	**0.23**	**0.27**
Cadmium (Cd)	0.10	0.01	0.10	**0.39**	0.01	**0.23**	0.03
Cobalt (Co)	0.05	0.00	0.05	0.07	0.27	0.00	**0.44**
Selenium (Se)	0.00	0.04	0.03	0.13	0.02	0.05	**0.29**
Copper (Cu)	0.02	0.01	0.04	0.07	0.11	0.06	0.00
Molybdenum (Mo)	0.17	0.00	0.00	0.00	0.05	0.00	0.13
Mercury (Hg)	0.07	0.07	0.05	0.09	0.21	0.13	0.03
Lead (Pb)	0.03	0.03	0.00	0.12	0.06	0.01	0.10

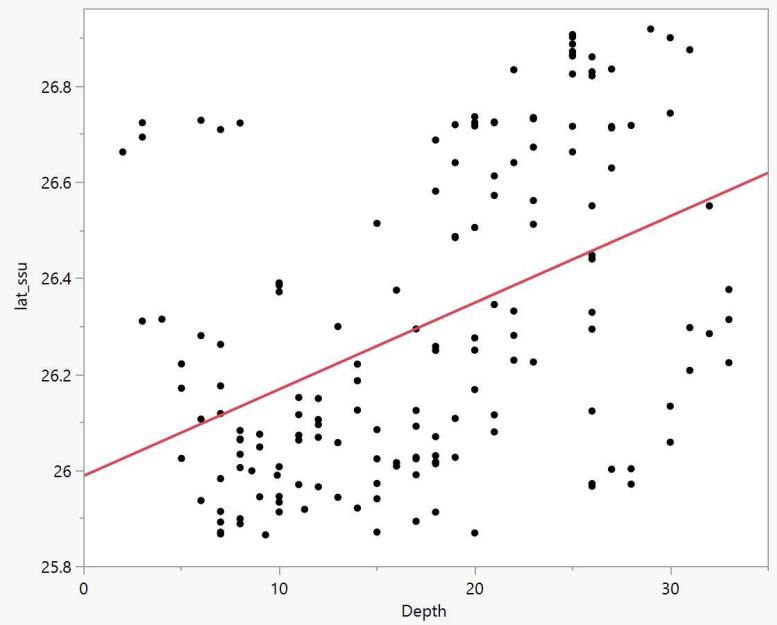

Figure 27. Scatterplot of the 2022 NCRMP sediment collection sites showing the relationship between site latitude and depth (m).Note the upper left quadrant has an absence of shallow sites in the north. The red line indicates the significant linear summary of fit (R^2 = 0.199).

A PERMANOVA of the heavy metal "community" at each site found a significant interaction with fixed factors Inlet Exposure Area and Depth Categories (sites classified into 5 m depth bins)

(p=0.001); Therefore, a bootstrap averages routine of the heavy metal communities by site based on the combined attributes of Inlet Contributing Area and Depth category in meters (0-5, 6-10, 11-15, 16-20, 21-25, 26-30, 31-33) was conducted to visualize the data (Figure 28). The plot illustrated the significant PERMANOVA results where the shallowest depths in the Government Cut, Haulover, and Port Everglades IEAs, which had the highest values of Arsenic (As), Vanadium (V), Chromium (Cr), Manganese (Mn), and Beryllium (Be) (pink stars and exes), plotted farthest away from the deep sites with the lowest heavy metal community in the Boynton IEA (gray diamonds).

A group average cluster analysis of heavy metal community data revealed that significant clusters of high similarity sites also clustered in space (Figure 29). The first large group (m-t) split from the others at 85.5% similarity (yellow sites). The second (j-l) split at 88% similarity (teal sites) and group h (red) and i (green) split at 91%. Sites in groups h and i were defined by high levels of Manganese (>4 mg/kg), Barium (>2.7), Chromium (>1.9), Vanadium (>1.6), Arsenic (1.4), and Zinc (1.3) compared to the first large group split (yellow). All of the sites in group h with highest heavy metal concentrations plotted south of Hillsboro inlet on the shallower habitats whereas the sites with the lowest concentrations (yellow) were located either in the deepest areas or in the Boynton IEA. Sites north of Lake Worth Inlet had a different heavy metal community than those in Boynton. The similarity percentages comparing these two groups is shown in Table 5.

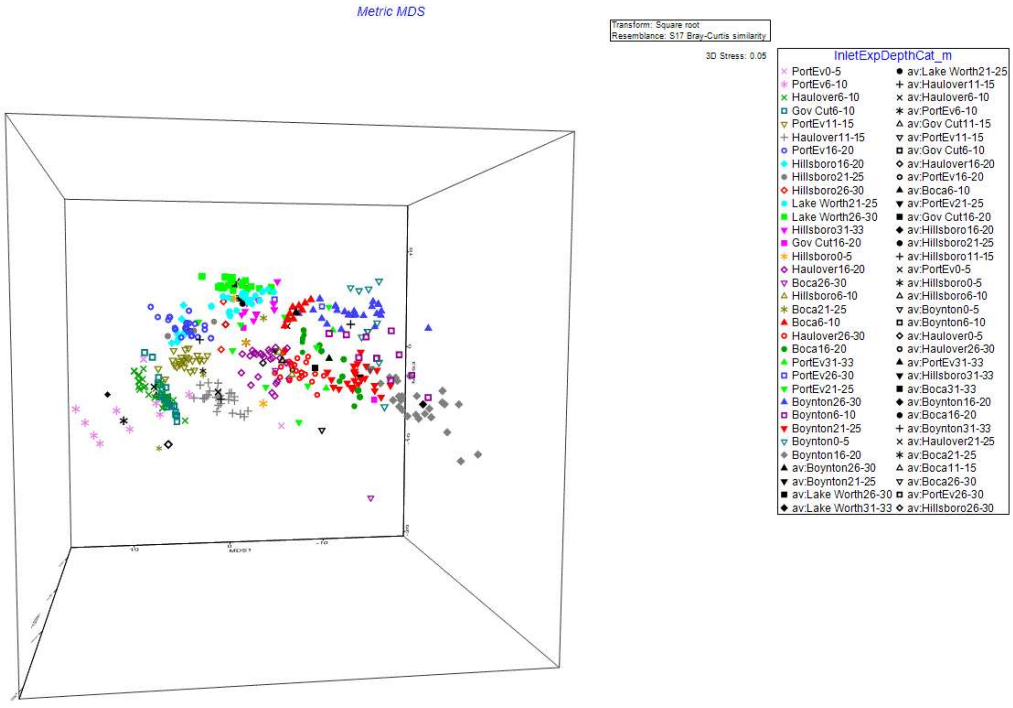

Figure 28. Three-dimensional plot of bootstrap averages of the heavy metal communities by site based on the combined attributes of Inlet Contributing Area. (Gov Cut, Haulover, PortEv, Hillsboro, Boca, Boynton, Lake Worth) and Depth category in meters (0-5, 6-10, 11-15, 16-20, 21-25, 26-30, 31-33). The

plot illustrates the permanova results where the shallowest depths near Government Cut, Haulover, and Port Everglades have the highest values of Arsenic (As), Vanadium (V), Chromium (Cr), Manganese (Mn), and Beryllium (Be) (pink stars and exes) while the heavy metal community was lowest at sites off of Boynton (gray diamonds).

Table 5. Similarity percentage comparison between the two most spatially distinct groups from the cluster analysis. Group m-t sites (yellow) were located in deep water or the Boynton IEA, whereas Group h sites (red) were in shallow habitats south of Hillsboro inlet.

Heavy Metal	Group h (91% sim) Av. Conc	Group m-t (85.5% sim) Av. Conc	Av.Diss	Diss/SD	Contrib%	Cum.%
Mn	4.43	3.31	3.74	2.65	20.74	20.74
V	2	0.94	3.58	3.45	19.83	40.57
As	1.36	0.63	2.45	3.59	13.6	54.17
Cr	2.07	1.45	2.09	2.19	11.59	65.76
Zn	1.21	0.87	1.47	1.33	8.17	73.93
Ba	2.46	2.44	1.17	1.36	6.5	80.43
Pb	1.05	0.89	0.75	1.37	4.18	84.61
Cu	0.55	0.39	0.75	1.13	4.14	88.75
Mo	0.22	0.14	0.54	1.22	2.99	91.75
Ni	0.69	0.59	0.37	1.52	2.07	93.81
Se	0.36	0.45	0.37	1.43	2.06	95.87
Hg	0.13	0.1	0.19	1.4	1.04	96.91
Be	0.14	0.14	0.16	1.4	0.88	97.79
Co	0.19	0.21	0.16	1.53	0.86	98.65
Ag	0.02	0.02	0.13	0.68	0.7	99.35
Cd	0.17	0.15	0.12	1.23	0.65	100

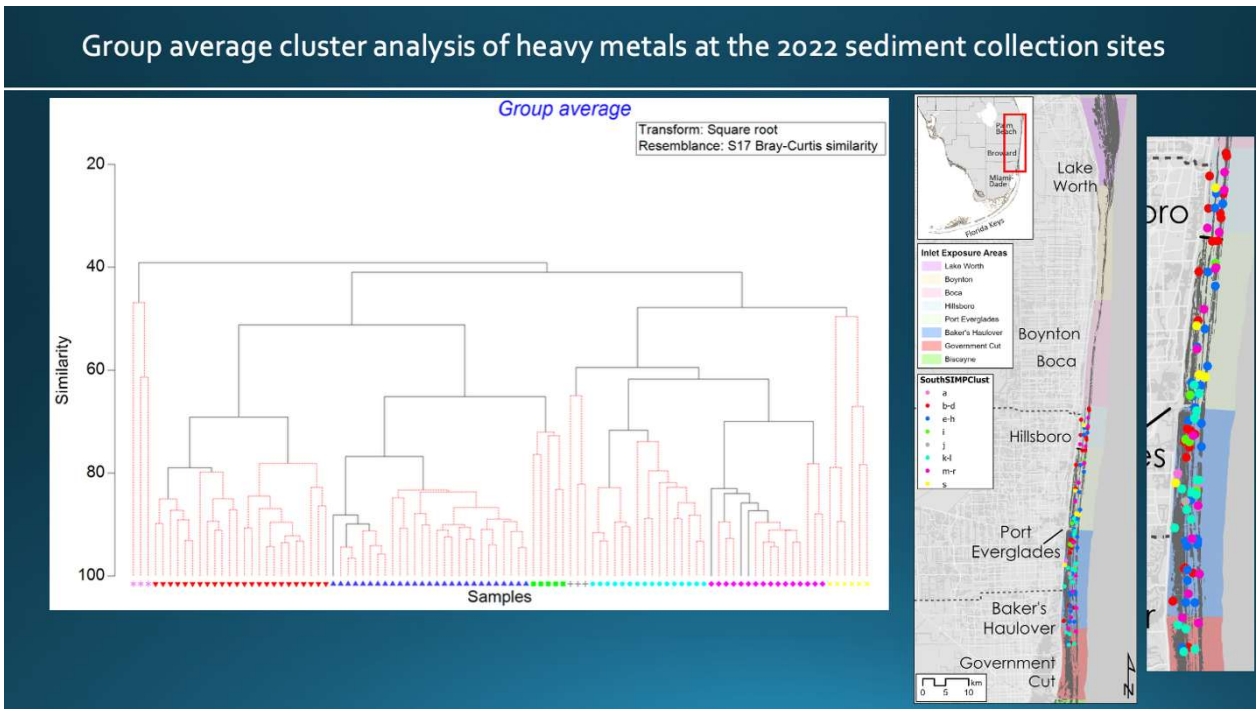

Figure 29. Group average cluster analysis of heavy metals at the 2022 sediment collection sites (top) and a map of the 2022 sediment monitoring sites categorized by similarity clusters (right).The yellow sites (m-t) split from the others at 85.5% similarity. Teal sites (j-l) split at 88% similarity and red (h) and green (i) split at 91%. Sites in groups h and i were defined by high levels of Manganese (>4 mg/kg), Barium (>2.7), Chromium (>1.9), Vanadium (>1.6), Arsenic (1.4), and Zinc (1.3) compared to the yellow sites. When excluding northern collections, Top 20 microbial families were not significantly different by IEA or depth

A two fixed factor PERMANOVA model of the heavy metal communities in the four southern IEAs (Hillsboro, Port Everglades, Haulover, and Government Cut) found that depth category had a significant effect as a single fixed factor (p=0.001). Out of 21 pairwise tests between depth categories, eleven were significant (Table 6). These results corroborated the linear fit models in Table 2 supporting that heavy metal communities are significantly different by depth.

Comparisons of mean concentrations within the southern IEAs (Hillsboro, Port Everglades, Haulover, and Government Cut) by depth category showed that Manganese (18.7 ± 1.8), Chromium (3.8 ± 0.2), Vanadium (2.9 ± 0.4), Zinc (1.9 ± 0.1), Beryllium (0.04 ± 0.004), and Arsenic (1.7 ± 0.3) were significantly highest in the shallow reefs and lower in the deeper ones (Mn = 13.9 ± 1.8; Cr = 2.8 ± 0.3; Va = 1.2 ± 0.3; Zn = 1.3 ± 0.2; Be = 0.02 ± 0.004; As = 0.5 ± 0.2) (Figure 30). Conversely, Barium (7.9 ± 0.7), Nickel (0.5 ± 0.04), and Cadmium (0.03 ± 0.04) were significantly higher in the deep reefs compared to the shallow ones (Ba = 5.9 ± 0.7; Ni = 0.4 ± 0.05; Cd = 0.02 ± 0.004). Lead, Selenium, and Cobalt were relatively consistent throughout and Copper and Molybdenum were highly variable across depths.

Table 6. Permutational ANOVA of the heavy metal communities showing that depth category had a significant effect as a fixed factor. Bold text indicates significant comparisons.

Permutational MANOVA (PERMANOVA)
Transform: Square root
Resemblance: D1 Euclidean distance
Sums of squares type: Type III (partial)
Fixed effects sum to zero for mixed terms

Depth Categories (m)	t	P(perm)	Unique perms
0-5 ,6-10	0.67	0.775	999
0-5, 11-15	0.81	0.622	999
0-5, 16-20	**1.74**	**0.037**	**997**
0-5, 21-25	**1.72**	**0.044**	**998**
0-5, 26-30	**2.94**	**0.002**	**999**
0-5, 31-33	1.77	0.066	984
6-10, 11-15	0.68	0.753	999
6-10, 16-20	**2.08**	**0.003**	**999**
6-10, 21-25	**1.80**	**0.019**	**999**
6-10, 26-30	**2.75**	**0.001**	**998**
6-10, 31-33	**1.85**	**0.008**	**999**
11-15, 16-20	1.23	0.191	998
11-15, 21-25	1.35	0.137	999
11-15, 26-30	**2.18**	**0.006**	**999**
11-15, 31-33	**1.62**	**0.048**	**998**
16-20, 21-25	1.11	0.253	999
16-20, 26-30	**2.00**	**0.005**	**999**
16-20, 31-33	**2.12**	**0.006**	**998**
21-25, 26-30	0.72	0.685	999
21-25, 31-33	1.10	0.3	994
26-30, 31-33	1.13	0.279	999

3.3 Task 4: Examining the relationships between reef sediment microbiomes and environmental conditions

3.3.1 Sediment Microbiome

The microbiome varied significantly by inlet contributing area (Permanova; Pseudo-F = 1.9, p = 0.01; Figure 30) and by the reef strata (Permanova; Pseudo-F = 1.7, p = 0.03), but there was no significant interaction between the two. Pairwise tests found the microbiome was significantly different between Boynton, where Bacillaceae abundance was high and Moraxellaceae abundance low, and Boca (t = 2.1, p = 0.008), Haulover (t = 2.1, p = 0.005) and Government Cut (t = 1.7, p < 0.05), Haulover and Hillsboro (t = 1.7, p = 0.03) and Haulover and Lake Worth (t = 1.7, p = 0.03). There was also significant variation in dispersion by inlet contributing area (Permdisp; F = 3.2, p = 0.04), but not by reef strata (Permdisp; F = 1.7, p = 0.3). Dispersion from the centroid was significantly greater in the Hillsboro contributing area than Boynton, Boca and Government Cut (Permdisp, p < 0.05). Dispersion from the centroid in the Port Everglades contributing area was significantly greater than for Government Cut (Permdisp, p = 0.04). The spatiotemporal model found the microbiome significantly varied by the interaction of inlet contributing area and month (Permanova, Pseudo-F = 1.6, p = 0.03) and month (Permanova,

Pseudo-F = 2.2, p = 0.02). There was significant variation in dispersion from the centroid by month though (Permdisp; F = 3.9, p = 0.03), with more dispersion in the microbiome between samples in June than July, August and September (Permdisp, p < 0.05).

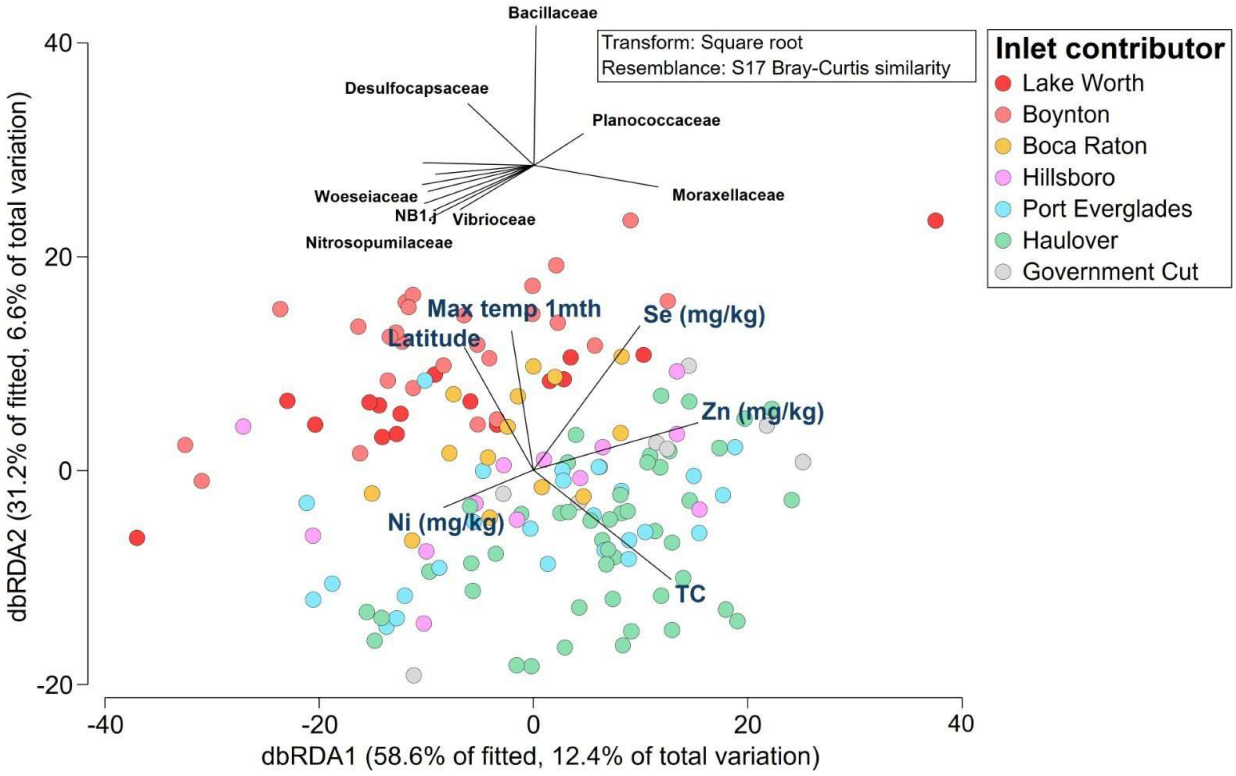

Figure 30. dbRDA ordination of the relationship between the sediment microbiome key environmental predictors identified in DISTLM based upon a Bray-Curtis similarity matrix of the square transformed microbiome within sample.Vectors explain 19 % variation in microbial community structure. Vectors at the origin show the direction and magnitude of the effect environmental predictors on variation in the microbiome. Max temp 1mth = maximum temperature the month before the sample taken; TC = total Carbon, Se = Selenium, Ni = Nickel, Zn = Zinc. All environmental predictors except Selenium were square root transformed for normality. The microbiome vectors have been moved vertically to aid visualization. Bacterial families listed have Pearson correlation coefficients >0.2. Colors reflect the inlet contributing area of the sample which significantly affected the microbiome.

3.3.2. Microbiome and environmental conditions

Distance-based linear model analysis (DISTLM) found multiple equivalent models containing multiple environmental factors. The most parsimonious model (i.e., the simplest model with an AIC within 2 of the lowest model) contained Total Carbon, Nickel, Zinc and Selenium (AIC = 1060.8; $R^2 = 0.19$), but marginal tests (Table 7) also showed highly significant effects of maximum temperature in the month prior to sample collection ($p = 0.002$) and latitude ($p = 0.004$). As the model containing all six of these predictors had a slightly lower AIC (1060.2) and a higher R^2 (0.21) it was chosen as the fitted model and used in the distance-based redundancy analysis (dbRDA) for ordination (Figure 30). Samples with higher total carbon, which were primarily found to the south of the sampling area in the Port Everglades and Haulover inlet contributing areas (Figure 31), higher Zinc concentration and lower Nickel concentration had a higher relative abundance of Moraxellaceae. Samples that had experienced higher maximum temperatures the previous month and had higher Selenium concentration had higher relative abundance of Bacillaceae (Figure 32). Samples with a more diverse microbiome, including a higher relative abundance of Nitrosococcaceae, NB1.j, Thermoaerobaculaceae, Desulfosarciceae and Woeseiaceae, had lower total carbon, lower Zinc concentrations and lower Selenium concentrations. There was a relatively clear latitudinal/temperature divide in the microbiome, with higher relative abundance of Bacillaceae and Desulfocapsaceae at northern sites which had experienced higher temperatures more recently.

Table 7. Marginal test results from distance-based linear model (DISTLM) showing variation in the microbiome explained by each variable.Environmental predictors in the fitted model bolded. Note, sqrt denotes that environmental predictor square root transformed prior to analysis. All predictors normalized prior to analysis.

Variable	**SS(trace)**	**Pseudo-F**	**P**	**Proportion explained variation**
Sqrt (Latitude)	**10819**	**8.83**	**0.0002**	**0.056**
Sqrt (Depth (m))	3868.7	3.04	0.03	0.020
Sqrt (Distance from shore (m))	2054.6	1.60	0.2	0.011
Sqrt (Distance to inlet (m))	556.13	0.43	0.8	0.003
Sqrt (Site temperature °C)	1801	1.40	0.2	0.009
Sqrt (Max.temp.1mth °C)	**6686.6**	**5.33**	**0.003**	**0.035**
Sqrt (SD.temp.1wk °C)	3190.5	2.50	0.06	0.017
Sqrt (SD.temp.1mth °C)	3307	2.59	0.05	0.017

Sqrt (Heat stress duration (days))	1222.1	0.95	0.4	0.006
Sqrt (TN) (ppm)	8136	6.54	0.001	0.042
Sqrt (TP) (ppm)	4355.4	3.43	0.02	0.023
Sqrt (TC) (ppm)	**10586**	**8.62**	**0.0002**	**0.055**
Sqrt (Co (mg/kg)	7108	5.68	0.002	0.037
Sqrt (Ni (mg/kg)	**1514.8**	**1.18**	**0.3**	**0.008**
Sqrt (Zn (mg/kg)	**10583**	**8.62**	**0.0001**	**0.055**
Se (mg/kg)	**9008.5**	**7.28**	**0.0002**	**0.047**
Sqrt (Cd (mg/kg)	1590.8	1.24	0.3	0.008
Ba (mg/kg)	1151.2	0.89	0.4	0.006
Pb (mg/kg)	4090.4	3.22	0.03	0.021

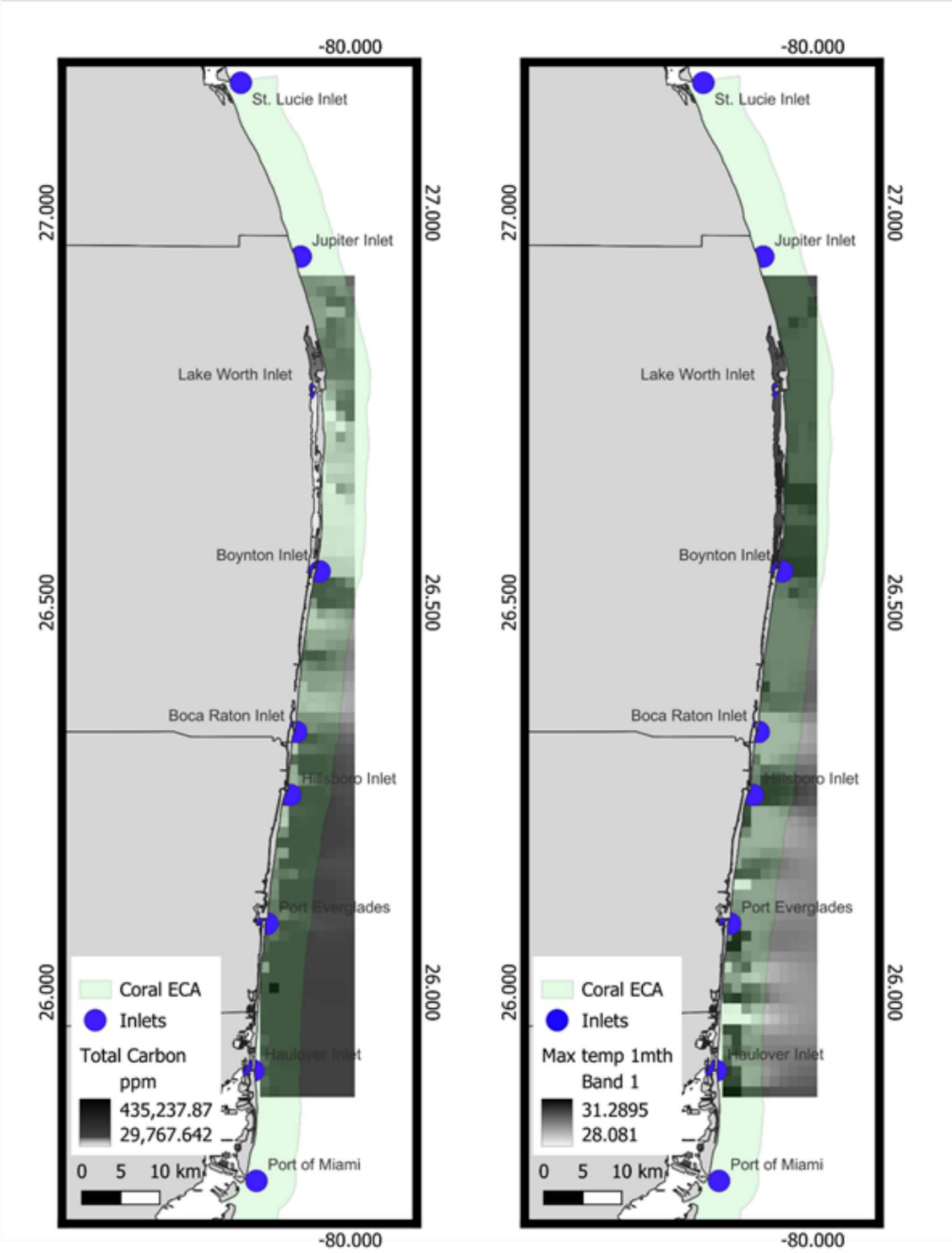

Figure 31. Inverse distance weighted interpolation at 0.01° showing spatiotemporal variation in a) Total carbon concentration (ppm) from collected sediment samples and b) Maximum temperature the month prior to sample collection (°C).

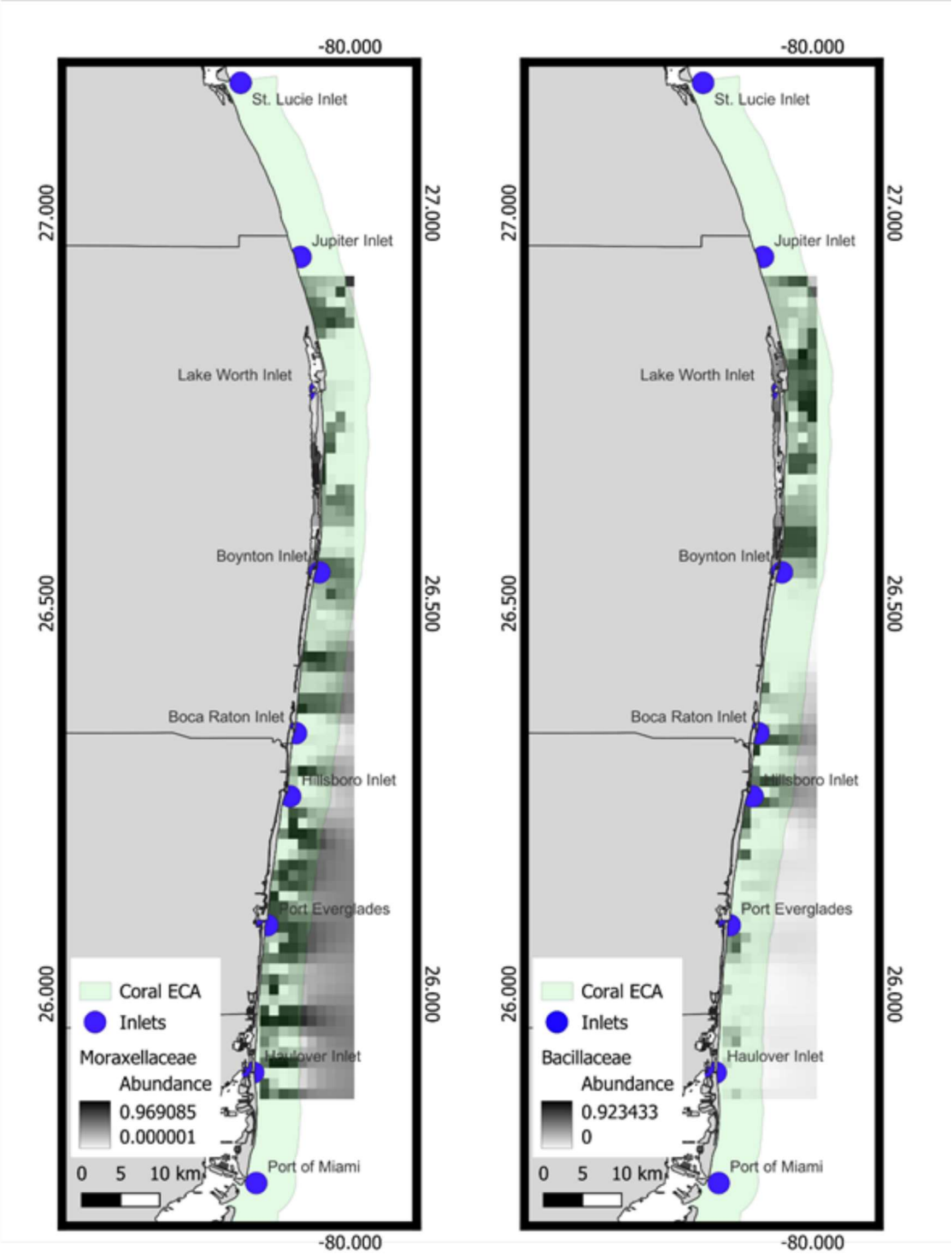

Figure 32. Inverse distance weighted interpolation at 0.01° showing spatial variation in bacterial relative abundance.In a) Moraxellaceae relative abundance which accounted for most variation in dbRDA1 and b) Bacillaceae relative abundance, which accounted for most variation in dbRDA2.

4. CONCLUSIONS AND RECOMMENDATIONS

4.1 Context with previous analyses

Sediments, both terrestrial or aquatic, hold some of the most diverse and complex microbial communities of any habitat (Baker et al, 2021; Capo et al, 2022). Therefore, genomics approaches have been pivotal in characterizing this diversity and their possible ecological functions (Thompson et al, 2017; Beale et al, 2022). Opportunistic sampling of reef sediments has enabled the generation of multiple environmental and microbiome-based datasets that can provide novel insights into factors that could affect reef health. Moreover, concerns about increased sedimentation in recent years has grown as another major stressor on corals alongside sea surface warming and ocean acidification (Fifer et al, 2022). In this context, characterization of the sediments proximal to reefs becomes tantamount.

Barring any major events, such extreme and sudden temperature shifts, hurricanes or pollutant spills, sediment microbial communities would be expected to remain fairly stable.

4.1.1 Past nutrient and trace metal research

Monitoring reef habitats has been an important, long-standing practice for ecosystem managers. Mapping by video transects and acoustics permit species counts and ground truthing. Understanding the effects of various land-based chemicals and pollutants from runoff on hard corals and adjacent residents of the ecosystem have been similarly deemed high priority (Reichelt-Brushett and Harrison 1999; Reichelt-Brushetta and McOrist 2003). In a recent study, colleagues Giarikos et al (2023) characterized heavy metals from Port Everglades sediment cores and found high levels of Arsenic (As), Cadmium (Cd), Lead (Pb) and Molybdenum (Mo), but they also only characterized a few samples from the most adjacent KJCAP reefs. Nonetheless, their results warned of the potential threats of resuspending bioavailable metals after dredging.

We participated in the follow-up project (FDEP agreement #C0FEDD), which had more extensive heavy metal analyses and our application of both 16S rRNA bacterial typing and metagenomics to the port core sediments. The finding of higher concentrations of metals, such as Al, As, Cu Fe, Mn, and Sn to the north of ports was consistent with our current project.

Unfortunately, extensive studies of potentially toxic chemicals, pollutants, organic pesticides etc are relatively sparse. A recent thesis has reviewed pollutant levels on S. Florida reefs which is helpful (Skelton 2023). Prior to this, on a study by McDonald (1994) was carried out.

In both of these studies, they report that the Florida Department of Environmental Protection (FDEP) had listed general threshold effect levels (TELs) and probable effects levels (PELs) for 10 metals. Only six of these – arsenic, copper, lead, mercury, silver, and zinc – had PELs that exceeded FDEP levels.

Moreover, application of molecular genomic methods, including eDNA and metabarcoding, can enhance habitat surveys and censuses because they capture cryptic, unculturable and smaller reef residents (Ip et al 2023). Moreover, when molecular-based microbiome data are coupled with the appropriate environmental metadata, the value of both datasets increases. Abiotic parameters

such as run-off chemicals and nutrients can help explain the presence of specific microbial and metazoan taxa.

4.1.2 Past Microbiome Characterizations on Florida's Coral Reefs and other Reef systems

Our MMG laboratory has been characterizing microbiomes from sediments, reefs, ambient seawater, and symbiotic reef organisms in Broward for almost a decade (Campbell et al, 2015; O'Connell et al, 2018; Krausfeldt and Lopez et al, 2023). The data provide important baselines to allow comparisons and assessments changes over time.

Other studies have identified beneficial bacteria such as *Ruegeria,*or those in the class of bacteria, Alteromonadaceae, which can serve as probiotic agents against possible coral diseases (Kitamura et al 2021)

In another example from a 2022- 2024 FL DEP collaboration with Dr. Mark Butler from Florida International University (FL DEP # C0856), sponges and their reef sediment habitats were characterized for microbiomes at multiple Florida reef sites. The sampling spanned 12 sites from Bahia Honda to Sugarloaf in the Florida Keys. As expected, using similar surface sediment grabs, the sediment communities appear diverse but did not show distinct structuring across any of the 12 sites.

Overall, the FL Keys bacterial sediment patterns differed from KJCAP data, which had more sites dominated by fewer taxa rather than more even diversity, though many taxa do overlap. For example, Family Woeseiaceae (with Genus *Woeseia)* (Mußmann et al 2017; Hoffman et al, 2020) are common members of marine sediments and found at every location in the FL Keys but not in KJCAP. This bacterial taxon is known as a chemoorganoheterotroph that lives on detritus by releasing a wide array of peptidases, potentially a pivotal role in organic compound recycling for sediment organisms (Ardnt et al 2013). Another bacterial group not observed in the top 15 KJCAP families was Pirellulaceae, a type of common planctomycete with roles involving aerobic chemoheterotrophy (Hernández-Zulueta et al, 2023). If common or probiotic reef community members such as Pirellula or *Woeseia*, are absent at impacted reef sites, could the lack be viewed as one indicator of an environmental disturbance and microbial dysbiosis?

4.2.1 Current Microbiome Characterizations

The finding of many of the same taxa (e.g. *Bacillus, Psychrobacter, Woeseia* and *Halomonas)* across sediment sites, along with no clear structure of bacterial distributions based on reef habitat type, underscores the complexity and dynamic nature of reef sediments (and their microbiomes). This could be partly attributable to the sediments not being deeply sampled; or rather the sampling was opportunistic and performed by surface grabs from the divers.

KJCAP communities differed from earlier sediment studies by showing very high relative abundances of *Psychrobacter* [Family Moraxellaceae]. The meaning of this is not clear. *Psychrobacter* and *Bacillus* have been previously found on corals or reef habitats (O'Connell et al, 2018, while some *Psychrobacter* species can participate in denitrification processes (Kennedy et al, 2024).

An interesting -omics study carried out on remote reefs of the southern Line Islands located in the Republic of Kiribati (Central Pacific) found that resident bacteria *Psychrobacter* [Family Moraxellaceae (Gammaproteobacteria)] relative abundances varied on a diel basis (Kelly et al, 2019). Along with cyanobacteria (from reef water column sampling), *Psychrobacter* appeared more prevalent in the day by up to two orders of magnitude compared to night times.

Although not fully analyzed or integrated with corresponding metadata, this project's 2024 microbiome dataset revealed the presence of various enterobacteria (fecal), such as *E. coli/Shigella* genera (Figure 12) at a few collection sites. These sites appear close to shore but could also have been affected by nearby sewage outfalls (e.g. in Boca Raton). Other fecal bacteria groups, such as Bacteroidetes, were also detected in reef sediments.

We were able to measure and include many environmental variables into this project, collected from various sources, and which could be applied to the microbiome distributions. Although microbiome patterns do not appear obvious now, they may be clarified if contaminants or more fine-grained approaches were taken. The integrated statistical analyses and environmental modeling from Task 4 suggested a structuring of the KJCAP into "inlet exposure areas (IEAs), which in turn are influenced by their closest inlet. This suggests that the northly currents have strong influences on run-off direction and eventual settlement on KJCAP reefs. "Southern" inlets (Port Everglades, Hillsboro, Haulover, Government Cut) showed higher signatures of heavy metals such as Ba, As, Zn and Hg compared to Boynton. However, Lake Worth did show elevated levels of Ba, Se and Ni compared to Boynton.

Heavy metals Tn, As and V appeared to drive some microbial differences in Broward and Miami-Dade county compared to more northern Palm Beach county. For example, Woeseiaceae increases with the Zn vector. Molybdenum, Selenium, Zinc, Nickel, and Copper appeared to fluctuate significantly with specific bacterial taxa.

How the diverse microbiomes are affected or follow the trace metal concentrations is not completely understood. More than likely other variables may more strongly affect specific microbiome compositions. Characterizing grain sizes of the different sediment samples and matching to the microbiome community together with other environmental variables could provide an even fuller picture of functions.

For example, Figure 28 as part of Task 4 modeling, indicates that Ni possibly has a strong influence on PEI microbes, while the variables of Total Carbon (TC) and Zn may have more influence Hillsboro and Haulover communities. This analyses also supports a general partitioning of northern and southern portions of KJCAP, partially defined by nutrient and microbiome presence.

Water depth showed interesting correlations with certain trace metals. Several data point to depth and location as possible significant drivers of microbiome composition.

4.3. Problems Encountered in Current Project

Although it is difficult to measure every parameter that could affect reef health in one study, we believe starting with microbial community characterizations, followed by nutrients and minerals analyses, help illustrate reef ecosystem functions.

This study only profiled a single year of sampling. As indicated above, we cannot make full comparisons between 2022 and 2024 microbiome data, since the 2024 NCRMP samples do not have corresponding environmental data (heavy metals, Hobo logger data collected once per year etc) available for the 2022 samples.

Moreover, we were unfortunately not able to measure sediment grain sizes for any of the 2022 reef samples due to insufficient material. This parameter has been shown to affect microbial community composition, but was not included in the budget for this project (e.g. prohibitive costs and time).

The qPCR approach was not able to be fully utilized as planned in this study, but other gene targets may be more informative, and require further trials. This does not fully obviate the use of qPCR, but we were limited in how many genes we could target and test.

The eukaryotic metabarcoding ran into technical problems with 18S rRNA sequencing. Nonetheless, the limited COI data sufficed to provide profiles which could help generate new hypotheses to test – e.g. what are the co-occurrences with each other and specific bacterial taxa? Besides being a detritus degrader, relatively little is known about Pythiaceae and other common water molds detected across multiple reef sediment samples.

The high incidence of genus *Bacillus* in many 2022 samples, and their predominance in northern sediment samples was puzzling and unexpected. Partial explanation is that samples obtained from Lake Worth had to remain in the field for at least week, even though stored cold by refrigeration before being brought to the MMG lab for processing. This extra time period could have enable growth of some *Bacillus* contaminants which is known to over grow quickly.

Nonetheless, we have learned important lessons on reef sediment sampling. Although we had sufficient quantities to complete trace metal and nutrient analyses for the 2022 sediment samples, future sampling will ensure the collection of a minimum of 40 grams of sediment per site instead of just 15 grams. Moreover, we will better protect against potential contamination by carrying out more discrete training of NCRMP dive staff to use gloves and preserve samples immediately. This will help improve and assure more robust environmental microbiome profiles going fororward

4.4 Significance and Future Directions

The new data from this project has added extra context to the 2022 NCRMP samples. The impetus of this project was to apply state-of-the-art molecular methods to obtain a snapshot of the Kristin Jacobs Coral Aquatic Preserve (KJCAP), the northernmost section of Florida's Coral Reef. This effort took advantage of bi-annual NCRMP sampling

(https://www.coris.noaa.gov/monitoring/). Simultaneously, we addressed specific hypotheses regarding the extent of port and inlet microbes previously characterized and land-based run-off influences on the surrounding KJCAP reefs. The hypothesis of PEI bacterial detection was partially supported both microbially and chemically: common port bacteria Thiotrichaceae, Desulfobulbaceae and Desulfobacteraceae were detected in 16S rRNA microbiome data. Desulfobacteraceae are strict anaerobic bacteria, obtain energy by reducing sulfates to sulfides and thus would not be expected to thrive in well aerated habitats.

The current datasets and effort also now provide a rich platform for future comparisons that can span, temporal, spatial and taxonomic boundaries. For example, multiple datasets of symbiotic microbiomes of resident reef invertebrates exist along the KJCAP and can be compared with the reef datasets. Having a two-year separation between 2022 and 2024 NCRMP samples is a long period to measure temporal changes, and too coarse when many other variables are likely to be introduced with no controls, and sediments shift over much shorter scales. For example, the 2023 marine heat wave occurred between the two NCRMP sampling events.

Therefore, we still recommend that managers take water and sediment samples to monitor microbial community composition and dynamics. This will enable comparative approaches and ecosystem functional assessments in the future. The efforts should also include collecting and integrating abiotic, environmental data whenever possible, as multiple parameters will enhance the interpretations of microbial functions. It is now well known that microbes (bacteria, protozoans, fungi and viruses) can strongly influence ecosystems -e.g. they can contribute to biochemical cycles, disease etiology and symbioses (Beale et al 2022).

Although still relatively rudimentary in this report, other trace metal analyses have been performed on various types of marine sediments for many years (Howard and Brown 1984; Shah 2021). It is beyond the scope of our study to determine the exact origins and fates of all potentially toxic heavy metals. For example, cadmium has been used an anti-corrosive on steel, older nickel-cadmium batteries and certain pigments. Barium is used in some steel alloys and superconducting materials, while zinc has anti-corrosive uses. Vanadium is routinely used in specialty steel and aluminum alloys, such as high-speed tools. The other elements would likewise be expected to occur in highly industrialized ports and large population coastal cities (Ansari et al, 2004).

We can recommend to reef managers that routinely monitoring or including heavy metal analyses in future reef conservation projects can be beneficial and serve important purposes (Giarikos et al, 2023). Furthermore, even though our sediment sampling may have been flawed (see above) partly due to the opportunistic start of the project (in 2022), the detection of higher concentrations of multiple heavy metals closer to busy ports should raise some alarms. For example, we can assume that surface sediment grabs, compared to sediment core samples, represent a mostly “ephemeral” sampling of shallow sediments which routinely experience a large amount of natural movement by normal wave actions and currents. However finding contaminated sediments close to ports and inlets indicates that these sites are likely still actively leaching and releasing potentially toxic and detectable levels of HMs even past their original generation and deposition events within the ports and inlets. We must ask the question - “are

HMs being detected in our study in the 2022 samples legacy elements, or are they still be generated at present?"

We recommend that trace heavy metal measurements continue to be taken in tandem with NCRMP sampling at least every two years. The NCRMP timeline did allay a large proportion of the overall project costs, since diving and boat time to sample the large span of sites of the KJCAP represent large efforts. In comparison, nutrient and trace metal analyses represent a small investment, and molecular microbiome profiling only slightly higher. A review of current literature finds a dearth of HM analyses of most reefs, exposing a lack of baseline environmental data on which to make comparisons. If funding is possible, FL DEP or other local agencies could take up sampling in even years.

Moreover, we found that ~172 samples in 2022 may not always be necessary, since obvious microbiome distribution patterns did not clearly emerge from the higher sampling coverage. Several adjacent spots could be eliminated, while others kept for statistical replication.

The characterization of eukaryotic meiofauna by metabarcoding was only rudimentary in this study, but reveals the need for more effort and analyses in this realm as well. Many of these organisms could exist as stable or acclimated residents of the KJCAP reefs, specifically interact with bacteria as prey or competitors and therefore should be included in future monitoring and models of reef ecosystem health. It could be very enlightening to look into the interactions in greater detail and determine how they may contribute to reef health.

5. REFERENCES

Alexander, J. B., Bunce, M., White, N., Wilkinson, S. P., Adam, A. A., Berry, T., ... & Richards, Z. T. (2020). Development of a multi-assay approach for monitoring coral diversity using eDNA metabarcoding. *Coral Reefs*, *39*, 159-171.

Anderson MJ (2001) A new method for non-parametric multivariate analysis of variance. Austral Ecol. 26, 32–46.

Andújar, C., Arribas, P., Yu, D. W., Vogler, A. P., & Emerson, B. C. (2018). Why the COI barcode should be the community DNA metabarcode for the metazoa.

Arndt, S., Jørgensen, B. B., LaRowe, D. E., Middelburg, J. J., Pancost, R. D., & Regnier, P. (2013). Quantifying the degradation of organic matter in marine sediments: A review and synthesis. *Earth-science reviews*, *123*, 53-86.

Ansari, T. M., Marr, I. L., & Tariq, N. (2004). Heavy metals in marine pollution perspective-a mini review. *Journal of Applied Sciences*, *4*(1), 1-20.

Baker, B. J., Appler, K. E., & Gong, X. (2021). New microbial biodiversity in marine sediments. *Annual Review of Marine Science*, *13*(1), 161-175.

Beale, D. J., Jones, O. A., Bose, U., Broadbent, J. A., Walsh, T. K., van de Kamp, J., & Bissett, A. (2022). Omics-based ecosurveillance for the assessment of ecosystem function, health, and resilience. *Emerging topics in life sciences*, *6*(2), 185-199.

Burnham KP, Anderson DR (2004) Multimodel inference: understanding AIC and BIC in model selection. Sociol. Methods Res. 33, 261–304.

Campbell, A. M. et al. (2015) Dynamics of marine bacterial community diversity of the coastal waters of the reefs, inlets, and wastewater outfalls of southeast Florida. *Microbio Open*, *4*(3), 390-408. https://doi: 10.1002/mbo3.245.

Capo, E., Monchamp, M. E., Coolen, M. J., Domaizon, I., Armbrecht, L., & Bertilsson, S. (2022). Environmental paleomicrobiology: using DNA preserved in aquatic sediments to its full potential. *Environmental Microbiology*, *24*(5), 2201-2209.

Caporaso, J. G. et al. (2011) Global patterns of 16S rRNA diversity at a depth of millions of sequences per sample. *PNAS, 108* (Supplement 1), 4516-4522. https://doi.org/10.1073/pnas.1000080107

Clarke K, Gorley R (2006) Primer-E, Plymouth.

Easson, CG., Boswell, KM, Tucker, N, Warren, JD, D.P. Sutton, TT, Lopez, JV. 2020. Combined Acoustics and E-DNA Analysis Reflects Diel Vertical Migration of Mixed Consortia in the Gulf of Mexico. Frontiers in Marine Science. 7:552. DOI:10.3389/fmars.2020.00552

Giarikos, D. G., White, L., Daniels, A. M., Santos, R. G., Baldauf, P. E., & Hirons, A. C. (2023). Assessing the ecological risk of heavy metal sediment contamination from Port Everglades Florida USA. *PeerJ*, *11*, e16152.

Hernández-Zulueta, J., Díaz-Pérez, L., Echeverría-Vega, A., Nava-Martínez, G. G., García-Salgado, M. Á., & Rodríguez-Zaragoza, F. A. (2023). An update of knowledge of the bacterial assemblages associated with the mexican caribbean corals Acropora palmata, Orbicella faveolata, and Porites porites. *Diversity*, *15*(9), 964.

Hoffmann, K., Bienhold, C., Buttigieg, P. L., Knittel, K., Laso-Pérez, R., Rapp, J. Z., ... & Offre, P. (2020). Diversity and metabolism of Woeseiales bacteria, global members of marine sediment communities. *The ISME journal*, *14*(4), 1042-1056.

Howard, L., & Brown, B. (1984). Heavy metals and reef corals. *Oceanography and Marine Biology, An Annual Review*, *22*, 192-208.

Ip, Y. C. A., Chang, J. J. M., Oh, R. M., Quek, Z. B. R., Chan, Y. K. S., Bauman, A. G., & Huang, D. (2023). Seq'and ARMS shall find: DNA (meta) barcoding of Autonomous Reef Monitoring Structures across the tree of life uncovers hidden cryptobiome of tropical urban coral reefs. *Molecular Ecology*, *32*(23), 6223-6242.

Jones NP, Figueiredo J, Gilliam DS (2020) Thermal stress-related spatiotemporal variations in high-latitude coral reef benthic communities. Coral Reefs 39:1661-1673. https://doi.org/10.1007/s00338-020-01994-8.

Jouffray, J. B., Wedding, L. M., Norström, A. V., Donovan, M. K., Williams, G. J., Crowder, L. B., ... & Nyström, M. (2019). Parsing human and biophysical drivers of coral reef regimes. *Proceedings of the Royal Society B*, *286*(1896), 20182544.

Kelly, L. W., Nelson, C. E., Haas, A. F., Naliboff, D. S., Calhoun, S., Carlson, C. A., ... & Rohwer, F. (2019). Diel population and functional synchrony of microbial communities on coral reefs. *Nature communications*, *10*(1), 1691.

Kennedy, S. J., Atkinson, C. G. F., Tubbs, T. J., Baker, B. J., & Shaw, L. N. (2024). Culture-dependent identification of rare marine sediment bacteria from the Gulf of Mexico and Antarctica. *bioRxiv*.

Kilfoyle, K., Walker, B.K., Gregg, K., Fiscoi, D.P., Spieler, D.E., 2018. Southeast Florida Coral Reef Fishery- Independent Baseline Assessment: 2012-2016 Summary Report. National Oceanic and Atmospheric Administration Coral Reef Conservation Program. https://floridadep.gov/rcp/coral/documents/southeast-floridacoral-reef-fishery-independent-baseline-assessment-2012-2016.

Kim, B.-R. et al. (2017). Deciphering diversity indices for a better understanding of microbial communities. *J. Microbio. Biotech.,* 27(12), 2089-2093.

Kitamura, R., Miura, N., Ito, M., Takagi, T., Yamashiro, H., Nishikawa, Y., ... & Kataoka, M. (2021). Specific detection of coral-associated *Ruegeria,* a potential probiotic bacterium, in corals and subtropical seawater. *Marine Biotechnology*, *23*, 576-589.

Knight R, Jansson J, Field D, Fierer N, Desai N et al. 2012. Designing Better Metagenomic Surveys: The role of experimental design and metadata capture in making useful metagenomic datasets for ecology and biotechnology. *Nature Biotech* 30:513–520.

Krausfeldt* L, Lopez*, JV, Bilodeau C., Lee HW, Casali, S. 2023. Change and stasis of distinct sediment microbiomes across Port Everglades Inlet (PEI) and the adjacent coral reefs. *PeerJ* 11:e14288 https://doi.org/10.7717/peerj.14288 (*dual first authors).

Lande, R. (1996). Statistics and partitioning of species diversity, and similarity among multiple communities. *Oikos*, 5-13.

Leray M, et al. (2013) A new versatile primer set targeting a short fragment of the mitochondrial COI region for metabarcoding metazoan diversity: Application for characterizing coral reef fish gut contents. Front Zool 10:34.

Legendre P, Anderson MJ (1999) Distance-based redundancy analysis: testing multispecies responses in multifactorial ecological experiments. Ecol. Monogr. 69, 1–24.

Lopez, JV. 2024 *Assessments and Conservation of Biological Diversity from Coral Reefs to the Deep Sea.* Academic Press. Paperback ISBN: 9780128241127.

McArdle BH, Anderson MJ (2001) Fitting multivariate models to community data: a comment on distance-based redundancy analysis. Ecology 82, 290–297.

MacDonald, D. (1994). *Approach to the assessment of sediment quality in Florida coastal waters* (Vol. 1). Florida department of environmental protection office of water policy.

Mougin, J., Roquigny, R., Travers, M. A., Grard, T., Bonnin-Jusserand, M., & Le Bris, C. (2020). Development of a mreB-targeted real-time PCR method for the quantitative detection of Vibrio harveyi in seawater and biofilm from aquaculture systems. *Aquaculture*, *525*, 735337.

Mußmann, M., Pjevac, P., Krüger, K., & Dyksma, S. (2017). Genomic repertoire of the Woeseiaceae/JTB255, cosmopolitan and abundant core members of microbial communities in marine sediments. *The ISME journal*, *11*(5), 1276-1281.

Newell, S. Y. (1992). Autumn distribution of marine Pythiaceae across a mangrove–saltmarsh boundary. *Canadian journal of botany*, *70*(9), 1912-1916.

NOAA Coral Reef Watch (2018) Updated daily. NOAA Coral Reef Watch Version 3.1 Daily Global 5km Satellite Coral Bleaching Degree Heating Week Product, Jun. 3, 2013-Jun. 2, 2014. College Park, Maryland, USA: NOAA Coral Reef Watch. Data set accessed 2020-09-01 at ftp://ftp.star.nesdis.noaa.gov/pub/sod/mecb/crw/data/5km/v3.1/nc/v1.0/daily/dhw/.

O'Connell, L. et al. (2018) Fine grained compositional analysis of PEI Everglades Inlet microbiome using high throughput DNA sequencing. *Peer J,* 6, e4671. https://doi.org/10.7717/peerj.4671.

Oksanen, J., et al. (2018) Vegan: Community Ecology Package.

Pawlowski, J., Bruce, K., Panksep, K., Aguirre, F. I., Amalfitano, S., Apothéloz-Perret-Gentil, L., ... & Fazi, S. (2022). Environmental DNA metabarcoding for benthic monitoring: A review of sediment sampling and DNA extraction methods. *Science of the Total Environment*, *818*, 151783.

Precht, W. F., Gintert, B. E., Robbart, M. L., Fura, R., and van Woesik, R. (2016). Unprecedented disease-related coral mortality in southeastern Florida. *Sci. Rep.* 6:31374. doi: 10.1038/srep31374.

Peixoto, R. S., Sweet, M., Villela, H. D., Cardoso, P., Thomas, T., Voolstra, C. R., ... & Bourne, D. G. (2021). Coral probiotics: premise, promise, prospects. *Annual review of animal biosciences*, *9*(1), 265-288.

Rainey, F. A., Ward-Rainey, N., Gliesche, C. G., & Stackebrandt, E. (1998). Phylogenetic analysis and intrageneric structure of the genus Hyphomicrobium and the related genus Filomicrobium. *International journal of systematic and evolutionary microbiology*, *48*(3), 635-639.

Reichelt-Brushett, A. J. & Harrison, P. L. (1999) The effect of copper, zinc and cadmium on fertilization success of gametes from scleractinian reef corals. *Mar Poll Bull*, 38:182-187.

Reichelt-Brushett, A. J. & McOrist, G. (2003). Trace metals in the living and nonliving components of scleractinian corals. *Mar Poll Bull*, 46(12):1573-1582.

Shah, S. B. (2021). Heavy metals in the marine environment—an overview. *Heavy metals in Scleractinian corals*, 1-26.

Shinzato, C., Narisoko, H., Nishitsuji, K., Nagata, T., Satoh, N., & Inoue, J. (2021). Novel mitochondrial DNA markers for scleractinian corals and generic-level environmental DNA metabarcoding. *Frontiers in Marine Science*, *8*, 758207.

Skelton, E. (2024). Assessment and prioritization of contaminants of concern along florida's coral reef . NSU Masters Thesis. NSUWorkds.

Studivan, M. S., Rossin, A. M., Rubin, E., Soderberg, N., Holstein, D. M., & Enochs, I. C. (2022). Reef Sediments Can Act As a Stony Coral Tissue Loss Disease Vector. *Frontiers in Marine Science, 8*. doi:10.3389/fmars.2021.815698.

Taberlet, P., Coissac, E., Pompanon, F., Brochmann, C., & Willerslev, E. (2012). Towards next-generation biodiversity assessment using DNA metabarcoding. *Molecular ecology*, *21*(8), 2045-2050.

Thompson, L. R. et al. (2017) A communal catalogue reveals Earth's multiscale microbial diversity. *Nature,* 551, 457-463.

Walker, B. K. (2012). Spatial analyses of benthic habitats to define coral reef ecosystem regions and potential biogeographic boundaries along a latitudinal gradient. *PloS one*, *7*(1), e30466.

Walker BK, Williams GJ, Aeby GS, Maynard JA and Whitall D. 2022. Environmental and human drivers of stony coral tissue loss disease (SCTLD) incidence within the Southeast Florida Coral Reef Ecosystem Conservation Area, 2021-22. Final Report. Florida DEP. Miami, FL., 36 p

6. APPENDICES

6.1 Sample IDs for 171 NCRMP collections in 2022

SiteID	lon_ssu	lat_ssu	strat	StratReg Ru	County	Depth	Date	Distance.from.shore	Closest.Inlet
3002	-80.01347	26.715884	DPRC	DPRC 15 0	Palm Beach	27	8/12/22	1942	Lake Worth Inlet
3004	-80.014336	26.716299	DPRC	DPRC 15 0	Palm Beach	25	8/8/22	1859	Lake Worth Inlet
3005	-80.012315	26.718172	DPRC	DPRC 15 0	Palm Beach	28	9/16/22	2084	Lake Worth Inlet
3006	-80.012018	26.830213	DPRC	DPRC 16 0	Palm Beach	26	8/10/22	2685	Lake Worth Inlet
3007	-80.009806	26.868336	DPRC	DPRC 16 0	Palm Beach	24	8/11/22	3763	Jupiter Inlet
3008	-80.014125	26.821413	DPRC	DPRC 16 0	Palm Beach	26	8/10/22	2235	Lake Worth Inlet
3010	-79.994424	26.875703	DPRC	DPRC 16 0	Palm Beach	31	9/16/22	5444	Jupiter Inlet
3011	-80.027487	26.865135	DPRC	DPRC 16 0	Palm Beach	25	8/11/22	1974	Jupiter Inlet
3012	-80.005982	26.862665	DPRC	DPRC 16 0	Palm Beach	25	8/11/22	4015	Jupiter Inlet
3013	-80.011687	26.829901	DPRC	DPRC 16 0	Palm Beach	26	8/10/22	2712	Lake Worth Inlet
3015	-80.009269	26.907303	DPRC	DPRC 16 0	Palm Beach	25	8/9/22	4896	Jupiter Inlet
3019	-79.997377	26.900713	DPRC	DPRC 16 0	Palm Beach	30	8/9/22	5881	Jupiter Inlet
3021	-80.013775	26.887554	DPRC	DPRC 16 1	Palm Beach	25	8/11/22	3922	Jupiter Inlet
3022	-80.008197	26.7437	DPRC	DPRC 16 1	Palm Beach	30	8/12/22	2667	Lake Worth Inlet
3023	-80.016626	26.834038	DPRC	DPRC 16 1	Palm Beach	22	8/9/22	2322	Lake Worth Inlet
3024	-79.99706	26.91891	DPRC	DPRC 16 1	Palm Beach	29	8/9/22	6422	Jupiter Inlet
3025	-80.020344	26.860962	DPRC	DPRC 16 1	Palm Beach	26	9/16/22	2577	Jupiter Inlet
3026	-80.019467	26.872116	DPRC	DPRC 16 1	Palm Beach	25	8/11/22	2936	Jupiter Inlet
3028	-80.004836	26.835609	DPRC	DPRC 16 1	Palm Beach	27	8/10/22	3506	Lake Worth Inlet
3029	-80.005727	26.902103	DPRC	DPRC 16 1	Palm Beach	25	8/9/22	5111	Jupiter Inlet
3033	-80.102159	25.970362	INNR	INNR 13 0	Miami-Dade	11	6/16/22	1635	Haulover Inlet
3034	-80.100003	25.943828	INNR	INNR 13 0	Miami-Dade	13	7/21/22	1964	Haulover Inlet
3035	-80.100261	26.048691	INNR	INNR 13 0	Broward	9	7/13/22	1166	Port Everglades
3036	-80.09695	26.063049	INNR	INNR 13 0	Broward	11	6/23/22	1365	Port Everglades
3037	-80.094241	26.118228	INNR	INNR 13 0	Broward	7	6/24/22	946	Port Everglades

3038	-80.097013	26.057783	INNR	INNR 13 0	Broward	13	8/23/22	1395	Port Everglades
3039	-80.102378	25.945675	INNR	INNR 13 0	Miami-Dade	10	7/21/22	1718	Haulover Inlet
3040	-80.09912	26.07526	INNR	INNR 13 0	Broward	9	6/17/22	1021	Port Everglades
3041	-80.097459	26.083	INNR	INNR 13 0	Broward	8	7/21/22	1164	Port Everglades
3043	-80.099491	25.871431	INNR	INNR 13 0	Miami-Dade	15	9/14/22	2031	Haulover Inlet
3045	-80.095341	26.073108	INNR	INNR 13 0	Broward	11	8/23/22	1418	Port Everglades
3047	-80.103327	25.944914	INNR	INNR 13 0	Miami-Dade	9	7/21/22	1626	Haulover Inlet
3048	-80.088442	26.149659	INNR	INNR 13 0	Broward	12	10/14/22	1172	Port Everglades
3050	-80.092665	26.105733	INNR	INNR 13 0	Broward	12	7/20/22	1232	Port Everglades
3051	-80.105925	25.871257	INNR	INNR 13 0	Miami-Dade	7	9/14/22	1387	Haulover Inlet
3053	-80.09192	26.11593	INNR	INNR 13 0	Broward	11	6/24/22	1176	Port Everglades
3054	-80.099795	25.965749	INNR	INNR 13 0	Miami-Dade	12	6/16/22	1879	Haulover Inlet
3055	-80.10204	26.00571	INNR	INNR 13 1	Broward	8	7/13/22	1367	Port Everglades
3056	-80.088558	26.151702	INNR	INNR 13 1	Broward	11	7/20/22	1135	Port Everglades
3059	-80.100031	25.933788	INNR	INNR 13 1	Miami-Dade	10	7/21/22	2071	Haulover Inlet
3060	-80.087353	26.17592	INNR	INNR 13 1	Broward	7	6/29/22	889	Hillsboro Inlet
3061	-80.100466	25.999738	INNR	INNR 13 1	Broward	12	7/13/22	1564	Port Everglades
3068	-80.1022	25.99901	INNR	INNR 13 1	Broward	8.6	8/16/22	1401	Port Everglades
3069	-80.1005	25.86575	INNR	INNR 13 1	Miami-Dade	9.3	9/14/22	1930	Haulover Inlet
3070	-80.1005	25.9189	INNR	INNR 13 1	Miami-Dade	11.3	6/28/22	2118	Haulover Inlet
3071	-80.1024	25.98994	INNR	INNR 13 1	Broward	9.9	8/23/22	1471	Haulover Inlet
3073	-80.10442	25.867564	INNR	INNR 13 1	Miami-Dade	7	9/14/22	1537	Haulover Inlet
3076	-80.101833	25.888842	INNR	INNR 13 1	Miami-Dade	8	8/16/22	1996	Haulover Inlet
3078	-80.10138	26.00755	INNR	INNR 13 1	Broward	10	7/13/22	1417	Port Everglades
3079	-80.091781	26.084793	MIDR	MIDR 13 0	Broward	15	6/24/22	1730	Port Everglades
3081	-80.09526	26.01609	MIDR	MIDR 13 0	Broward	16	6/23/22	1963	Port Everglades
3082	-80.095214	25.972767	MIDR	MIDR 13 0	Miami-Dade	15	6/16/22	2316	Haulover Inlet
3083	-80.08122	26.18661	MIDR	MIDR 13 0	Broward	14	6/29/22	1350	Hillsboro Inlet

3085	-80.07683	26.2212	MIDR	MIDR 13 0	Broward	14	6/29/22	1280	Hillsboro Inlet
3086	-80.094263	25.940909	MIDR	MIDR 13 0	Miami-Dade	15	7/21/22	2561	Haulover Inlet
3091	-80.092766	25.91311	MIDR	MIDR 13 0	Miami-Dade	18	6/28/22	2910	Haulover Inlet
3093	-80.084965	26.124769	MIDR	MIDR 13 0	Broward	17	6/21/22	1776	Port Everglades
3094	-80.096071	26.008838	MIDR	MIDR 13 0	Broward	16	6/23/22	1939	Port Everglades
3097	-80.089261	26.091843	MIDR	MIDR 13 0	Broward	17	6/24/22	1655	Port Everglades
3098	-80.09909	25.92151	MIDR	MIDR 13 0	Miami-Dade	14	8/16/22	2242	Haulover Inlet
3099	-80.093159	26.068823	MIDR	MIDR 13 0	Broward	12	8/23/22	1709	Port Everglades
3101	-80.0867	26.125389	MIDR	MIDR 13 0	Broward	14	6/21/22	1599	Port Everglades
3103	-80.06066	26.38536	MIDR	MIDR 14 0	Palm Beach	10	8/12/22	559	Boca Raton Inlet
3104	-80.06062	26.39027	MIDR	MIDR 14 0	Palm Beach	10	10/14/22	505	Boca Raton Inlet
3105	-80.062494	26.371778	MIDR	MIDR 14 0	Palm Beach	10	7/11/22	455	Boca Raton Inlet
3109	-80.080218	26.16819	MIDR	MIDR 13 1	Broward	20	7/20/22	1696	Port Everglades
3110	-80.08654	26.10809	MIDR	MIDR 13 1	Broward	19	6/24/22	1774	Port Everglades
3112	-80.091053	26.095281	MIDR	MIDR 13 1	Broward	12	6/24/22	1402	Port Everglades
3114	-80.091567	26.070189	MIDR	MIDR 13 1	Broward	18	8/23/22	1842	Port Everglades
3115	-80.07174	26.249769	MIDR	MIDR 13 1	Broward	18	10/12/22	1256	Hillsboro Inlet
3119	-80.095759	25.990751	MIDR	MIDR 13 1	Broward	17	9/14/22	2125	Haulover Inlet
3120	-80.085261	26.115508	MIDR	MIDR 13 1	Broward	21	6/24/22	1843	Port Everglades
3121	-80.09283	25.86967	MIDR	MIDR 13 1	Miami-Dade	20	8/16/22	2691	Haulover Inlet
3122	-80.067371	26.294385	MIDR	MIDR 14 1	Broward	17	7/20/22	979	Boca Raton Inlet
3123	-80.069219	26.280945	MIDR	MIDR 14 1	Broward	22	10/12/22	904	Hillsboro Inlet
3124	-80.068113	26.299452	MIDR	MIDR 14 1	Broward	13	7/11/22	835	Boca Raton Inlet
3126	-80.06364	26.27572	MIDR	MIDR 14 1	Broward	20	10/12/22	1512	Hillsboro Inlet
3127	-80.104917	26.019365	NEAR	NEAR 13 0	Broward	8	6/23/22	974	Port Everglades
3128	-80.10992	25.89236	NEAR	NEAR 13 0	Miami-Dade	7	8/16/22	1224	Haulover Inlet
3130	-80.11306	25.982823	NEAR	NEAR 13 0	Broward	7	6/16/22	509	Haulover Inlet
3136	-80.101093	26.065362	NEAR	NEAR 13 0	Broward	8	6/23/22	937	Port Everglades

3139	-80.102533	26.063605	NEAR	NEAR 13 0	Broward	8	8/23/22	802	Port Everglades
3141	-80.09609	26.10659	NEAR	NEAR 13 0	Broward	6	6/24/22	876	Port Everglades
3143	-80.11536	25.91446	NEAR	NEAR 13 0	Miami-Dade	7	8/16/22	644	Haulover Inlet
3144	-80.086195	26.221669	NEAR	NEAR 13 0	Broward	5	10/12/22	344	Hillsboro Inlet
3145	-80.109511	26.033507	NEAR	NEAR 13 0	Broward	8	6/17/22	432	Port Everglades
3149	-80.10575	25.89924	NEAR	NEAR 13 0	Miami-Dade	8	8/16/22	1678	Haulover Inlet
3150	-80.102148	25.913343	NEAR	NEAR 13 0	Miami-Dade	10	6/28/22	1970	Haulover Inlet
3152	-80.07565	26.28055	NEAR	NEAR 14 0	Broward	6	6/27/22	272	Hillsboro Inlet
3153	-80.076843	26.26228	NEAR	NEAR 14 0	Broward	7	10/12/22	281	Hillsboro Inlet
3154	-80.074278	26.310713	NEAR	NEAR 14 0	Broward	3	6/27/22	119	Boca Raton Inlet
3156	-80.035623	26.662808	NEAR	NEAR 15 0	Palm Beach	2	9/15/22	66	Lake Worth Inlet
3157	-80.030995	26.693869	NEAR	NEAR 15 0	Palm Beach	3	8/11/22	260	Lake Worth Inlet
3159	-80.031325	26.728926	NEAR	NEAR 16 0	Palm Beach	6	8/9/22	347	Lake Worth Inlet
3177	-80.08859	26.17106	NEAR	NEAR 13 1	Broward	5	6/29/22	842	Hillsboro Inlet
3178	-80.11182	26.02488	NEAR	NEAR 13 1	Broward	5	6/17/22	252	Port Everglades
3179	-80.028455	26.709576	NEAR	NEAR 15 1	Palm Beach	7	8/11/22	445	Lake Worth Inlet
3182	-80.02953	26.72322	NEAR	NEAR 16 1	Palm Beach	8	8/8/22	501	Lake Worth Inlet
3183	-80.030714	26.723844	NEAR	NEAR 16 1	Palm Beach	3	8/8/22	389	Lake Worth Inlet
3189	-80.08717	26.02401	OFFR	OFFR 13 0	Broward	15	6/17/22	2722	Port Everglades
3190	-80.089058	26.030535	OFFR	OFFR 13 0	Broward	18	7/21/22	2483	Port Everglades
3193	-80.089795	25.97243	OFFR	OFFR 13 0	Miami-Dade	26	7/21/22	2860	Haulover Inlet
3194	-80.088374	26.023986	OFFR	OFFR 13 0	Broward	17	6/17/22	2601	Port Everglades
3195	-80.089693	26.027249	OFFR	OFFR 13 0	Broward	17	6/17/22	2445	Port Everglades
3200	-80.06647	26.25029	OFFR	OFFR 13 0	Broward	20	10/12/22	1620	Hillsboro Inlet
3201	-80.09046	26.01376	OFFR	OFFR 13 0	Broward	18	6/17/22	2462	Port Everglades
3202	-80.068977	26.22424	OFFR	OFFR 13 0	Broward	33	6/29/22	2046	Hillsboro Inlet
3204	-80.058683	26.314054	OFFR	OFFR 14 0	Broward	33	6/27/22	1624	Boca Raton Inlet
3205	-80.053392	26.376553	OFFR	OFFR 14 0	Palm Beach	33	7/20/22	1321	Boca Raton Inlet

3206	-80.018739	26.672966	OFFR	OFFR 15 0	Palm Beach	23	8/8/22	1707	Lake Worth Inlet
3207	-80.027718	26.561831	OFFR	OFFR 15 0	Palm Beach	23	10/14/22	1230	Boynton Inlet
3208	-80.018077	26.687709	OFFR	OFFR 15 0	Palm Beach	18	8/8/22	1597	Lake Worth Inlet
3209	-80.040744	26.4846	OFFR	OFFR 15 0	Palm Beach	19	7/12/22	1312	Boynton Inlet
3211	-80.019711	26.629556	OFFR	OFFR 15 0	Palm Beach	27	9/15/22	1706	Boynton Inlet
3212	-80.017141	26.663139	OFFR	OFFR 15 0	Palm Beach	25	8/8/22	1894	Lake Worth Inlet
3213	-80.034273	26.508284	OFFR	OFFR 15 0	Palm Beach	20	7/12/22	1617	Boynton Inlet
3214	-80.027412	26.550777	OFFR	OFFR 15 0	Palm Beach	32	9/16/22	1438	Boynton Inlet
3215	-80.018349	26.717001	OFFR	OFFR 16 0	Palm Beach	20	8/10/22	1471	Lake Worth Inlet
3216	-80.015932	26.734684	OFFR		Palm Beach	23	8/8/22	1880	Lake Worth Inlet
3218	-80.068337	26.225584	OFFR	OFFR 13 1	Broward	23	6/29/22	2103	Hillsboro Inlet
3219	-80.088548	26.002333	OFFR	OFFR 13 1	Broward	27	7/13/22	2732	Port Everglades
3220	-80.06863	26.22934	OFFR	OFFR 13 1	Broward	22	6/29/22	2036	Hillsboro Inlet
3221	-80.089188	25.97121	OFFR	OFFR 13 1	Miami-Dade	28	6/16/22	2928	Haulover Inlet
3222	-80.089515	25.967054	OFFR	OFFR 13 1	Miami-Dade	26	6/16/22	2899	Haulover Inlet
3224	-80.08709	26.02718	OFFR	OFFR 13 1	Broward	19	6/17/22	2706	Port Everglades
3230	-80.088613	26.003362	OFFR	OFFR 13 1	Broward	28	7/13/22	2727	Port Everglades
3232	-80.064678	26.25819	OFFR	OFFR 13 1	Broward	18	10/12/22	1518	Hillsboro Inlet
3233	-80.084564	26.080083	OFFR	OFFR 13 1	Broward	21	6/23/22	2465	Port Everglades
3235	-80.090311	26.01747	OFFR	OFFR 13 1	Broward	18	6/23/22	2445	Port Everglades
3236	-80.088957	25.893989	OFFR	OFFR 13 1	Miami-Dade	17	6/28/22	3323	Haulover Inlet
3237	-80.057311	26.331666	OFFR	OFFR 14 1	Palm Beach	22	6/27/22	1396	Boca Raton Inlet
3239	-80.062966	26.271323	OFFR	OFFR 14 1	Broward	21	10/12/22	1607	Hillsboro Inlet
3240	-80.055717	26.345315	OFFR	OFFR 14 1	Palm Beach	21	6/27/22	1357	Boca Raton Inlet
3241	-80.054778	26.375115	OFFR	OFFR 14 1	Palm Beach	16	7/20/22	1193	Boca Raton Inlet
3243	-80.022617	26.613005	OFFR	OFFR 15 1	Palm Beach	21	8/12/22	1387	Boynton Inlet
3244	-80.031789	26.512256	OFFR	OFFR 15 1	Palm Beach	23	10/14/22	1763	Boynton Inlet
3245	-80.032761	26.514232	OFFR	OFFR 15 1	Palm Beach	15	7/12/22	1616	Boynton Inlet

3246	-80.024437	26.581304	OFFR	OFFR 15 1	Palm Beach	18	10/14/22	1299	Boynton Inlet
3248	-80.014652	26.71285	OFFR	OFFR 15 1	Palm Beach	27	8/12/22	1816	Lake Worth Inlet
3249	-80.045246	26.447717	OFFR	OFFR 15 1	Palm Beach	26	7/11/22	1405	Boynton Inlet
3250	-80.046712	26.440057	OFFR	OFFR 15 1	Palm Beach	26	7/11/22	1371	Boynton Inlet
3252	-80.027389	26.550904	OFFR	OFFR 15 1	Palm Beach	26	9/16/22	1439	Boynton Inlet
3253	-80.03951	26.48697	OFFR	OFFR 15 1	Palm Beach	19	7/12/22	1381	Boynton Inlet
3254	-80.034541	26.5057	OFFR	OFFR 15 1	Palm Beach	20	7/12/22	1633	Boynton Inlet
3255	-80.01555	26.73186	OFFR	OFFR 16 1	Palm Beach	23	8/8/22	1917	Lake Worth Inlet
3257	-80.087657	25.939768	PTDP	PTDP 13 0	Miami-Dade	27	6/28/22	3231	Haulover Inlet
3258	-80.085016	26.058559	PTDP	PTDP 13 0	Broward	30	6/23/22	2591	Port Everglades
3259	-80.061008	26.284696	PTDP	PTDP 14 0	Broward	32	7/20/22	1690	Hillsboro Inlet
3260	-80.05926	26.297318	PTDP	PTDP 14 0	Broward	31	6/27/22	1749	Boca Raton Inlet
3262	-80.018742	26.640762	PTDP	PTDP 15 0	Palm Beach	22	9/15/22	1851	Boynton Inlet
3263	-80.018068	26.723756	PTDP	PTDP 16 0	Palm Beach	21	8/9/22	1634	Lake Worth Inlet
3264	-80.01789	26.724254	PTDP	PTDP 16 0	Palm Beach	20	8/10/22	1661	Lake Worth Inlet
3273	-80.069414	26.208173	PTDP	PTDP 13 1	Broward	31	6/29/22	2216	Hillsboro Inlet
3274	-80.078086	26.133625	PTDP	PTDP 13 1	Broward	30	6/21/22	2429	Port Everglades
3275	-80.079772	26.123554	PTDP	PTDP 13 1	Broward	26	6/21/22	2305	Port Everglades
3279	-80.056609	26.329079	PTDP	PTDP 14 1	Palm Beach	26	6/27/22	1582	Boca Raton Inlet
3280	-80.060262	26.294045	PTDP	PTDP 14 1	Broward	26	7/20/22	1690	Boca Raton Inlet
3282	-80.051885	26.396544	PTDP	PTDP 15 1	Palm Beach	25	7/11/22	1296	Boca Raton Inlet
3284	-80.025791	26.572429	PTDP	PTDP 15 1	Palm Beach	21	10/14/22	1269	Boynton Inlet
3285	-80.016219	26.825173	PTDP	PTDP 16 1	Palm Beach	25	8/10/22	2184	Lake Worth Inlet
3286	-80.01788	26.72541	PTDP	PTDP 16 1	Palm Beach	21	8/12/22	1675	Lake Worth Inlet
3292	-80.021038	26.640706	PTSH	PTSH 15 2	Palm Beach	19	9/15/22	1622	Boynton Inlet
3293	-80.019132	26.719753	PTSH	PTSH 16 2	Palm Beach	19	9/16/22	1450	Lake Worth Inlet
3294	-80.019243	26.736325	PTSH	PTSH 16 2	Palm Beach	20	8/10/22	1551	Lake Worth Inlet

6.2. Sample IDs and sites for NCRMP collections in 2024

Sample	lat_degree	lon_degree	depth
3001	26.72276000	-80.02931100	8.8
3006	26.71763000	-80.02969700	7.5
3014	26.72505000	-80.01680600	21.6
3015	26.86834000	-80.01740200	21.7
3023	26.83609500	-80.01175900	21.3
3030	26.95574600	-80.01139600	23.0
3031	26.86302100	-79.99618500	31.1
3037	26.85148900	-80.00089000	30.8
3041	26.92875800	-80.03519300	23.1
3080	26.11672200	-80.09458200	7.1
3084	25.91110300	-80.10266000	9.3
3097	26.05629900	-80.10206700	6.7
3098	26.07464300	-80.10737000	5.2
3099	26.04502900	-80.10263600	8.3
3100	26.21600300	-80.08537300	3.5
3101	26.03707800	-80.10421500	8.3
3105	26.11054400	-80.09714700	5.2
3107	25.90954300	-80.10121500	11.1
3109	26.12623300	-80.09844400	6.0
3110	25.89793500	-80.10211300	9.9
3114	26.26076300	-80.07701600	7.6
3115	26.38084600	-80.06149900	9.1
3117	26.32536100	-80.07225400	2.8
3121	26.68301800	-80.03148500	3.8
3122	26.68103089	-80.03098667	6.7
3124	26.68790514	-80.03216070	3.3
3125	26.03986900	-80.09931700	8.5
3126	26.01965400	-80.10033100	9.9
3127	26.08651900	-80.10407800	4.8
3128	26.02872500	-80.10091800	8.2
3130	26.21569700	-80.08181400	10.1
3132	26.17700200	-80.09333500	5.4
3135	26.06551200	-80.09973800	8.8
3136	26.04790300	-80.10568300	5.8
3137	25.93891000	-80.10890800	5.1
3139	26.03373300	-80.09947100	10.3
3151	26.31879200	-80.06696300	11.9

3152	26.38195000	-80.06115900	9.7
3155	26.71013300	-80.02962600	4.0
3156	26.66240397	-80.03559151	2.7
3163	26.02185500	-80.08839900	17.4
3174	26.99955100	-80.10033600	12.4
3185	25.96605900	-80.09734000	13.3
3189	25.99497100	-80.09941800	12.2
3195	25.88826000	-80.10020200	13.8
3200	26.26412600	-80.07207900	13.2
3201	26.30044700	-80.06761000	13.6
3206	26.62038500	-80.02285200	16.7
3207	26.69130200	-80.01792000	16.5
3208	26.52945600	-80.03020900	21.9
3209	26.42366900	-80.05003300	17.2
3213	26.04498600	-80.09395200	15.9
3220	26.13679000	-80.08315500	18.1
3226	26.15602900	-80.08165300	21.8
3229	26.05896100	-80.09140500	17.0
3237	26.17643900	-80.07409200	17.4
3240	26.26670600	-80.06505500	20.2
3241	26.27140000	-80.07070700	13.6
3243	26.37468700	-80.05461327	16.6
3244	26.32640600	-80.05788400	19.9
3246	26.52139000	-80.03164000	17.7
3248	26.62636700	-80.02329300	13.7
3249	26.46692300	-80.04382600	20.7
3257	25.92602900	-80.08734300	31.3
3259	26.37418400	-80.05255700	26.5
3260	26.38784900	-80.05120000	28.0
3262	26.51760600	-80.03006200	32.2
3266	26.58932900	-80.02337400	23.3
3267	26.61282300	-80.02115400	29.9
3270	25.89831600	-80.08783200	23.0
3274	26.14087319	-80.07738500	26.2
3275	26.21113000	-80.06898500	32.7
3276	26.03602100	-80.08573000	25.2
3280	26.16532200	-80.07371900	30.7
3289	26.29270300	-80.06011600	25.4
3295	26.47324300	-80.04184100	22.0
3296	26.54341400	-80.02749100	26.0
3299	26.68345000	-80.01764900	22.0

3600	26.72854600	-80.03133100	5.6
3601	26.72708500	-80.03196500	4.4
3603	26.72375100	-80.03095500	7.4
3609	26.77797900	-80.01135100	15.8

6.3 Candidate qPCR sequences

Gene target and ID	Primer Sequences	
fucose LVEMEA F	CTCGTGGAAATGGAGGCAGT	
fucose GPRDNF rc	CGAAGTTATCTCGGGGTCCG	
fucose 2 -QERSCK- F	CAGGAACGTAGCTGCAAGGA	
fucose 2-RC	CTGAGCCTGAACCAAGAGCA	
Epimerase 5-PPMDMF- F	ACCGCCCATGGATATGTTCC	
Epimerase 5 RC	GCCGTCGCCCCAGATAATAA	
Epimerase 6 -DILCQA -F	AGATATCCTGTGCCAAGCCG	
Epimerase 6 RC	AACATATCCATGGGCGGTCC	
PEI Bathyarchaeia Catalase F	ACGTGGTTCTGCCGATACAG	
PEI Bathyarchaeia Catalase RC	GGTCAAGACTATGCACCCCC	
Hexulose-FormAssimil F	GTAACGATCTCGGGTCTGGC	
Hexulose-FormAssimil RC	TTGAGCTGTACACGGTGGAG	

6.3 Similarity percentages of the Top 20 sediment microbial families by Inlet Exposure Area.

Group Lake Worth					
Average similarity: 55.71					
Species	**Av.Abund**	**Av.Sim**	**Sim/SD**	**Contrib%**	**Cum.%**
Bacillaceae	0.43	11.87	1.06	21.3	21.3
Moraxellaceae	0.44	10.7	0.72	19.21	40.51
Pirellulaceae	0.19	5.97	3.59	10.71	51.22
uncultured	0.14	3.87	1.99	6.94	58.17
Woeseiaceae	0.12	2.72	1.5	4.89	63.06
Thermoanaerobaculaceae	0.09	2.25	1.6	4.04	67.1
Nitrosococcaceae	0.1	2.23	1.37	4.01	71.11
Rhodobacteraceae	0.07	1.96	1.53	3.52	74.63
Hyphomicrobiaceae	0.06	1.95	2.71	3.49	78.13
Nitrosopumilaceae	0.08	1.84	1.38	3.3	81.42
Rhizobiaceae	0.06	1.76	1.99	3.16	84.58
Desulfosarcinaceae	0.07	1.74	1.7	3.12	87.7
NB1-j	0.09	1.68	0.94	3.01	90.71
Kiloniellaceae	0.09	1.64	1.01	2.94	93.65
Desulfocapsaceae	0.05	1.24	1.27	2.22	95.87
Flavobacteriaceae	0.04	0.94	1.44	1.69	97.57
Planococcaceae	0.07	0.6	0.34	1.08	98.65
Vibrionaceae	0.05	0.57	0.89	1.02	99.68
Pseudoalteromonadaceae	0.02	0.17	0.39	0.31	99.98
Halomonadaceae	0	0.01	0.15	0.02	100

Group Boynton					
Average similarity: 59.89					
Species	**Av.Abund**	**Av.Sim**	**Sim/SD**	**Contrib%**	**Cum.%**
Bacillaceae	0.51	14.14	1.06	23.6	23.6
Moraxellaceae	0.33	6.39	0.59	10.67	34.28
Pirellulaceae	0.17	5.75	3.71	9.61	43.89
uncultured	0.13	4.19	3.21	6.99	50.88
Rhodobacteraceae	0.14	4.1	2.62	6.84	57.72
Desulfocapsaceae	0.11	3.24	2.16	5.41	63.13
Woeseiaceae	0.11	2.87	1.96	4.79	67.92
Desulfosarcinaceae	0.1	2.85	2.23	4.76	72.68
Hyphomicrobiaceae	0.08	2.67	3.52	4.46	77.14
Rhizobiaceae	0.08	2.43	3.08	4.06	81.2
Thermoanaerobaculaceae	0.07	2.16	2.93	3.61	84.81
Planococcaceae	0.1	2.09	0.78	3.48	88.29
Flavobacteriaceae	0.07	2.04	2.61	3.4	91.7
Nitrosococcaceae	0.06	1.56	1.83	2.61	94.31
NB1-j	0.06	1.17	1.06	1.95	96.25
Kiloniellaceae	0.06	1.11	1.03	1.86	98.11
Nitrosopumilaceae	0.04	0.5	0.63	0.84	98.95
Vibrionaceae	0.08	0.5	0.3	0.83	99.78
Pseudoalteromonadaceae	0.01	0.07	0.2	0.11	99.9
Halomonadaceae	0.01	0.06	0.27	0.1	100

Group Boca					
Average similarity: 56.24					
Species	**Av.Abund**	**Av.Sim**	**Sim/SD**	**Contrib%**	**Cum.%**
Moraxellaceae	0.55	15.62	1.17	27.78	27.78
Rhodobacteraceae	0.17	5.17	2.83	9.18	36.96
Pirellulaceae	0.14	4.49	3.54	7.98	44.95
uncultured	0.12	3.29	2.41	5.85	50.8
Bacillaceae	0.2	2.96	0.59	5.27	56.07
Woeseiaceae	0.12	2.74	1.78	4.88	60.94
Rhizobiaceae	0.07	2.44	4.67	4.33	65.27
Desulfocapsaceae	0.08	2.35	2.46	4.18	69.45
Hyphomicrobiaceae	0.07	2.33	5.1	4.15	73.6
Desulfosarcinaceae	0.1	2.16	1.46	3.83	77.44
Flavobacteriaceae	0.12	2.07	0.91	3.68	81.11
Planococcaceae	0.15	2.06	0.85	3.66	84.77
NB1-j	0.09	1.46	0.83	2.59	87.36
Thermoanaerobaculaceae	0.07	1.42	1.23	2.52	89.89
Kiloniellaceae	0.08	1.28	0.75	2.28	92.17
Halomonadaceae	0.14	1.28	0.44	2.27	94.45
Nitrosococcaceae	0.07	1.17	0.98	2.08	96.52
Nitrosopumilaceae	0.08	1.15	0.71	2.05	98.57
Vibrionaceae	0.04	0.58	0.86	1.03	99.6
Pseudoalteromonadaceae	0.06	0.23	0.17	0.4	100

Group Hillsboro					
Average similarity: 48.71					
Species	**Av.Abund**	**Av.Sim**	**Sim/SD**	**Contrib%**	**Cum.%**
Bacillaceae	0.43	10.06	0.7	20.65	20.65
Planococcaceae	0.19	4.58	0.83	9.39	30.04
Pirellulaceae	0.14	4.48	3.12	9.2	39.24
Moraxellaceae	0.29	4.48	0.41	9.19	48.43
uncultured	0.13	3.33	1.7	6.85	55.28
Rhodobacteraceae	0.13	3.3	2.28	6.78	62.05
Woeseiaceae	0.11	2.63	1.5	5.39	67.44
Hyphomicrobiaceae	0.07	2.31	2.51	4.74	72.19
Desulfosarcinaceae	0.11	2.28	1.46	4.68	76.87
Rhizobiaceae	0.07	1.89	2.03	3.88	80.75
Desulfocapsaceae	0.07	1.65	1.23	3.4	84.15
Thermoanaerobaculaceae	0.07	1.61	1.3	3.3	87.45
Nitrosococcaceae	0.07	1.45	1.3	2.98	90.43
Kiloniellaceae	0.08	1.2	0.72	2.45	92.88
NB1-j	0.07	1.12	0.8	2.29	95.18
Flavobacteriaceae	0.05	1	1.25	2.05	97.23
Nitrosopumilaceae	0.06	0.87	0.76	1.8	99.02
Vibrionaceae	0.02	0.3	0.5	0.62	99.65
Halomonadaceae	0.06	0.14	0.28	0.28	99.93
Pseudoalteromonadaceae	0.01	0.04	0.32	0.07	100

Group PortEver					
Average similarity: 49.43					
Species	**Av.Abund**	**Av.Sim**	**Sim/SD**	**Contrib%**	**Cum.%**
Moraxellaceae	0.53	15.99	0.83	32.36	32.36
Pirellulaceae	0.14	4.67	2.5	9.45	41.8
Bacillaceae	0.22	3.59	0.53	7.27	49.07
Rhodobacteraceae	0.11	3.51	2.65	7.09	56.16
uncultured	0.11	2.96	1.8	6	62.16
Hyphomicrobiaceae	0.08	2.94	4.4	5.94	68.1
Rhizobiaceae	0.07	2.35	3.09	4.76	72.86
Woeseiaceae	0.09	1.91	1.1	3.86	76.72
Desulfocapsaceae	0.06	1.73	1.69	3.49	80.21
Flavobacteriaceae	0.08	1.64	1.05	3.32	83.52
Desulfosarcinaceae	0.07	1.43	1.21	2.9	86.42
Thermoanaerobaculaceae	0.06	1.19	1.16	2.41	88.83
Kiloniellaceae	0.06	1.16	0.97	2.34	91.17
Planococcaceae	0.08	0.91	0.35	1.84	93.01
Nitrosococcaceae	0.05	0.82	0.71	1.66	94.67
NB1-j	0.05	0.79	0.67	1.59	96.26
Nitrosopumilaceae	0.05	0.75	0.67	1.51	97.77
Pseudoalteromonadaceae	0.11	0.5	0.14	1.01	98.78
Halomonadaceae	0.07	0.39	0.26	0.8	99.58
Vibrionaceae	0.02	0.21	0.48	0.42	100

Group Haulover					
Average similarity: 53.42					
Species	**Av.Abund**	**Av.Sim**	**Sim/SD**	**Contrib%**	**Cum.%**
Moraxellaceae	0.59	19.72	1.2	36.91	36.91
Pirellulaceae	0.16	4.73	2.33	8.86	45.76
Rhodobacteraceae	0.13	3.58	1.93	6.69	52.46
Bacillaceae	0.19	3.27	0.63	6.12	58.58
uncultured	0.11	2.91	1.61	5.44	64.02
Hyphomicrobiaceae	0.09	2.77	2.54	5.19	69.21
Woeseiaceae	0.1	2.17	1.29	4.06	73.26
Planococcaceae	0.15	2.15	0.48	4.02	77.28
Rhizobiaceae	0.07	2.03	1.95	3.8	81.08
Flavobacteriaceae	0.1	1.86	0.94	3.49	84.57
Desulfocapsaceae	0.08	1.83	1.51	3.43	88
Desulfosarcinaceae	0.07	1.37	1.03	2.56	90.56
Thermoanaerobaculaceae	0.05	1.01	1.05	1.9	92.46
Kiloniellaceae	0.05	0.85	0.78	1.58	94.04
Nitrosococcaceae	0.04	0.8	1.04	1.49	95.53
NB1-j	0.05	0.75	0.64	1.4	96.93
Nitrosopumilaceae	0.04	0.7	0.81	1.3	98.23
Halomonadaceae	0.09	0.62	0.28	1.16	99.38
Vibrionaceae	0.06	0.27	0.18	0.51	99.9
Pseudoalteromonadaceae	0.02	0.06	0.15	0.1	100

Group Gov Cut					
Average similarity: 63.09					
Species	**Av.Abund**	**Av.Sim**	**Sim/SD**	**Contrib%**	**Cum.%**
Moraxellaceae	0.58	16.53	1.28	26.2	26.2
Pirellulaceae	0.22	7.12	4.37	11.29	37.49
uncultured	0.16	4.64	2.44	7.36	44.85
Rhodobacteraceae	0.16	4.5	2.74	7.13	51.98
Hyphomicrobiaceae	0.14	4.46	3.43	7.07	59.05
Woeseiaceae	0.15	3.6	1.5	5.7	64.75
Desulfocapsaceae	0.1	3.15	3.6	5	69.75
Rhizobiaceae	0.1	3.07	3.28	4.86	74.61
Bacillaceae	0.16	2.65	0.7	4.21	78.81
Desulfosarcinaceae	0.1	2.43	1.85	3.86	82.67
Flavobacteriaceae	0.08	2.01	2.03	3.19	85.87
Thermoanaerobaculaceae	0.07	1.88	2.45	2.99	88.85
Kiloniellaceae	0.09	1.77	1.64	2.81	91.66
NB1-j	0.07	1.32	1.04	2.1	93.76
Planococcaceae	0.1	1.12	0.38	1.77	95.53
Nitrosococcaceae	0.07	1.05	0.91	1.66	97.18
Nitrosopumilaceae	0.05	0.74	1.41	1.17	98.36
Vibrionaceae	0.03	0.68	2.35	1.07	99.43
Halomonadaceae	0.03	0.28	0.43	0.45	99.88
Pseudoalteromonadaceae	0.03	0.08	0.41	0.12	100

6.4. **BioSample Objects and Accession numbers for all NCRMP samples uploaded to NCBI for 2022-2024**

Accession	Sample Name	SPUID	Organism	Tax ID	
SAMN49078318	Sed.3002.2022	Sed.3002.2022	metagenome	256318	
SAMN49078319	Sed.3004.2022	Sed.3004.2022	metagenome	256318	
SAMN49078320	Sed.3005.2022	Sed.3005.2022	metagenome	256318	
SAMN49078321	Sed.3006.2022	Sed.3006.2022	metagenome	256318	
SAMN49078322	Sed.3007.2022	Sed.3007.2022	metagenome	256318	
SAMN49078323	Sed.3008.2022	Sed.3008.2022	metagenome	256318	
SAMN49078324	Sed.3010.2022	Sed.3010.2022	metagenome	256318	
SAMN49078325	Sed.3011.2022	Sed.3011.2022	metagenome	256318	
SAMN49078326	Sed.3012.2022	Sed.3012.2022	metagenome	256318	
SAMN49078327	Sed.3013.2022	Sed.3013.2022	metagenome	256318	
SAMN49078328	Sed.3015.2022	Sed.3015.2022	metagenome	256318	
SAMN49078329	Sed.3019.2022	Sed.3019.2022	metagenome	256318	
SAMN49078330	Sed.3021.2022	Sed.3021.2022	metagenome	256318	
SAMN49078331	Sed.3022.2022	Sed.3022.2022	metagenome	256318	
SAMN49078332	Sed.3023.2022	Sed.3023.2022	metagenome	256318	
SAMN49078333	Sed.3024.2022	Sed.3024.2022	metagenome	256318	

SAMN49078334	Sed.3025.2022	Sed.3025.2022	metagenome	256318
SAMN49078335	Sed.3026.2022	Sed.3026.2022	metagenome	256318
SAMN49078336	Sed.3028.2022	Sed.3028.2022	metagenome	256318
SAMN49078337	Sed.3029.2022	Sed.3029.2022	metagenome	256318
SAMN49078338	Sed.3033.2022	Sed.3033.2022	metagenome	256318
SAMN49078339	Sed.3034.2022	Sed.3034.2022	metagenome	256318
SAMN49078340	Sed.3035.2022	Sed.3035.2022	metagenome	256318
SAMN49078341	Sed.3036.2022	Sed.3036.2022	metagenome	256318
SAMN49078342	Sed.3037.2022	Sed.3037.2022	metagenome	256318
SAMN49078343	Sed.3038.2022	Sed.3038.2022	metagenome	256318
SAMN49078344	Sed.3039.2022	Sed.3039.2022	metagenome	256318
SAMN49078345	Sed.3040.2022	Sed.3040.2022	metagenome	256318
SAMN49078346	Sed.3041.2022	Sed.3041.2022	metagenome	256318
SAMN49078347	Sed.3043.2022	Sed.3043.2022	metagenome	256318
SAMN49078348	Sed.3045.2022	Sed.3045.2022	metagenome	256318
SAMN49078349	Sed.3047.2022	Sed.3047.2022	metagenome	256318
SAMN49078350	Sed.3048.2022	Sed.3048.2022	metagenome	256318
SAMN49078351	Sed.3050.2022	Sed.3050.2022	metagenome	256318
SAMN49078352	Sed.3051.2022	Sed.3051.2022	metagenome	256318
SAMN49078353	Sed.3053.2022	Sed.3053.2022	metagenome	256318
SAMN49078354	Sed.3054.2022	Sed.3054.2022	metagenome	256318
SAMN49078355	Sed.3055.2022	Sed.3055.2022	metagenome	256318
SAMN49078356	Sed.3056.2022	Sed.3056.2022	metagenome	256318
SAMN49078357	Sed.3059.2022	Sed.3059.2022	metagenome	256318
SAMN49078358	Sed.3060.2022	Sed.3060.2022	metagenome	256318
SAMN49078359	Sed.3061.2022	Sed.3061.2022	metagenome	256318
SAMN49078360	Sed.3068.2022	Sed.3068.2022	metagenome	256318
SAMN49078361	Sed.3069.2022	Sed.3069.2022	metagenome	256318
SAMN49078362	Sed.3070.2022	Sed.3070.2022	metagenome	256318
SAMN49078363	Sed.3071.2022	Sed.3071.2022	metagenome	256318
SAMN49078364	Sed.3072.2022	Sed.3072.2022	metagenome	256318
SAMN49078365	Sed.3073.2022	Sed.3073.2022	metagenome	256318
SAMN49078366	Sed.3076.2022	Sed.3076.2022	metagenome	256318
SAMN49078367	Sed.3078.2022	Sed.3078.2022	metagenome	256318
SAMN49078368	Sed.3079.2022	Sed.3079.2022	metagenome	256318
SAMN49078369	Sed.3081.2022	Sed.3081.2022	metagenome	256318
SAMN49078370	Sed.3082.2022	Sed.3082.2022	metagenome	256318
SAMN49078371	Sed.3083.2022	Sed.3083.2022	metagenome	256318
SAMN49078372	Sed.3085.2022	Sed.3085.2022	metagenome	256318
SAMN49078373	Sed.3086.2022	Sed.3086.2022	metagenome	256318
SAMN49078374	Sed.3091.2022	Sed.3091.2022	metagenome	256318
SAMN49078375	Sed.3093.2022	Sed.3093.2022	metagenome	256318
SAMN49078376	Sed.3094.2022	Sed.3094.2022	metagenome	256318
SAMN49078377	Sed.3097.2022	Sed.3097.2022	metagenome	256318
SAMN49078378	Sed.3098.2022	Sed.3098.2022	metagenome	256318
SAMN49078379	Sed.3099.2022	Sed.3099.2022	metagenome	256318

SAMN49078380	Sed.3101.2022	Sed.3101.2022	metagenome	256318
SAMN49078381	Sed.3103.2022	Sed.3103.2022	metagenome	256318
SAMN49078382	Sed.3104.2022	Sed.3104.2022	metagenome	256318
SAMN49078383	Sed.3105.2022	Sed.3105.2022	metagenome	256318
SAMN49078384	Sed.3109.2022	Sed.3109.2022	metagenome	256318
SAMN49078385	Sed.3110.2022	Sed.3110.2022	metagenome	256318
SAMN49078386	Sed.3112.2022	Sed.3112.2022	metagenome	256318
SAMN49078387	Sed.3114.2022	Sed.3114.2022	metagenome	256318
SAMN49078388	Sed.3115.2022	Sed.3115.2022	metagenome	256318
SAMN49078389	Sed.3119.2022	Sed.3119.2022	metagenome	256318
SAMN49078390	Sed.3120.2022	Sed.3120.2022	metagenome	256318
SAMN49078391	Sed.3121.2022	Sed.3121.2022	metagenome	256318
SAMN49078392	Sed.3122.2022	Sed.3122.2022	metagenome	256318
SAMN49078393	Sed.3123.2022	Sed.3123.2022	metagenome	256318
SAMN49078394	Sed.3124.2022	Sed.3124.2022	metagenome	256318
SAMN49078395	Sed.3126.2022	Sed.3126.2022	metagenome	256318
SAMN49078396	Sed.3127.2022	Sed.3127.2022	metagenome	256318
SAMN49078397	Sed.3128.2022	Sed.3128.2022	metagenome	256318
SAMN49078398	Sed.3130.2022	Sed.3130.2022	metagenome	256318
SAMN49078399	Sed.3136.2022	Sed.3136.2022	metagenome	256318
SAMN49078400	Sed.3139.2022	Sed.3139.2022	metagenome	256318
SAMN49078401	Sed.3141.2022	Sed.3141.2022	metagenome	256318
SAMN49078402	Sed.3143.2022	Sed.3143.2022	metagenome	256318
SAMN49078403	Sed.3144.2022	Sed.3144.2022	metagenome	256318
SAMN49078404	Sed.3145.2022	Sed.3145.2022	metagenome	256318
SAMN49078405	Sed.3149.2022	Sed.3149.2022	metagenome	256318
SAMN49078406	Sed.3150.2022	Sed.3150.2022	metagenome	256318
SAMN49078407	Sed.3152.2022	Sed.3152.2022	metagenome	256318
SAMN49078408	Sed.3153.2022	Sed.3153.2022	metagenome	256318
SAMN49078409	Sed.3154.2022	Sed.3154.2022	metagenome	256318
SAMN49078410	Sed.3156.2022	Sed.3156.2022	metagenome	256318
SAMN49078411	Sed.3157.2022	Sed.3157.2022	metagenome	256318
SAMN49078412	Sed.3159.2022	Sed.3159.2022	metagenome	256318
SAMN49078413	Sed.3177.2022	Sed.3177.2022	metagenome	256318
SAMN49078414	Sed.3178.2022	Sed.3178.2022	metagenome	256318
SAMN49078415	Sed.3179.2022	Sed.3179.2022	metagenome	256318
SAMN49078416	Sed.3182.2022	Sed.3182.2022	metagenome	256318
SAMN49078417	Sed.3183.2022	Sed.3183.2022	metagenome	256318
SAMN49078418	Sed.3189.2022	Sed.3189.2022	metagenome	256318
SAMN49078419	Sed.3190.2022	Sed.3190.2022	metagenome	256318
SAMN49078420	Sed.3193.2022	Sed.3193.2022	metagenome	256318
SAMN49078421	Sed.3194.2022	Sed.3194.2022	metagenome	256318
SAMN49078422	Sed.3195.2022	Sed.3195.2022	metagenome	256318
SAMN49078423	Sed.3200.2022	Sed.3200.2022	metagenome	256318
SAMN49078424	Sed.3201.2022	Sed.3201.2022	metagenome	256318
SAMN49078425	Sed.3202.2022	Sed.3202.2022	metagenome	256318

SAMN49078426	Sed.3204.2022	Sed.3204.2022	metagenome	256318
SAMN49078427	Sed.3205.2022	Sed.3205.2022	metagenome	256318
SAMN49078428	Sed.3206.2022	Sed.3206.2022	metagenome	256318
SAMN49078429	Sed.3207.2022	Sed.3207.2022	metagenome	256318
SAMN49078430	Sed.3208.2022	Sed.3208.2022	metagenome	256318
SAMN49078431	Sed.3209.2022	Sed.3209.2022	metagenome	256318
SAMN49078432	Sed.3211.2022	Sed.3211.2022	metagenome	256318
SAMN49078433	Sed.3212.2022	Sed.3212.2022	metagenome	256318
SAMN49078434	Sed.3213.2022	Sed.3213.2022	metagenome	256318
SAMN49078435	Sed.3214.2022	Sed.3214.2022	metagenome	256318
SAMN49078436	Sed.3215.2022	Sed.3215.2022	metagenome	256318
SAMN49078437	Sed.3216.2022	Sed.3216.2022	metagenome	256318
SAMN49078438	Sed.3218.2022	Sed.3218.2022	metagenome	256318
SAMN49078439	Sed.3219.2022	Sed.3219.2022	metagenome	256318
SAMN49078440	Sed.3220.2022	Sed.3220.2022	metagenome	256318
SAMN49078441	Sed.3221.2022	Sed.3221.2022	metagenome	256318
SAMN49078442	Sed.3222.2022	Sed.3222.2022	metagenome	256318
SAMN49078443	Sed.3224.2022	Sed.3224.2022	metagenome	256318
SAMN49078444	Sed.3230.2022	Sed.3230.2022	metagenome	256318
SAMN49078445	Sed.3232.2022	Sed.3232.2022	metagenome	256318
SAMN49078446	Sed.3233.2022	Sed.3233.2022	metagenome	256318
SAMN49078447	Sed.3235.2022	Sed.3235.2022	metagenome	256318
SAMN49078448	Sed.3236.2022	Sed.3236.2022	metagenome	256318
SAMN49078449	Sed.3237.2022	Sed.3237.2022	metagenome	256318
SAMN49078450	Sed.3239.2022	Sed.3239.2022	metagenome	256318
SAMN49078451	Sed.3240.2022	Sed.3240.2022	metagenome	256318
SAMN49078452	Sed.3241.2022	Sed.3241.2022	metagenome	256318
SAMN49078453	Sed.3243.2022	Sed.3243.2022	metagenome	256318
SAMN49078454	Sed.3244.2022	Sed.3244.2022	metagenome	256318
SAMN49078455	Sed.3245.2022	Sed.3245.2022	metagenome	256318
SAMN49078456	Sed.3246.2022	Sed.3246.2022	metagenome	256318
SAMN49078457	Sed.3248.2022	Sed.3248.2022	metagenome	256318
SAMN49078458	Sed.3249.2022	Sed.3249.2022	metagenome	256318
SAMN49078459	Sed.3250.2022	Sed.3250.2022	metagenome	256318
SAMN49078460	Sed.3252.2022	Sed.3252.2022	metagenome	256318
SAMN49078461	Sed.3253.2022	Sed.3253.2022	metagenome	256318
SAMN49078462	Sed.3254.2022	Sed.3254.2022	metagenome	256318
SAMN49078463	Sed.3255.2022	Sed.3255.2022	metagenome	256318
SAMN49078464	Sed.3257.2022	Sed.3257.2022	metagenome	256318
SAMN49078465	Sed.3258.2022	Sed.3258.2022	metagenome	256318
SAMN49078466	Sed.3259.2022	Sed.3259.2022	metagenome	256318
SAMN49078467	Sed.3260.2022	Sed.3260.2022	metagenome	256318
SAMN49078468	Sed.3262.2022	Sed.3262.2022	metagenome	256318
SAMN49078469	Sed.3263.2022	Sed.3263.2022	metagenome	256318
SAMN49078470	Sed.3264.2022	Sed.3264.2022	metagenome	256318
SAMN49078471	Sed.3273.2022	Sed.3273.2022	metagenome	256318

SAMN49078472	Sed.3274.2022	Sed.3274.2022	metagenome	256318
SAMN49078473	Sed.3275.2022	Sed.3275.2022	metagenome	256318
SAMN49078474	Sed.3279.2022	Sed.3279.2022	metagenome	256318
SAMN49078475	Sed.3280.2022	Sed.3280.2022	metagenome	256318
SAMN49078476	Sed.3282.2022	Sed.3282.2022	metagenome	256318
SAMN49078477	Sed.3284.2022	Sed.3284.2022	metagenome	256318
SAMN49078478	Sed.3285.2022	Sed.3285.2022	metagenome	256318
SAMN49078479	Sed.3286.2022	Sed.3286.2022	metagenome	256318
SAMN49078480	Sed.3292.2022	Sed.3292.2022	metagenome	256318
SAMN49078481	Sed.3293.2022	Sed.3293.2022	metagenome	256318
SAMN49078482	Sed.3294.2022	Sed.3294.2022	metagenome	256318
SAMN49078483	Sed.3001.2024	Sed.3001.2024	metagenome	256318
SAMN49078484	Sed.3014.2024	Sed.3014.2024	metagenome	256318
SAMN49078485	Sed.3015.2024	Sed.3015.2024	metagenome	256318
SAMN49078486	Sed.3030.2024	Sed.3030.2024	metagenome	256318
SAMN49078487	Sed.3031.2024	Sed.3031.2024	metagenome	256318
SAMN49078488	Sed.3037.2024	Sed.3037.2024	metagenome	256318
SAMN49078489	Sed.3041.2024	Sed.3041.2024	metagenome	256318
SAMN49078490	Sed.3080.2024	Sed.3080.2024	metagenome	256318
SAMN49078491	Sed.3084.2024	Sed.3084.2024	metagenome	256318
SAMN49078492	Sed.3097.2024	Sed.3097.2024	metagenome	256318
SAMN49078493	Sed.3098.2024	Sed.3098.2024	metagenome	256318
SAMN49078494	Sed.3099.2024	Sed.3099.2024	metagenome	256318
SAMN49078495	Sed.3100.2024	Sed.3100.2024	metagenome	256318
SAMN49078496	Sed.3101.2024	Sed.3101.2024	metagenome	256318
SAMN49078497	Sed.3105.2024	Sed.3105.2024	metagenome	256318
SAMN49078498	Sed.3107.2024	Sed.3107.2024	metagenome	256318
SAMN49078499	Sed.3109.2024	Sed.3109.2024	metagenome	256318
SAMN49078500	Sed.3110.2024	Sed.3110.2024	metagenome	256318
SAMN49078501	Sed.3114.2024	Sed.3114.2024	metagenome	256318
SAMN49078502	Sed.3115.2024	Sed.3115.2024	metagenome	256318
SAMN49078503	Sed.3117.2024	Sed.3117.2024	metagenome	256318
SAMN49078504	Sed.3121.2024	Sed.3121.2024	metagenome	256318
SAMN49078505	Sed.3125.2024	Sed.3125.2024	metagenome	256318
SAMN49078506	Sed.3126.2024	Sed.3126.2024	metagenome	256318
SAMN49078507	Sed.3127.2024	Sed.3127.2024	metagenome	256318
SAMN49078508	Sed.3128.2024	Sed.3128.2024	metagenome	256318
SAMN49078509	Sed.3130.2024	Sed.3130.2024	metagenome	256318
SAMN49078510	Sed.3132.2024	Sed.3132.2024	metagenome	256318
SAMN49078511	Sed.3135.2024	Sed.3135.2024	metagenome	256318
SAMN49078512	Sed.3136.2024	Sed.3136.2024	metagenome	256318
SAMN49078513	Sed.3137.2024	Sed.3137.2024	metagenome	256318
SAMN49078514	Sed.3139.2024	Sed.3139.2024	metagenome	256318
SAMN49078515	Sed.3151.2024	Sed.3151.2024	metagenome	256318
SAMN49078516	Sed.3152.2024	Sed.3152.2024	metagenome	256318
SAMN49078517	Sed.3155.2024	Sed.3155.2024	metagenome	256318

SAMN49078518	Sed.3163.2024	Sed.3163.2024	metagenome	256318
SAMN49078519	Sed.3174.2024	Sed.3174.2024	metagenome	256318
SAMN49078520	Sed.3185.2024	Sed.3185.2024	metagenome	256318
SAMN49078521	Sed.3189.2024	Sed.3189.2024	metagenome	256318
SAMN49078522	Sed.3195.2024	Sed.3195.2024	metagenome	256318
SAMN49078523	Sed.3201.2024	Sed.3201.2024	metagenome	256318
SAMN49078524	Sed.3206.2024	Sed.3206.2024	metagenome	256318
SAMN49078525	Sed.3207.2024	Sed.3207.2024	metagenome	256318
SAMN49078526	Sed.3208.2024	Sed.3208.2024	metagenome	256318
SAMN49078527	Sed.3209.2024	Sed.3209.2024	metagenome	256318
SAMN49078528	Sed.3213.2024	Sed.3213.2024	metagenome	256318
SAMN49078529	Sed.3220.2024	Sed.3220.2024	metagenome	256318
SAMN49078530	Sed.3226.2024	Sed.3226.2024	metagenome	256318
SAMN49078531	Sed.3229.2024	Sed.3229.2024	metagenome	256318
SAMN49078532	Sed.3237.2024	Sed.3237.2024	metagenome	256318
SAMN49078533	Sed.3240.2024	Sed.3240.2024	metagenome	256318
SAMN49078534	Sed.3241.2024	Sed.3241.2024	metagenome	256318
SAMN49078535	Sed.3243.2024	Sed.3243.2024	metagenome	256318
SAMN49078536	Sed.3244.2024	Sed.3244.2024	metagenome	256318
SAMN49078537	Sed.3248.2024	Sed.3248.2024	metagenome	256318
SAMN49078538	Sed.3257.2024	Sed.3257.2024	metagenome	256318
SAMN49078539	Sed.3259.2024	Sed.3259.2024	metagenome	256318
SAMN49078540	Sed.3260.2024	Sed.3260.2024	metagenome	256318
SAMN49078541	Sed.3262.2024	Sed.3262.2024	metagenome	256318
SAMN49078542	Sed.3266.2024	Sed.3266.2024	metagenome	256318
SAMN49078543	Sed.3270.2024	Sed.3270.2024	metagenome	256318
SAMN49078544	Sed.3274.2024	Sed.3274.2024	metagenome	256318
SAMN49078545	Sed.3275.2024	Sed.3275.2024	metagenome	256318
SAMN49078546	Sed.3276.2024	Sed.3276.2024	metagenome	256318
SAMN49078547	Sed.3280.2024	Sed.3280.2024	metagenome	256318
SAMN49078548	Sed.3289.2024	Sed.3289.2024	metagenome	256318
SAMN49078549	Sed.3295.2024	Sed.3295.2024	metagenome	256318
SAMN49078550	Sed.3296.2024	Sed.3296.2024	metagenome	256318
SAMN49078551	Sed.3299.2024	Sed.3299.2024	metagenome	256318
SAMN49078552	Sed.3601.2024	Sed.3601.2024	metagenome	256318
SAMN49078553	Sed.3603.2024	Sed.3603.2024	metagenome	256318
SAMN49078554	Sed.3609.2024	Sed.3609.2024	metagenome	256318

6.5. Heavy metal depth scatterplots by region (attached and available in shared folder as filed named “Heavy Metal by Depth Inlet Exp scatterplots BW 6 2025.doc”)